ANALYSIS AND RECOMBINANT AAV DELIVERY OF RIBOZYMES AGAINST THE *rd* MUTATION IN MICE

By

WEIMING YAN

A DISSERTATION PRESENTED TO THE GRADUATE SCHOOL OF THE
UNIVERSITY OF FLORIDA IN PARTIAL FULFILLMENT OF THE
REQUIREMENTS FOR THE DEGREE OF
DOCTOR OF PHILOSOPHY

UNIVERSITY OF FLORIDA

1998

Copyright 1998

By

Weiming Yan

ACKNOWLEDGEMENTS

I would like first to thank my mentor, Dr. William Hauswirth, for his advice, understanding and encouragement during this research. This work would not have been possible without his unlimited guidance and support. I especially appreciate for his patience and time in proofreading my English.

I would also like to thank my committee members, Drs. Alfred Lewin, Nicolas Muzyczka and Paul Hargrave, for their advice and guidance.

My thanks are extended to Chrissie, Vince, Ad, Qiuhong and other colleagues in Dr. Hauswirth's laboratory. Their support and encouragement make this research more enjoyable. I would also thank the fellows in Dr. Lewin's laboratory for their advice and assistance. I am grateful to the staff in the Department of Molecular Genetics and Microbiology for their help whenever I need.

I am most appreciative to Drs. Chandu Ammini and Hyma Tirupati, who taught me how to do science from the very beginning, and gave me support during the difficult time.

Finally, I am very grateful to my family, the people love me and I love, for their understanding and encouragement during those years.

TABLE OF CONTENTS

ACKNOWLEDGEMENTS....iii

KEYS TO SYMBOLS....vi

ABSTRACT....ix

CHAPTERS

1. INTRODUCTION....1
   - Retinal Structure and Visual Signal Transduction....1
   - Ribozymes for Gene Therapy....20
   - Adeno-associated Virus as a Gene Delivery Vector....27
   - Focus of Dissertation....36

2. *IN VITRO* ANALYSIS OF THE BOVINE RHODOPSIN PROMOTER....38
   - Introduction....38
   - Materials and Methods....41
   - Results....51
   - Discussion....60

3. SELECTIVE DEGRADATION *IN VIVO* OF NONSENSE BETA PHOSPHODIESTERASE mRNA IN THE HETEROZYGOUS *rd* MOUSE....65
   - Introduction....65
   - Materials and Methods....68
   - Results....71
   - Discussion....82

4. *IN VITRO* ANALYSIS OF HAMMERHEAD RIBOZYMES SPECIFICTO THE mRNA OF cGMP PHOSPHODIESTERASE BETA SUBUNIT....88
   - Introduction....88
   - Materials and Methods....91
   - Results....100
   - Discussion....126

5. THE EFFECT OF hnRNP A1 ON THE CLEAVAGE REACTION OF HAMMERHEAD RIBOZYME pRZ636....130

Introduction..130
Materials and Methods..134
Results...140
Discussion...147

6. *IN VIVO* CHARACTERIZATION OF A HAMMERHEAD RIBOZYME SPECIFIC TO A NONSENSE TRANSCRIPT OF THE MOUSE cGMP PHOSPHODIESTERASE BETA SUBUNIT...152
Introduction..152
Materials and Methods..155
Results...163
Discussion...164

7. CONCLUSIONS AND PERSPECTIVES...169

LIST OF REFERENCES...176

BIOGRAPHICAL SKETCH..199

KEY TO SYMBOLS

AS	antisense
ATP	adenosine 5’-triphosphate
β actin	beta actin
β-PDE	beta subunit of cGMP phosphodiesterase
β-globin	beta globin
bp	base pair
BSA	bovine serum albumin
°C	degrees centigrade
cGMP	cyclic guanosine monophosphate
CTP	cytidine 5’-triphosphate
DNA	deoxyribonucleic acid
DNase I	deoxyribonucleic acid nuclease I
DTT	dithiothreitol
EDTA	ethylenediamene tetraacetic acid, disodium salt
GDP	guanosine 5’-diphosphate
GTP	guanosine 5’-triphosphate
HEPES	N-2-hydroxyethylpiperazine-N’-2-ethanesulfonic acid
IRBR	interphotoreceptor retinoid binding protein
kb	kilobase
kd	kilodalton
M	molar
μCi	microcurie
μl	microliter
μm	micrometer
μM	micromolar

mCi	millicurie
mg	microgram
min	minute
ml	milliliter
mM	millimolar
mo	months
mRNA	messenger ribonucleic acid
ng	nanogram
NP-40	nonidet P-40
ONL	outer nuclear layer
^{32}P	phosphorus 32
PCR	polymerase chain reaction
PDE	phosphodiesterase
PDE_{α}	α subunit of cGMP phosphodiesterase
PDE_{β}	β subunit of cGMP phosphodiesterase
PDE_{γ}	γ subunit of cGMP phosphodiesterase
PMSF	phenylmethylsulfonyl fluoride
PR	photoreceptor
pre-mRNA	pre messenger ribonucleic acid
RNA	ribonucleic acid
RNase	Ribonuclease A
rpm	revolution per minutes
rRNA	ribosomal ribonucleic acid
S	sense
SDS	sodium dodecyl sulfate
T	transducin
T_{α}	α subunit of transducin
T_{β}	β subunit of transducin
T_{γ}	γ subunit of transducin
Tris	Tris(hydroxymethyl)aminomethane
UTP	uridine 5'-triphosphate

UV	ultra violet
w/v	weight per volume
x g	times gravity

Abstract of Dissertation Presented to the Graduate School
of the University of Florida in Partial Fulfillment of the
Requirements for the Degree of Doctor of Philosophy

ANALYSIS AND RECOMBINANT AAV DELIVERY OF RIBOZYMES AGAINST THE *rd* MUTATION IN MICE

By

Weiming Yan

December, 1998

Chairperson: William W. Hauswirth
Major Department: Molecular Genetics and Microbiology

Retinal degeneration is currently untreatable. Understanding the molecular mechanism causing specific forms of retinal degeneration and searching for novel therapies should help to cure or alleviate this disease. The general focus of this dissertation is to develop such therapies. My specific focus will be to understand the molecular mechanisms of Retinitis Pigmentosa using the *rd* mouse as a model, and to develop a recombinant adeno-associated virus based ribozyme therapy for its treatment. Toward this end several topics were investigated.

Understanding the function of *cis* elements in the rod opsin promoter will identify a promoter sequence for achieving high level, photoreceptor-specific therapeutic gene expression. An *in vitro* transcription system using bovine retinal nuclear extract was set up and used to dissect *cis* regulatory elements.

Specific degradation of nonsense mRNA of the β subunit of cGMP phosphodiesterase in the photoreceptor of *rd* mice was documented by RT-PCR and RFLP. This mechanism might protect the retina of heterozygous *rd*/+ mice from degeneration by eliminating deleterious nonsense transcripts. These results might be extended to other nonsense mutations causing different retinal degenerations.

A hammerhead ribozyme was designed to specifically decrease levels of nonsense transcripts of β-PDE. The ultimate aim was to alleviate the deleterious effect of such transcripts and extend the rescue of retinal degeneration in transgenic *rd/rd*/+ mice. Another hammerhead ribozyme specific to the wild type transcript of β-PDE was also designed and tested. This ribozyme might induce retinal degeneration in heterozygous *rd*/+ mice by creating an imbalance between different subunits of cGMP phosphodiesterase, leading to an animal model for further study of retinal degeneration. The activities of those ribozymes were tested *in vitro*, and their kinetic constants determined.

The gene for each ribozyme was packaged into recombinant adeno-associated viruses, and delivered into *rd*/+ mice by subretinal injection. The ribozyme specific to nonsense transcripts of β-PDE can function *in vivo* to decrease nonsense transcript levels in photoreceptors of the *rd*/+ mouse.

The effect of hnRNP A1 on the activity of the ribozyme was determined *in vitro*. Although no positive effect was found, the hnRNP A1 binding site might still function inside cells. The aim was to increase the efficiency of the ribozyme reaction by linking an hnRNP A1 binding site to the ribozyme sequence.

CHAPTER 1
INTRODUCTION

Retinal Structure and Visual Signal Transduction

Morphology

The retina is located between the vitreous chamber and the choroidal layer of the vertebrate eye. It is composed of several well-defined layers (Figure 1-1): the ganglion cell layer (GCL), the inner plexiform layer (IPL), the inner nuclear layer (INL), the outer plexiform layer (OPL), the outer nuclear layer (ONL) and retinal pigment epithelial cell layer (RPE). The ganglion cell layer, closest to the vitreous humor, consists of ganglion neural cells and Müller glial cells. The long axons of ganglion cells bundle together to form the optic nerve that exits the eye toward the brain. Ganglion cells have synaptic connections to cells of the inner nuclear layer within the inner plexiform layer. The inner nuclear layer consists of several classes of neural cells (amacrine, horizontal and bipolar) and Müller glial cells. The neural cells of the inner nuclear layer form synaptic connections within the outer plexiform layer and transmit neural signals between the outer nuclear layer and ganglion cell layer. Müller cell bodies extend throughout the entire retinal layer, providing structural support and metabolic function for all retinal cell types (Blomhoff et al., 1990).

The photoreceptor cell is the major cell-type in outer retinal layer and comprises about 50% of all cells in the mammalian retina. The nuclei of photoreceptors form the outer

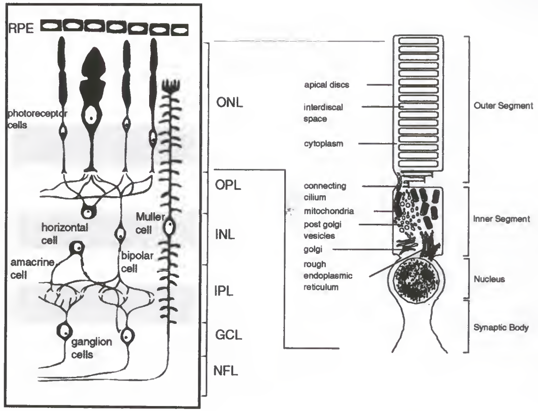

Retina

Photoreceptor

Figure 1-1: Schematic structure of the retina and rod photoreceptor (adapted from Miyoshi et al, 1997 with minor modification). ONL, outer nuclear layer; OPL, outer plexiform layer; INL, inner nuclear layer; IPL, inner plexiform layer; GCL, ganglion cell layer; NFL, nerve fiber layer. The photoreceptor cell contains a cell body with the nucleus (NL), an inner segment, an outer segment and a synaptic body.

nuclear layer. There are two kinds of photoreceptors: rods and cones. About 90% of human photoreceptors are rods, the cells responsible for monochromatic vision in dim light. The rest are cone cells, and are responsible for the color vision and perception of fine detail in fairly bright light. The fovea is a circular, cone rich region of the retina close to optic nerve in the central retina of the primates. The majority of cone nuclei are located within the outer portion of the outer nuclear layer; more than 50% of cone nuclei are adjacent to the outer limiting membrane. In the peripheral retina of primates and in most other mammals, cones are separated from one another by several rod cells and their outer segments are shorter than those of rods (Carter Dawson and LaVail., 1979a). About 90% of human cones contain middle/long wavelength pigments (red or green sensitive), and the remaining contain a short wavelength pigment (blue sensitive).

The visual transduction cascade occurs within the outer segments of photoreceptors (Stryer, 1986). Light-induced hyperpolarization of photoreceptor plasma membrane causes a decrease of Ca^{2+} influx at the synapse that leads to a decrease in the release rate of the neurotransmitter glutamate from photoreceptors to neighboring bipolar cells. Since the neurotransmitter inhibits most postsynaptic neurons, lower concentrations of transmitter excites the neurons, producing a neural signal. This signal is then transmitted to the visual cortex of the brain through a ganglion cell process that create the optic nerve (Kaneko, 1979).

Photoreceptors (PRs) contain several distinct compartments: the synaptic body, the nuclear region (N), the inner segments (IS) and the outer segments (OS) (Hargrave and McDowell, 1992) (Figure 1-1). The synaptic body connects PRs to second-order neurons, such as bipolar and horizontal cells. Rhodopsin is synthesized in the rod inner segment, transported into outer segment and incorporated into plasma membrane. Each outer segment contains about two thousand disk-like structures, which are formed by pinching off from plasma membrane at the base of the outer segment. About 90% of the protein integrated in the disk membrane is rhodopsin. Other structural proteins, such as peripherin and rim protein, are also necessary to maintain the integrity of this bilayer disk.

The retinal pigment epithelia cell (RPE) cell has multiple functions important for visual transduction. Since it is behind PRs in the visual light pathway, it absorbs excess light and prevents light scatter back toward PRs. It also provides nutrients and other factors essential for the photoreceptor, such as retinoids. RPE cells renew visual pigments and photoreceptor outer segments by recycling the 11-*cis* retinal chromophore and by phagocytosing approximately 10% of each outer segment per day (Bok, 1985). In the PR, light activates photoisomerization of the chromophore of rhodopsin, 11-*cis* retinaldehyde, from its 11-*cis* to an all-*trans* configuration. The chromophore is then renewed by exchanging the all-*trans* retinal for 11-*cis* retinal supplied by the RPE cells. The all-*trans* retinal is reduced to all-*trans* retinol in the outer segment before being transported to RPE cells. Within the RPE, all-*trans* retinol is isomerized to the 11-*cis* configuration, and then oxidized before transport back to the photoreceptor outer segment (Bridges and Alvarez, 1987). This large scale transport between RPE and photoreceptor involves the interphotoreceptor retinol binding protein (IRBP) since the retinol has low solubility in water. IRBP is an extracellular protein secreted into subretinal space by PRs. It acts as a carrier to shuttle retinol and other nutrients such as fatty acids between photoreceptors and retinal pigment epithelium cells (Lai et al., 1982). Beside retinoids and vitamin A, vitamin E is also important for photoreceptor function, and provides protection for photoreceptors from oxidation products due to light absorption (Blomhoff et al., 1990; Berson et al., 1993).

Visual Transduction Cycle

Retinal photoreceptors are very sensitive to incident light. A single photon can trigger the visual excitation (Stryer and Bourne, 1986). The details of visual transduction in rod cells has been studied extensively over the past 25 years, and most of the genes involved in this process have been cloned and sequenced. In outline, light activates a biochemical cascade that results in the closing of cation-specific gated channels in the plasma membrane and production of a neural signal (Figure 1-2).

Rhodopsin is the key initial player in this signal cascade (Hargrave and McDowell, 1992). It is a 40 kd (348 amino acids) protein, which contains a chromophore, 11-*cis* retinal, attached to lysine 296 by a protonated Schiff base linkage. The hydrophobic amino acids occur in clusters, forming 7 transmembrane domains separated by hydrophilic loops. The carboxyl terminus is located in the cytoplasm and the amino terminus is on the intradiscal face of the plasma membrane. Cysteines within the C-terminal domain are palmitoylated through thioester bonds. It has been suggested that the palmitates are inserted into the disk lipid bilayer creating a fourth loop structure. There is also a binding site for transducin (see below) on the cytoplasmic loops. Phosphorylation of serines and threonines in this region by rhodopsin kinase or protein kinase C is crucial to the quenching of the light-induced signal. The N terminus is acetylated and two nearby asparagines are glycosylated. The proper folding of rhodopsin is critical for its

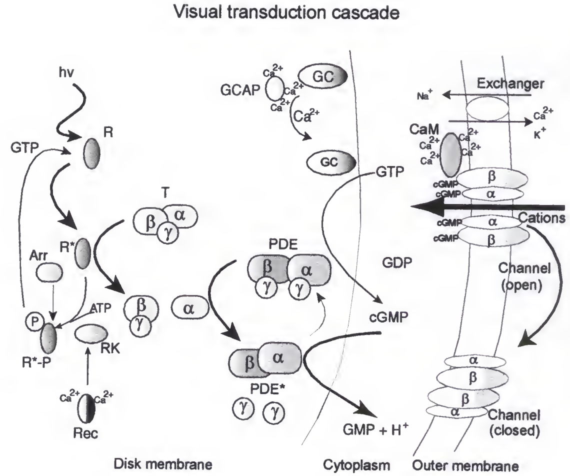

Figure 1-2: Schematic diagram of the visual signal transduction cycle (adapted from Polans et al, 1996 with minor modification). R, rhodopsin; R*, photolyzed rhodopsin; R*-P, phosphorylated rhodopsin; Arr, arrestin; RK, rhodopsin kinase; Rec, recoverin; T, transducin; PDE, cGMP phosphodiesterase; GC, guanylate cyclase; GCAP, guanylate cyclase activating protein; CaM, calmodulin; Channel, cGMP-gated channel; Exchanger, Na^+/Ca^{2+}-K^+ exchanger.

function, as suggested by the more than 80 mutations in this protein which alter rhodopsin structure and lead to degenerative retinal diseases.

The 11-*cis* retinal chromophore is isomerized to the an all-*trans* configuration by photon absorption, and this generates a structurally altered photoexcited metarhodopsin II. Metarhodopsin activates bound transducin by promoting exchange of free GTP for transducin bound GDP. Transducin is a heterotrimeric G-protein located in the peripheral disk membrane. It consists of α (39 Kd), β (36 Kd) and γ (8 Kd) subunits. The α subunit has a binding site for GTP or GDP and GTPase activity. In its inactive dark form, transducin β and γ subunits ($T_{\beta\gamma}$) are associated with transducin α subunit (T_α). Light activated rhodopsin leads to a T_α exchange of GTP for GDP resulting in the release of T_α from $T_{\beta\gamma}$ subunits. T_α can then activate cGMP phosphodiesterase (PDE), and metarhodopsin II can then activate another transducin T_α subunit. The activation of hundreds of transducins by a single light activated rhodopsin is the first amplification step in the visual cascade. This step is estimated to achieve about a 500-fold amplification.

The cGMP PDE is a heterotetramer also located on the peripheral disk membrane and consists of one α (88 Kd), one β (85 Kd) and two γ (9 Kd) subunits. In its active state, T_α-GTP extracts $PDE_{\gamma 2}$ from the intact $PDE_{\alpha\beta\gamma 2}$, releasing active $PDE_{\alpha\beta}$ to rapidly hydrolyze cGMP. This step increases the cGMP hydrolytic activity of PDE nearly 1,500 fold. PDE is an efficient enzyme, possessing a K_{cat}/K_m ($6 \times 10^7\ M^{-1}s^{-1}$), close to the limit of diffusion-controlled encounters between enzyme and substrate (Hurley and Stryer, 1982). In the dark state, cGMP binds cGMP gate channel proteins, keeping the channel open. The light-induced decrease of cGMP in the cytosol leads to this channel closing and hyperpolarization of the plasma membrane. This inhibits release of neurotransmitters at the PR synapse and generation of a neural signal.

To restore the dark state, the cation channel needs to reopen by restoration of intracellular cGMP levels. This key recovery step is necessary for proper visual sensing. The GTPase activity in transducin α subunits contributes to recovery from light activation by hydrolyzing its bound GTP, deactivating transducin and releasing $PDE_{\gamma 2}$. This, in turn, allows $PDE_{\gamma 2}$ to rebind to $PDE_{\alpha\beta}$, deactivating PDE. The γ subunit of PDE might also act as a GTPase-activating protein (GAP), thus accelerating GTP hydrolysis by transducin α subunits. A retinal specific protein (RGS-r) also has GAP function, and competes with PDE_{γ} for T_{α} to facilitate signal termination (Wieland et al., 1997).

Simultaneously it is necessary to quench rhodopsin. Rhodopsin kinase, a 68 kd cytosolic protein phosphorylates active rhodopsin at multiple serines and threonines near the C-terminus of rhodopsin. Arrestin, a 48 Kd cytosolic protein then binds to phosphorylated rhodopsin to further prevent interaction between rhodopsin and transducin. Light sensitive rhodopsin is regenerated by release of arrestin, C-terminal dephosphorylation by phosphatase 2A and reinsertion of 11-*cis* retinal.

Guanylate cyclase is also activated after light absorption to help restore the dark state. It works through recoverin, a calcium-sensitive stimulatory protein that interacts with Ca^{2+} in the dark state. In the dark, bound cGMP keeps the cGMP-gated channel open. Therefore, Na^{+} and Ca^{2+} can enter PRs through this cGMP-gated channel while K^{+} flows out through the plasma membrane. The import of Ca^{2+} via cGMP gated channels is balanced by its export through the glycoprotein sodium-calcium exchanger, powered by the influx of three Na^{+} and the efflux of one K^{+}. After light activation, the decrease of cGMP in the cytosol leads to closing of the cGMP-gated channel, and the influx of Ca^{2+} ceases. However, the export of Ca^{2+} by the sodium-calcium exchanger continues, which leads to a decrease in cytosolic Ca^{2+} levels. This light-triggered lowering of Ca^{2+} releases recoverin to stimulate guanylate cyclase. Guanylate cyclase then converts GTP into cGMP, elevating cGMP levels and reopening cGMP channels.

Regulation of Photoreceptor Gene Expression

Eukaryotic cells can regulate their gene expression at several levels: transcription, post-transcriptional processing, translation and post-translational modification. The major point of regulation in most cells is at transcription. Extracellular or intracellular signals can trigger different signaling pathways and alter the transcription of certain genes. Selective activation or inactivation of genes can also control development and differentiation. Several model systems have been adopted for studying transcriptional regulation. These include *in vitro* transcription, genetic analysis (usually in yeast or *Drosophila*), *in vivo* analysis of endogenous cellular genes or transient transfection with exogenous genes. Through these systems of transcriptional analysis, we have achieved a reasonable level of understanding of promoter structure, transcription factors, transcription initiation and chromatin effects on transcription.

A promoter is a DNA region containing the majority of *cis*-elements for RNA polymerase II transcriptional regulation (Zawel and Reinberg, 1995; Roeder, 1996). All promoters can be dissected into core and regulatory regions (enhancers and silencers). The core region is very conserved for most protein encoding genes. The TATA box found in many pol II promoters and located about 30 bp upstream of the transcription start site is the focus of the proximal promoter. The basal transcription apparatus recognizes the TATA box and/or a pyrimidine-rich initiator (Inr) close to the transcription start site (Kaufmann and Smale, 1994), and initiates transcription. Regions regulating the strength of basal transcription are modular and diverse among different genes. *Cis*-elements in regulatory regions interact with DNA binding proteins, which in turn, are involved in protein-protein interactions with other *trans*-acting regulatory proteins. Enhancer elements, also in the regulatory region, can affect gene transcription in a distance and orientation independent manner. Multiple sequence-specific activators and DNA bending proteins bound to the same promoter form an enhanceosome complex. Enhancesomes aid in recruiting RNA polymerase II to the TATA complex and, in synergy with transcription factors and other coactivators, stimulate transcription. Phosphorylation of activators in enhanceosomes by kinase-dependent signal pathways are likely to further regulate transcription (Carey, 1998).

The basal transcription apparatus consists of RNA polymerase II and the general transcription factors: TATA-binding protein (TBP), TFIIA, TFIIB, TFIIE, TFIIF and TFIIH (Halle and Meisterernst, 1996). These factors are conserved between yeast, *drosophila* and human, and are functional on most proximal promoters. TBP recognizes the TATA box, and recruits TFIIB to form the initiation complex. TAFs (TBP-associated factors) recognize the non-TATA core promoter, and interact with multiple regulatory proteins. TFIIB recruits RNA polymerase II, and determines the transcription start site. TFIIF forms a holoenzyme with RNA polymerase II, and TFIIE helps to recruit the TFIIH to the initiation complex (Ohkuma et al., 1995). TFIIH has ATPase and helicase activities, which locally unwind the DNA templates for transcription (Holstege et al., 1996). The protein kinase activity of TFIIH can phosphorylate the carboxyl-terminal domain (CTD) of RNA polymerase II, a prerequisite for initiation and pre-mRNA splicing (Koleske and Young, 1995; Steinmetz, 1997).

Cis-elements in regulatory regions are also responsible for tissue-specific and gene-specific expression. Different activator or repressor proteins interact with those elements and TBP/TAFs to selectively activate essential genes (Ptashne and Gann, 1997). Some transcription factors act as bridges between the basal transcription apparatus and activators. Mediator proteins in yeast and TAFs in *Drosophila* have this function. Mediators bind within the CTD of RNA polymerase II and form a holoenzyme (Verrijzer and Tjian, 1996). TAFs may also form a complex with TBP (TFIID), and interact through this complex with activators to regulate gene expression (Sauer et al., 1996; Verrijzer and Tjian, 1996).

The DNA in eukaryotic cells is organized into particles using DNA-bound histone proteins. Approximately every 146 bp of DNA is wrapped around a nucleosome, an octamer of two each of four different histones (H2A, H2B, H3 and H4). Nucleosomes are then organized into higher order structures, ultimately compacting DNA several thousand fold. This compact chromatin structure inhibits transcription by serving as a barrier for entry of basal transcription factors or regulatory proteins (Peterson and Tamkun, 1995). Some factors, such as the SWI-SNF complex of yeast, can unwind and open chromatin, and facilitate the accessibility of transcription factors. In yeast cells, the SWI-SNF complex can promote GAL4-4H, a transcription activator, to form a ternary complex with double-stranded DNA and histone proteins *in vitro* (Cote et al., 1994). The hydrolysis of ATP by the DNA-stimulated ATPase activity in SWI-SNF might provide the energy for promoting the release of histone H2A-H2B dimer from chromatin. A human and *Drosophila* homolog to subunit SWI2 have been identified (Tamkun et al., 1992; Khavari et al., 1993), and might have a function similar to SWI-SNF in yeast.

Levels of histone acetylation/deacetylation also affect chromatin structure in the cells (Grunstein, 1997). Acetylation of the amino termini of histone neutralizes a positively charged lysine residue, and increases the accessibility of the nucleosome to regulatory proteins (Durrin et al., 1991; Lee et al., 1993). Some transcription factors have intrinsic histone acetyltransferase activity. Examples include yeast GCN5, p300/CBP (Ogryzko et al., 1996), and TAFII250 (Mizzen et al., 1996). These transcription factors, by virtue of their ability to acetylate histones, recruit other transcriptional activators. Deacetylation also regulates transcription, but in a negative sense. Histone deacetylase (HDAC1), by forming a complex with the transcription repressor Mad/Max and corepressor mSin3 (Hassig et al., 1997), is required to completely repress transcription (Pazin and Kadonaga, 1997).

Rod opsin expression, as studied primarily in rodents, is controlled by transcriptional activation. Opsin mRNA levels increase from postnatal day 2 (P2) to P12, and remain at adult levels thereafter. The transcription rate of opsin increases 30 fold during this same developmental period and is correlated with the appearance of differentiated photoreceptors (Treisman et al., 1988). Since the basal transcription machinery is similar for most genes, it has been important to identify the *cis*-elements in the rhodopsin promoter controlling photoreceptor-specific gene expression. Transgenic animal studies using serial overlapping opsin promoters linked to *lacZ* constructs delineated broad promoter regions essential for photoreceptor gene expression (Zack, 1993). The bovine rod opsin proximal promoter from –222 to +70 bp is sufficient for correct tissue and developmental expression in some mouse transgenic lines, but not all. A larger promoter (-2174 to +70 bp) gives higher level and more consistent rod-specific expression (Zack et al., 1991). Therefore *cis*-elements between –222 and –2174 bp appear to control a higher level, more uniform, and precise temporal gene expression.

The human red-green cone promoter has also been studied in transgenic mouse lines (Wang et al., 1992). There is a conserved locus control region (LCR) that appears essential for cone pigment expression. This 600-bp conserved region contains a core 37-bp domain of perfect identity among mammals, embedded in 200 bp of 70% identity among human, bovine and mouse. The LCR might selectively activate the tandemly arranged red and green pigment genes. Another 150-200 bp conserved region adjacent to the transcription start site contains proximal promoter functions. A 6.5 kd red-green cone promoter (-6.5 kb to +1) can direct an inferior to superior gradient of cone pigment expression for both red-green and blue cones in mice. This gradient of expression is similar to early fetal expression patterns and therefore might control early spatial expression across the retina.

Multiple transcription factors controlling very early retinal and photoreceptor development have been identified (Cepko et al., 1996; Freund et al., 1996). The best studied are homeodomain transcription factors, such as *Pax*6 (Freund et al., 1996), *Chx*10 (Liu et al., 1994), and *Rax* (Furukawa et al., 1997a). Several basic helix-loop-helix and zinc finger transcription factors are also involved in the development of the eye. Some of those factors may also function in opsin transcription. Nr1, one such *trans*-acting factor, is a basic motif-leucine zipper transcription factor, which can activate rhodopsin gene expression (Kumar et al., 1996). Recently, mutations in a photoreceptor-specific homeobox gene (*CRX*) have been found to lead to one form of cone-rod dystrophy (Freund et al., 1997b). *Crx* can bind and transactivate sequences which are upstream of several photoreceptor-specific genes, including rhodopsin (Furukawa et al., 1997). However, the actual targets of *Crx* remain to be elucidated.

The development of the mouse retina is dependent on both intrinsic cell properties and cell-cell interaction (Watanabe et al., 1990). Using a retroviral vector containing *lacZ* (Turner and Ceplo, 1987) or fluorescent dextran (Wetts and Fraser, 1988) as markers, cell lineage studies showed that the progenitor neuroepithelial cells are multipotent; a single progenitor cell can generate all types of retinal neurons as well as Müller glia cells. Retinal cell type determination is also dependent on environmental signals (Turner et al., 1990).

Tritiated-thymidine labeling has been used to determine the timing of cell genesis for the mouse photoreceptor. Cone photoreceptors are generated over a short period of time during fetal development and reach a peak on embryonic days 13-14 (E13-14), finishing on E16. Rod photoreceptor genesis begins on E13, but does not reach its peak until P0, and continues until P5 (Carter Dawson et al., 1979b). Interestingly, retinal cell genesis in the monkey is quite different (LaVail et al., 1991). Cones are generated earlier than rods, but rods complete genesis before birth. The generation of cones starts at 1 month of gestation, and reaches a peak at 1.5 months. The generation of rod cells starts at 2-months gestation and continues until birth. Whether transcriptional regulation by species-specific factors controls the different development patterns between rodent and primates remains to be determined.

Retinal Degeneration

The genetic basis of retinal degeneration has been extensively studied. This is primarily because many of the genes involved in vision signal transduction have been cloned and sequenced, and the majority have been found to be photoreceptor specific. Using forward genetic approaches, mutations in several of these genes were identified by screening and relating pedigree patterns to retinal degeneration (Dryja, 1997). Positional cloning and other reverse genetic approaches have also identified several other genes or chromosomal loci determinant for retinal degeneration. Currently, more than 40 genes or loci likely linked to retinal diseases have been mapped to specific chromosomal sites (Bird, 1995; Daiger et al., 1995).

Some of the disease gene loci have been identified. A mutation in a guanine nucleotide exchange factor homolog was related to X-linked Retinitis Pigmentosa (Meindl et al., 1996). The gene encoding a geranylgeranyl transferase was identified as responsible for choroideraemia (Seabra et al., 1993), and mutations in ornithine aminotransferase cause gyrate atrophy (Mitchell et al., 1989). Sorsby's fundus dystrophy was mapped to a tissue-specific inhibitor of metalloproteinase-3 (Weber et al., 1994) and the gene for Norrie disease was also defined (Meindl et al., 1992; Meitinger et al., 1993). Recently, mutations in a photoreceptor cell-specific ATP-binding cassette transporter gene (ABCR) were linked to autosomal recessive Stargardt's macular dystrophy (Allikmets et al., 1997b), which is an early onset form of macular degeneration. ABCR is identical to rim protein (RmP), a moderately abundant protein in the outer segments of photoreceptors. It is thought that ABCR is involved in the recycling of fatty acids for outer segments or in the uptake of vitamin E, essential for quenching photo-oxidative damage. This gene may also be responsible for age-related macular degeneration (Allikmets et al., 1997a), but this linkage remains controversial. A gene encoding a trabecular meshwork-induced glucocorticoid response protein (TIGR) has been linked to primary open angle glaucoma (Stone et al., 1997). TIGR might regulate intraocular pressure by controlling the drainage of fluid from the eye. Mutations in this gene therefore might increase the eye pressure and cause degeneration of the optical nerve.

Mutations in photoreceptor-specific transcription factors also cause retinal disease. A homeodomain transcription factor (*CRX*) has been linked to autosomal dominant cone-rod dystrophy (Freund et al., 1997). This mutation might act either through a dominant negative effect or through haploinsufficiency. Recently a non-photoreceptor-specific gene, *night blindness a* (*nba*) related to a dominant form retinal degeneration was cloned from *zebrafish* (Li et al., 1997). A human homolog to the *Drosophila* retinal degeneration C (*rdgC*) gene has also been cloned (Sherman et al., 1997). When their biochemical functions are elucidated, these new genes should provide more understanding of the diversity of retinal degeneration mechanisms.

One major degenerative retinal disease is retinitis pigmentosa (RP), a hereditary rod photoreceptor cell degeneration. RP is first noted clinically by the development of night blindness, or nyctalopia, associated with the loss of rod photoreceptors. Continued degeneration of peripheral rods leads to loss of peripheral vision. Eventually the vessels supplying blood to the retina attenuate and cone cells die off late in RP. As rods die, the RPE invades the retina, causing pigment deposits in the retina thus giving RP its name. Eventually all the vision is lost in some patients. At the genetic level, RP constitutes a group of heterogeneous progressive rod photoreceptor degenerations leading to blindness.

It affects 1 in 3,000 individuals in the U.S. About 25% of RP is autosomal dominant, 15% is autosomal recessive, 10% is X-linked, and 20% are syndromic forms. The remaining 30% are simplex cases of unknown etiology (Daiger et al., 1995). Thus far, mutations for RP have been found in rhodopsin, transducin α subunit, rod cGMP-gated cation channel α subunit, peripherin/*rds* (Farrar et al., 1991), α, β subunits of cGMP phosphodiesterase (Huang et al., 1995; McLaughlin et al., 1995), rhodopsin kinase and an opsin disc membrane gene ROM1 (Dryja, 1997). Some mutations in these genes are also related to other retinal diseases (Cideciyan et al., 1998). Although defects in some visual transduction genes have not been assigned yet to retinal disease, transgenic knock-out mice (such as those for arrestin or γ subunit of PDE) show a phenotype similar to classic RP (Tsang et al., 1996; Xu et al., 1997). Therefore, more genes are likely to be identified from the continuous screening effort underway. Mutations in many of the above genes appear to cause photoreceptor death by apoptosis (Portera et al., 1994; Wong, 1994). Currently, little information is available on the biochemical reasons for these mutant proteins to lead to rod apoptosis. Mutations might produce dominant negative proteins, or accumulate at abnormal sites in the retina (Portera et al., 1994; Roof et al., 1994; Sung et al., 1994; Colley et al., 1995). There is presently no effective therapy available for RP.

Several animal models with mutations identical or similar to human RP defects simulate the clinical course of human retinal disease. The *rds* mouse contains mutations in peripherin, which appears to be a structural protein within the rims of the outer segment discs. The *rds* mouse develops an autosomal dominant RP-like disease (Connell et al., 1991; Travis et al., 1992). A nonsense mutation in guanylate cyclase of the *rd* chicken, causes a degeneration similar to Leber's congenital amaurosis (Semple Rowland et al., 1998). The RCS (Royal College of Surgeons) rat mimics human retinal degeneration owing to the inability of the RPE to phagocytize PR outer segments. The mutant gene is expressed specifically in RPE cells but is yet to be identified. Transgenic mouse lines with mutations in or knock-outs of rhodopsin, arrestin, γ-PDE and rhodopsin kinase have been constructed (Olsson et al., 1992; Chen et al., 1995; Humphries et al., 1997; Xu et al., 1997), and show a degeneration pattern similar to the corresponding human gene mutations.

Many autosomal recessive forms of RP result from mutations in the β subunit of cGMP phosphodiesterase (McLaughlin et al., 1993). A mutation in this gene is also responsible for autosomal dominant congenital stationary night blindness (CSNB) (Gal et al., 1994). The *rd* mouse model has been very useful for understanding this form of RP. A nonsense mutation in codon 347 and/or a retroviral insertion in intron 1 of β subunit of cGMP phosphodiesterase cause this degeneration (Pittler and Baehr, 1991; Bowes et al., 1993). The Irish setter dog also has a nonsense mutation in β-PDE resulting in rod-cone dysphasia (*rcdl*) (Suber et al., 1993).

Having identified the genetic basis for a number of retinal degenerations, it is possible to consider gene transfer methods to rescue the retinal degeneration. Therapeutic genes can be, in theory, delivered to retinal cells by viral vectors or by physical methods. For recessive mutations, a wild type copy gene could be provided *in trans* to provide the missing gene function. Antisense nucleotides or ribozymes could be used to selectively degrade a dominant negative mutant at the transcript level. Cytokines, neurotrophins or growth factors might also be used since they have shown therapeutic effect in some neuronal diseases, such as Huntington's Disease (Emerich et al., 1997) and motor neuron disease (Haase et al., 1997). In rodents these classes of agents can also protect the retinas from light damage (Faktorovich et al., 1990; LaVail et al., 1992). Continually expressing any of these factors in the appropriate cell type might protect the function of photoreceptors from genetic retinal degeneration.

One major problem of gene therapy relates to obtaining high level expression of a therapeutic gene in the appropriate cell type. A *lacZ* reporter gene delivered by Adenovirus, AAV or herpes simplex vector is expressed in reasonable levels in mouse retina using a CMV promoter (Bennett et al., 1994; Li et al., 1994; Ali et al., 1996; Bennett et al., 1996). However, the CMV promoter is capable of being expressed in essentially all retinal cell types. The first use of a rod specific promoter involved rAAV containing green fluorescent protein driven by 470 bp mouse opsin promoter (Flannery et al., 1997) . This construct gave high level, photoreceptor-specific expression. Soon afterward, a lentiviral vector containing GFP with 2.1 Kb mouse opsin promoter yielded a similar result (Miyoshi et al., 1997).

A key step in developing a gene therapy for retinal degeneration is demonstration of proof-of-principle. A rod β-subunit of phosphodiesterase gene driven by a CMV promoter partially delayed the retinal degeneration in *rd* mouse from 10 days to 6 weeks when delivered in a recombinant Adenovirus (Bennett et al., 1996). Since most of the photoreceptors in those genetic diseases are lost by apoptosis, it is possible to rescue the photoreceptors by knocking out one or more of the genes involved in this process. Photoreceptors in the c-*fos* knock out mouse were resistant to light-induced photoreceptors loss (Hafezi et al., 1997). Finally, a transgenic mouse line overexpressing

Bcl-2 could also decrease the damaging effect in light exposure (Chen et al., 1996), although this observation remains controversial.

In summary, there are multiple target genes causing retinal degeneration. Individual and multiple strategies could be employed for dealing with each genetic disease. The advantages of a gene therapy approach for retinal diseases include the depth of genetic analysis and the number of animal models currently available.

Ribozymes for Gene Therapy

Ribozymes are catalytic RNAs that can break and reform covalent bonds within themselves or within another RNA. The original ribozyme was a 413-nucleotide Group I intron of *Tetrahymena themophila* rRNA precursor (Cech, 1990). RNase P is another 400-nt RNA that can cleave its precursor tRNA substrate. The self-splicing in Group I and Group II introns creates cleavage products containing a 3' hydroxyl group, and a 5'-phosphate group. Although, these classes of catalytic RNA can be used for gene therapy purposes, their application is limited by difficulties of design for targeting different substrates.

Another group of catalytic RNAs are small ribonucleotides, originally identified in a number of small plant pathogenic RNAs. These RNAs can self-cleave and produce 5' hydroxyl, and 2', 3, cyclic phosphate products. Two of these catalytic RNAs have been named according to their secondary structures. Four motifs have been discovered: hammerheads, hairpins, delta motifs, and a motif from *Neurospora*. All members are small RNAs that can be dissected into the enzymatic molecule (ribozyme) and the substrate site which can exist on a separate molecule (for *trans* cleavage). The requirement for substrate sequences is quite flexible, and this has been very useful for gene therapy purposes.

The hammerhead ribozyme motif is derived from the positive strand of satellite RNA of tobacco ringspot virus. It is also found in avocado sunblotch viroid and several satellite RNAs of RNA plant viruses (Long and Uhlenbeck, 1993). These RNAs are replicated by an RNA dependent RNA polymerase using a rolling circle mechanism *in vivo*. This replication produces concatameric progeny RNA from which intramolecular site-specific cleavage will produce the monomers of the viral genome. The autocatalytic reaction leading to this processing can occur *in vitro* in the presence of magnesium and other divalent cations. The cleavage can also occur *in trans* by separating the RNA into substrate and enzyme domains. In this bimolecular reaction the ribozyme (enzymatic domain) can act in a multiple turnover manner (Uhlenbeck, 1987). A putative conserved hammerhead motif was proposed as the active site (Forster and Symons, 1987), and extensive mutagenesis has confirmed these sequence requirements (Ruffner et al., 1990). A 50 nucleotide long RNA containing the hammerhead structure is sufficient for the cleavage with only 11 nucleotides in the catalytic core absolutely unchangeable (Figure 1-3). These nucleotides are directly involved in either the cleavage reaction or in formation of the required tertiary structures.

The hairpin ribozyme is naturally found in the minus strand of satellite RNA of tobacco ringspot virus. Conserved aspects of this structure were identified by mutagenesis (Anderson et al., 1994) (Figure 1-3). Interestingly, both cleavage and ligation are possible, thus the reaction is formally reversible (Hegg and Fedor, 1995).

A. Hammmerhead ribozyme conserved sequence

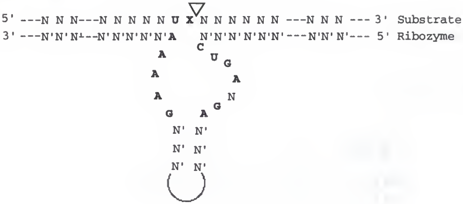
5' ---N N N---N N N N N U X N N N N N N ---N N N --- 3' Substrate
3' ---N'N'N'--N'N'N'N'N'A N'N'N'N'N'N'---N'N'N'--- 5' Ribozyme
C
A U G
A A
A N
G A G
N' N'
N' N'
N' N'

B. Hairpin ribozyme conserved sequence

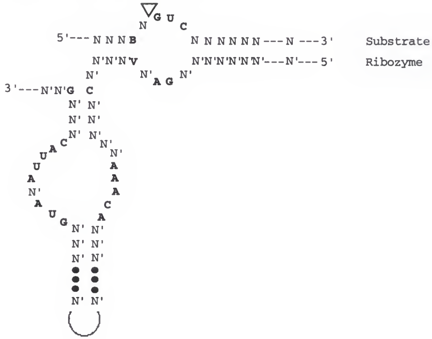

Figure 1-3: Consensus sequence for the hammerhead and hairpin ribozymes (adapted from Ruffer et al, 1990 and Anderson et al, 1992 with minor modification). N: any nucleotide in the substrate; N': any nucleotide in the ribozyme; B: G, U or C; X: U, A or C; V: C, A, G. The open triangle indicates the substrate cleavage site.

Hairpin catalysis can proceed without divalent ions, although at a much lower rate (Chowrira et al., 1993).

The delta ribozyme motif is found in the hepatitis delta virus (Kuo et al., 1988; Sharmeen et al., 1988) and consists of about 100 nucleotides folded into an "axehead" secondary structure. It is believed that two helices form a pseudoknot tertiary structure, while two helical domains form stems as in the hairpin ribozyme (Been, 1994). The delta motif is also able to self-cleave a rolling circle replication intermediate. Even though the corresponding bimolecular reaction can be carried out, the stringent sequence requirement for delta ribozymes limits their application for gene therapy.

The last well-studied ribozyme motif comes from two mitochondrial RNAs in *Neurospora*. This ribozyme structure is less well characterized and contains minimal sequence homology with other catalytic RNAs (Guo and Collins 1995). The mechanism of these mitochondrial ribozymes is not clear yet.

It is entirely possible more ribozyme sequences exist in other transcripts because of their small size and modest sequence requirements. Database searches and *in vitro* selection has identified a number of such additional potentially self-cleaving RNA sequences (Jayasena and Gold, 1997).

Hammerhead and hairpin ribozymes are the best characterized. Their unimolecular and bimolecular kinetics and optimal cleavage conditions have been studied extensively *in vitro*. Divalent cations are necessary for the transester-cleavage reaction. Magnesium ion attacks the 5' phosphate group and initiates the cleavage reaction, and it also acts to aid H_2O in the catalytic reaction. Divalent cations also promote the functional folding of RNA and this serves to further increase the rate of cleavage. The catalytic core within the RNA structure accepts a proton from the 2'-hydroxyl and a nearby acidic function provides a proton to create the 5' hydroxyl at the cleavage site. Km values (30-700 nM) of hammerhead ribozymes are in the range of conventional protein enzymes, but K_{cat} (0.03-2.1) values are much lower. It is likely that the cleavage rates of ribozyme might be much different *in vivo* due to micro-intracellular environment and the possible effects of cellular RNA binding proteins.

The substrate sequence requirement for hammerheads is NUX↓N (N = any nucleotides, X = A, U and C) (Ruffner et al., 1990). This is less stringent than that of hairpin (NBN↓GUC, N = any nucleotides; B = G, U and C) (Anderson et al., 1994). The absence of sequence requirements for helices I and III in the hammerhead and helices I and II in the hairpin provides the flexibility to target cellular mRNA sequences. The bimolecular reaction *in vivo* would, in theory, destroy the target mRNA and block gene expression. Therefore, it has been thought that ribozymes could be used for controlling pathogen expression or suppressing an undesired cellular trait. The catalytic property of ribozymes gives them an advantage over antisense therapy because of the inability of antisense molecules to turn over RNA substrates.

The idea of ribozyme therapy was initially tested in a model system by targeting chloramphenicol acetyl transferase mRNA *in vitro* (Haseloff and Gerlach, 1988; Couture and Stinchcomb), and was rapidly adapted for different target genes. *In vivo* applications have been tested in a number of cases. Ribozymes were designed to target different regions of HIV mRNA, including the LTR, *gag*, *tat*, *nef* and *vif* genes (Heidenreich and Eckstein, 1992; Sarver and Rossi, 1993). In general, these ribozymes decrease virus mRNA expression, but none eliminate all virus production (Yu et al., 1993a). Ribozymes have also been used in cancer therapy by targeting oncogene mRNAs (Scanlon et al., 1991; Poeschla and Wong, 1994). Alternatively, ribozymes have been employed to eliminate specific gene expression and simulate a mutant phenotype. A ribozyme specific to the mRNA of wild type *fushi tarazu* (*ftz*) gene in *Drosophila* can generate a trait similar to that of a *ftz* mutation (Zhao and Pick, 1993). Recently, a ribozyme specific to zebrafish *no tail* gene also produced a similar mutant phenotype in *zebrafish* (Xie et al., 1997).

Even though the results of ribozyme applications are promising in most cases, there are still many problems related to ribozyme gene therapy. To suppress gene expression *in vivo*, a high level of the ribozyme might be needed inside the cell. Intracellular mRNAs are bound with several classes of RNA-binding proteins, and the effect of these proteins on the efficiency of ribozyme cleavage is unknown. The intracellular ionic environment is also not easy to duplicate *in vitro*. In some cases, RNA binding proteins such as hnRNP A1, HIV-NCp7, *E. coli* S12 ribosomal protein (Coetzee et al., 1994) and glyceraldehyde-3-phosphate dehydrogenase can enhance the hammerhead activity and Group I intron splicing (Herschlag, 1995). Those proteins promote nucleic acid strand exchange, and might act as cofactors to stabilize the active ribozyme conformation. Even though the host immune response against nucleotides is weak, it has been found that some sequences are particularly immunogenic, particular CG repeats. It is necessary to attempt to predict and avoid these immunogenic sequences. Ribozyme efficiency will increase if it is co-localized with its target mRNA substrate (Sullenger and Cech, 1993) and inclusion of 3' or 5' untranslated regions to ribozymes appears to improve *in vivo* efficiency.

The length and base composition of the annealing helices have a substantial effect on substrate selection and catalytic efficiency. A long annealing arm will increase the suppression efficiency, but the specificity and turnover rate of the ribozyme will decrease dramatically. A low specificity ribozyme might not distinguish mutant mRNAs with only a single point mutation difference from its wild type counterpart, and thus be of limited therapeutic use. Therefore, it is critical to screen mRNA cleavage *in vitro* to obtain the most active and selective ribozyme. An A/U rich sequence can be selected to reach the minimal free energy required for a stable annealing arm (about –16 Kcal/mol) so that the possible longest target sequence can be chosen. Additionally, ribozymes might be able to tolerate G-U base pairs, and, therefore, it may better to avoid G-U base pairs (Bertrand et al., 1994). Computer-assisted secondary structure modeling as well as *in vitro* and *in vivo* selection have been employed for determining the most accessible site on an mRNA, and this approach has shown promising results for human growth factor (Lieber and Strauss, 1995; Fujita et al., 1997). Ways to increase catalytic efficiency without losing target specificity remain a significant challenge. Even though choosing the optimal site in the target mRNA might increase ribozyme efficiency, this may not be useful for many specific mutations that are remote to the optimal ribozyme cleavage site.

The *in vivo* stability of ribozymes inside the cell is also a problem. One solution is to modify a ribosyl side chain with different reagents, such as 2'- fluorecytidine substitution (Heidenreich and Eckstein, 1992). This serves to increase stability but appears to lower the catalytic rate. Additionally, modified nucleic acids might have unpredicted behavior inside cells similar to that seen with phosphorothioates for antisense therapy (Roush, 1997). Producing ribozymes inside the cell at very high levels using a strong promoter is another option. The RNA pol III promoter can be used if the expression of ribozyme does not need to be tissue specific. Embedding the ribozyme in a stable RNA also increases its stability. For example, ribozymes inserted into a region devoid of stable tertiary structure in U1, U5, U6 RNA or tRNA extends the *in vivo* half-life (Bertrand et al., 1994; Michienzi et al., 1996).

As noted above, many mutations related to retinal degeneration have been identified, and several animal models are available that simulate the disease course. Mutation specific ribozymes can in theory be delivered to photoreceptors of the animal models of dominant diseases to determine whether ribozymes in these systems can delay or diminish retinal degeneration. This is an especially useful approach for autosomal dominant diseases such as AdRP. The hypothesis to be tested here is that a ribozyme-related decrease in a dominant deleterious mRNA will allow transcript from the wild type allele to provide normal PR function and hence rescue the retinal degeneration.

Adeno-associated Virus as a Gene Delivery Vector

The concept of gene therapy is simple in principle: to alleviate or cure diseases by introducing new genetic materials into cells. Started in the early 1980's, gene therapy developed in parallel with our understanding of gene expression and virology. There have been several successes in different disease models, and currently more than 200 clinical trials are underway (Crystal, 1995; Kay et al., 1997).

Even though the idea sounds simple, many problems need to be addressed to obtain a therapeutic effect *in vivo* using gene therapy. Major questions include how to deliver the gene to target cells, how to obtain sufficient and controllable gene expression and how to overcome the host immune response. Each is key for a successful gene therapy scheme.

There are two basic ways to deliver genes to target cells, either with or without packaging into recombinant viral vectors. I will first discuss methods involving non-viral techniques. Genetic material can be directly injected into the host, either as pure nucleic acid or a mixture with packaging agents such as polylysine or cationic lipids to aid in crossing the cell membrane. It is relatively easy to prepare large amounts of DNA/lipid complexes, and there is no limit to the size of transgene. The host immune reaction often appears to be low due to lack of carrier protein, and little potential for chromosomal insertional mutation exists due to the extremely low integration rate. Some successes have been achieved by those methods, especially in tissue culture systems (Wu et al., 1991; Nabel et al., 1993; Liu et al., 1997). However, the general problem with nonviral delivery techniques has been their low efficiency of gene expression, partly due to low efficiency of effective gene delivery. Most artificial packaging reagents rely on receptor-mediated uptake of a DNA-polypeptide ligand, and genetic materials are transferred to endocytic vesicles. These vesicles frequently fuse with lysosomes and lead to degradation of the nucleic acids. Another problem is that a majority of the transgene frequently stays in the cytoplasm where expression is not possible. Finally, gene expression usually lasts for only a short period of time. Additionally, most artificial packaging reagents are cytotoxic and will need careful modification before their application to humans. Currently, other reagents are being tested to increase nucleic acid delivery efficiency (Liu et al., 1996; Oudrhiri et al., 1997). One possibility is cholesterol based lipids that can induce disruption of the endosome after internalization, thus allowing packaged nucleic acids to escape the lysosomal-degradaion pathway. A conjugated fusagenetic approach is being evaluated that involves adding hemagglutinin and adenoviral capsid proteins to help transgenes escape from intracellular endosomes (Curiel et al., 1991; Sarver and Rossi, 1993). Another new reagent, chylomicron remnant particles consisting of lipoprotein has also been used to transfer *lacZ* gene to mouse liver by systemic injection (Hara et al., 1997). Additionally, linking a nuclear localization signal to the transgene will increase transgene concentration in the nucleus.

Direct injection of naked DNA into muscle cells has shown progress in achieving transduction in recent years (Wolff et al., 1990; Taubes, 1997). Naked DNA is apparently recognized by an unknown vesicular system in muscle cells, and is expressed in the cell nucleus. Expression levels varied for different transgenes, and was found to be dependent on the specific promoter used and on the host immune response (Acsadi et al., 1991). Even though the net gene expression level is relatively low, this approach might still be useful for vaccine purposes. A naked HIV DNA vaccine encoding *env*, *rev* and *gag/pol* can provide protection in chimpanzees (Boyer et al., 1997). Even though the simplicity of this method makes it very attractive, a number of problems need to be addressed before applying it to patients. One is the inconsistency of gene expression. Variation among inoculations can range from 20% to 90%. So far details of the gene transfer pathway are unknown, and this pathway might be unique to muscle cells and therefore of limited general value. Since gene delivery and expression may be quite different between mouse and human muscle cells, it remains untested whether the same delivery pathway exists in human muscle cells.

Viral vectors are the other major alternative for transgene delivery *in vivo*. This approach takes advantage of specific mechanisms virus have developed to deliver encapsidated target genes through cell membrane to the nucleus. Most of recombinant viruses are modified to alleviate or eliminate all or most pathogenic effects. Retroviral, lentiviral, herpes simplex viral, adenoviral vector and adeno-associated viral vectors are currently the most studied. Modifications to these existing vectors are in development, as are efforts to bring on line new vectors based on different viruses, such as Epstein-Barr virus, vaccinia virus, simian virus 40, papilloma, hepatitis, Sindbis virus, and Semliki Forest virus. Each vector has its own unique features, and it is critical to select the most suitable one for each intended use.

Retroviruses are relatively small RNA viruses. The RNA genome of retrovirus must be converted into complimentary DNA and integrated into the host genome for gene expression. A packaging sequence (ψ) in the retrovirus genome is necessary and sufficient for recombinant virus assembly. Transgenes with this packaging sequence can be packaged into recombinant virus by providing *gag, env,* and *pol* proteins *in trans* from a separate plasmid DNA lacking the ψ sequence. Transgene expression can be controlled by the retrovirus long terminal repeat (LTR), which contains a strong enhancer-promoter function or by an added promoter. However, the LTR frequently dominates the added tissue-specific promoter. The immune response is relatively low to these vectors. However, their inability to transduce nondividing cells and the low virus titers obtainable are their major disadvantages. An important safety consideration is the random integration feature of retroviral vectors. This leads to a potential risk of inactivating tumor suppressor genes or activating oncogenes *in vivo*.

The major use of retroviral vectors today involves cells treated *ex vivo* and transplanted back into the host. Successes have been seen in Factor IX expression in mouse using this approach (Dai et al., 1992). Fibroblasts transformed with β-glucuronidase (GUSB) can be transplanted into mucopolysaccharidosis type VII (MPS VII) mouse brain, allowing survival over 5 months without inflammatory reaction (Taylor and Wolfe, 1997). However, GUSB expression lasted for just 4 weeks. The majority of retroviral transgene expression is shut off after a short period of time due to unknown mechanisms (Palmer et al., 1991). One possibility is the deletion or partial deletion of the transgene during chromosomal integration.

The lentivirus, Human Immunodeficiency Virus (HIV), is also a member of retrovirus family, and has advantages over other retroviral vectors. Besides *gag*, *env*, *pol* genes, lentiviruses have several accessory genes not found in classical retroviruses, including *tat, rev, vpr, vpu, nef* and *vif.* Although these proteins have important functions in viral expression (Poznansky et al., 1991; Buchschacher and Panganiban, 1992), many or all of them can be deleted without affecting virus packaging and infection. There remain many candidate *cis* elements in the lentiviral genome, making it difficult to completely eliminate sequences critical for the pathogenesis without affecting the production of effective recombinant viruses.

Since lentiviral vectors infect both dividing and non-dividing cells, their range of uses is broader *in vivo* than conventional retroviral vectors (Naldini, et al., 1996). The CD4+ specific *env* gene can be replaced with other retroviral *env* genes or with VSV-G glycoprotein to increase the infection spectrum. Transgene expression can persist for long periods of time, and the host immune response is limited. However random vector integration remains a safety problem for lentiviral vectors.

Adenoviral vectors can also infect both dividing and non-diving cells. This vector can carry about 30 kb of transgene DNA. However, replication-deficient adenoviruses remain in an episomal form in the host nucleus and this limits the duration of transgene expression. In initial adenovirus vectors, transgene and promoter sequences replaced the viral E1 gene that is essential for viral replication. High-level *lacZ* expression in hetapocytes, muscle cells and neurons was achieved by recombinant adenovirus (Jaffe et al., 1992; Quantin et al., 1992; Le et al., 1993). A cystic fibrosis transmembrane conductance regulator cDNA and the human α-1 antitrypsin cDNA have been delivered to the lung epithelium of rats by first generation adenoviral vectors, but expression lasted for only about 2 weeks (Rosenfeld et al., 1992a). This short duration of expression appears to be due to strong host immune responses to adenoviral capsid proteins. Human α-1 antitrysin can also be transferred to the CNS and secreted into cerebral spinal fluid for 1 week (Bajocchi et al., 1993). A *lacZ* reporter delivered by an second generation adenoviral vector containing larger viral gene deletions (E1A, E1B, and E3) could express transgenes in the CNS up to 8 weeks (Davidson et al., 1993). A new form of adenoviral vector (the gutless vector) containing no viral genes has been developed to extend gene expression by avoiding at least part of the host immune response (Mitani et al., 1995; Lieber et al., 1996; Chen et al., 1997). The dystrophin gene delivered by a gutless adenoviral vector expressed up to 84 days in mice (Parks et al., 1996). Recently, another type of adenoviral vector (Adenovirus dodecahedron) has been constructed and has exhibited efficient gene transfer and expression in cultured Hela cells (Fender et al., 1997). This vector was made of adenoviral pentones (a complex of pentone pentameric base and trimeric fiber) and appears to elicit a lower host immune response because it contains just two adenoviral proteins instead of the normal 11 proteins in the adenovirus virion.

Herpes virus vectors are neurotropic, allowing them to efficiently infect neuronal cells (Breakefield and Deluca, 1991; Kaplitt et al., 1994a). The large herpesvirus genome (~200 kb) allows more transgenes to be packaged. Recombinant herpesviruses can also infect postmitotic cells. There are two categories of vectors available: recombinant HSV and defective HSV. Transgenes can be cloned into a plasmid flanked with HSV-1 sequences. Recombinant HSV vectors are then produced by homologous recombination. Some HSV genes, such as IE3, can be deleted to minimize the toxicity and pure recombinant virus stocks can produce useful high titers. Defective HSV vectors have only an HSV DNA replication origin and DNA packaging signal (Spaete and Frenkel, 1982), and require a helper HSV to be amplified and packaged. However it is difficult to completely purify defective viruses from the helper virus. For neither defective nor recombinant vector can all the viral genes be eliminated. The cytotoxicity of the remaining viral proteins is a severe disadvantage for current HSV vectors. There persists a strong host immune response to vector HSV proteins, and the role of many viral proteins in eliciting this response is still unclear.

Adeno-associated virus (AAV) is a very small single stranded DNA virus. AAV can infect a broad range of human cell types, but it needs some gene products from a co-infecting helper virus (Adenovirus, Herpes simplex virus or Vaccinia virus) to replicate. Without helper viruses, AAV establishes a latent phase and integrates at a single site in human chromosome 19 in the presence of viral *rep* protein (Kotin et al., 1990). One possible safety concern is that this chromosomal region might be involved in chromosomal rearrangements in chronic B-cell leukemia (Mulligan, 1993). It appears that rAAV might have more or less random integration sites without the help of viral *rep* protein. The *rep* and *cap* genes located between the inverted terminal repeats (ITRs) are the only viral genes and both can be deleted and replaced with transgenes and promoters (McLaughlin et al., 1988). The ITRs are necessary for viral replication, integration and packaging (Hermonat and Muzyczka, 1984). Since ITRs do not have a strong promoter function, exogenous promoters can be linked to the transgene to obtain cell type specific expression. Although up to 80% of the normal human population may be latently infected with AAV, no disease has been linked to this common virus. This non-pathogenic feature of AAV is a very promising property for safety in human gene therapy. The host immune response to recombinant AAV vectors is weak, and a transgene (Factor IX) can express in immunocompetent mice for over six months (Herzog et al., 1997; Snyder et al., 1997). *LacZ* gene expression also persists in the muscle cells for over 240 days by rAAV delivery (Fisher et al., 1997).

Recombinant AAV can infect both dividing and nondividing cells. The transduction efficiency in nondividing cells appears to vary with the cell type. In some cases, such as human peripheral blood cells, the transduction efficiency is 200 fold less in nondividing cells than that in dividing cells. However, for bone marrow progenitor cells, the transduction efficiency can reach 80%. AAV vector transduction might require DNA synthesis since DNA damaging agents can increase the transduction of nondividing cells 750 fold (Alexander et al., 1994).

The size of AAV is about 4.7 kb, and rAAV can package about 4.5 kb of foreign DNA sequence. This size limitation prohibits consideration of large cDNA transgenes such as dystrophin (12 kb). The packaging process is also labor-intensive but improvements in efficiency are making this procedure less of a problem. The rAAV particle titer can reach 10^{13}/ml or greater, even though just 1 in 100 - 1000 particles are typically infectious by standard assays. The fate of rAAV in the host cells is not entirely clear yet and may depend on the specific host cell. Since the *rep* protein is not present, rAAV is likely to remain as an episome early after infection or randomly integrate into host genome after longer residency in a cell. It has been reported that rAAV containing a *lacZ* reporter gene can form head to tail concatamers (Fisher et al., 1997), a replicative characteristic of latent AAV replication.

There are a growing number of reports of transgene delivery and expression using rAAV. Recombinant AAV can effectively transfer genes to postmitotic cells in the CNS with stable gene expression (Kaplitt et al., 1994b). Recombinant AAV can also transduce skeletal muscle cells (Fisher et al., 1997), lung epithelial cells (Flotte et al., 1993), hepatocytes (Snyder et al., 1997) and hematopoietic cells (Miller, 1992). It is reported that gene expression with rAAV is initially low due to the rate limiting step of second strand synthesis, a process that can be enhanced by the presence of adenovirus (Ferrari et al., 1996; Fisher et al., 1996). But results in muscle cells show that rAAV alone can reach high levels of gene transfer (about 50% cells positive) after several weeks. A recombinant AAV containing Factor IX gene has been shown to produce therapeutic amount of proteins for over 9 months without toxicity (Herzog et al., 1997; Snyder et al., 1997). Recently, GFP expression was found to persist for 21 months in the photoreceptors of rat (Yan et al., unpublished).

Focus of Dissertation

Since Retinitis Pigmentosa affects 1 in 3,000 people in the U.S and no effective therapy currently exists, it is worth while to develop novel treatments for curing or alleviating this disease. This project aims to develop a rAAV-based gene therapy approach for retinal degeneration by taking advantage of recombinant adeno-associated virus vector and the high specificity of ribozymes. There are several critical criteria for the successes of gene therapy. There needs to be an animal model to mimic the disease; the mutation in the gene causing the disease should be identified; the therapeutic gene needs to be delivered by an effective way. The *rd* mouse is a well-characterized retinal degeneration model, and the nonsense mutation and/or the retroviral insertion in intron 1 in rod cGMP β-PDE has been identified as the cause of retinal degeneration. Recombinant adeno-associated viruses have been found to be an effective method for gene delivery. Therefore, the *rd* mouse appears to be an ideal model for developing gene therapy for retinal degeneration.

To obtain a high level and photoreceptor-specific therapeutic gene expression, it is critical to identify a suitable promoter. The rod opsin promoter can direct a high level of opsin expression in rod photoreceptors, and therefore appears to be a good promoter for therapeutic gene expression in photoreceptors. It is necessary to understand the regulation of opsin expression so that this promoter can be effectively used to control therapeutic gene expression. I first developed an *in vitro* transcription system to dissect the *cis*-elements in the rod opsin promoter. This helped us select a proper rod opsin promoter for high level and photoreceptor-specific therapeutic gene expression.

I then characterized β-PDE mRNA levels in the *rd* mouse. Since expression of mutant β-PDE contributes to retinal degeneration in the *rd* mouse, understanding PDE expression and mRNA degradation mechanisms are necessary for eventually using ribozymes to treat retinal degeneration in the *rd* mouse model.

Ribozymes specific for wild type or mutant β-PDE mRNA were designed and tested for the efficiency and substrate specificity *in vitro*. These ribozymes were packaged into rAAV virus and delivered into *rd*/+ mouse retinas. Expression of these ribozymes in the photoreceptors were determined. The therapeutic effects of those ribozymes will be tested in transgenic *rd*/*rd*/+ mice or heterozygous *rd*/+ mice.

To further understand the function of ribozymes, I tested whether hnRNP A1 protein can improve their activity. Several RNA binding proteins have been found to accelerate the turnover rate of ribozymes, and this might be critical for obtaining maximal ribozyme activity inside cells. Since an hnRNP A1 binding site has been identified by *in vitro* selection, it is of interest to determine whether we can improve ribozyme activity by linking an A1 binding site to the ribozyme. This might aid in developing more efficient ribozymes against different deleterious mRNAs.

CHAPTER 2
IN VITRO ANALYSIS OF THE BOVINE RHODOPSIN PROMOTER

Introduction

Rhodopsin, an essential protein for visual signal transduction, is a rod photoreceptor-specific protein. At least 80 mutations in rhodopsin are known or suspected to cause Retinitis Pigmentosa (RP). To develop effective gene therapy for RP, it is necessary to understand regulation of rhodopsin transcription so that effective, rod-specific promoters can be identified and included in the appropriate vector.

Rhodopsin expresses in a cell-type specific and developmentally regulated pattern. Transcriptional activation during fetal development is the major step in opsin regulation. Transcriptional levels and rates of the rod opsin gene expression increase coordinately along with the appearance of the earliest differentiated rod photoreceptor (Treisman et al., 1988; Timmers et al., 1993). To understand this transcriptional regulation, it is important to define the *cis* DNA elements and *trans*-acting proteins defining this promoter. Early transgenic animal studies have shown that a proximal promoter (-222 to +70) is sufficient for photoreceptor-specific expression (Zack et al., 1991). A 2.1 kb opsin upstream region results in a higher level and topographically correct gene expression. Mouse rod opsin 4.4 kb and 0.5 kb upstream fragments can also direct photoreceptor-specific expression in transgenic mice (Lem et al., 1991). Since the 4.4 kb mouse rhodopsin promoter has activity in both cone and rod cells, *cis*-elements controlling rod specific expression might not be contained in this 4.4 kb promoter (Woodford et al., 1994). In another transgenic animal study, an 11 kb mouse genomic rod opsin fragment containing more than 5 kb of upstream sequence was shown to support rod-specific expression. Therefore, the *cis*-elements for rod specific expression might be located in rhodopsin introns, in the 3' untranslated region or up to 5 kb from the transcriptional start site (Chen et al., 1995).

A highly conserved 100 bp region from –2044 to –1943 bp in the bovine opsin promoter was identified as an enhancer element (RER, rhodopsin enhancer region) (Nie et al., 1996). This element in the cow is related to similarly positioned human, and mouse domains. It also has similarity to the cone locus control region (LCR). Using DNase I protection and gel mobility shift techniques, three regions in rat rod opsin promoter were found to contain retinal-specific protein binding ability. Protein binding to Ret 1 (-138 to –132 bp) is correlated with developmentally regulated opsin gene expression (Morabito et al., 1991). Ret 2 (-255 to –222bp) and Ret 3 (-1460 to –1432 bp) appear to bind with the same retina-specific factor but their developmental binding pattern is less clear (Yu et al., 1993b). Another region, Ret 4 (-48 to –44 bp), also binds retinal-specific factor(s), and activates opsin transcription (Chen and Zack, 1996) like Ret 1.

Several other DNA domains in a 2.0 kb upstream bovine opsin region were also identified by DNA footprints during fetal development (DesJardin and Hauswirth, 1996). Since such footprint only indicates where protein-DNA interactions occur, it is necessary to use functional analysis to determine the true role of the proteins protecting regions in transcription regulation. Some of those elements appear related to already-known elements, such as RER1 and Ret 3. By comparing protection patterns with nuclear extracts prepared from different fetal stage retinas, some of those elements were assigned negative regulatory roles during photoreceptor development (DesJardin and Hauswirth, 1996). From transgenic mouse experiments (Lem et al., 1991; Zack et al., 1991), the upstream region beyond the proximal promoter (about 200 bp) might be important for high level, temporally and spatially correct expression. Several footprinting sequences in this promoter region are candidates for this function.

Trans-acting proteins critical for early fetal photoreceptor cell determination and development have been identified (Cepko et al., 1996). Some are photoreceptor-specific, and might regulate photoreceptor-specific gene expression later in development. Others are non-photoreceptor-specific factors that appear to control photoreceptor cell determination from pluripotent embryonic precursors. Most of these proteins are transcription factors, and control gene expression at the transcriptional level. It has been shown that these retina-specific transcription factors are essential for eye development (Freund et al., 1996). Nr 1 is a basic-motif leucine zipper, and can positively regulate opsin expression (Rehemtulla et al., 1996). *Crx*, a newly identified homeobox gene, interacts with and transactivates the rhodopsin proximal promoter (Furukawa et al., 1997b). Mutations in the transcription factors can dramatically affect early gene transcription and result in retinal degeneration (Freund et al., 1997).

To dissect the rhodopsin promoter more completely , I developed an *in vitro* transcription system to determine the function of those elements that can be footprinted *in vitro*. The aim was to further define promoter regions having a suspected role in transcriptional regulation. Serial constructs of the bovine opsin promoter were made according the footprinting data of DesJardin and Hauswirth (1996). By comparing transcription levels from this serial set of promoter constructs, it was anticipated that the transcription function of some footprinted elements might be more clearly understood.

The bovine retina was used to prepare nuclear extracts for *in vitro* transcription. Bovine retina was chosen based on several considerations: it is easy to obtain a large numbers of retinas; fetal bovine retina is abundantly available for developmental studies; *cis*-elements of suspected transcriptional regulatory function are well characterized. The most important reason for using the bovine retina is that the photoreceptor development in the cow is similar to that in human and unlike that in mouse and rat. Development of bovine rod photoreceptors occurs mainly during the final fetal trimester, and is finished before the day of birth, whereas rodent PR development does not begin until about PN0 and continues until about PN9-10. The gestational period of the cow is also quite similar to human, and appears to properly and closely mimic the timing of development of the human retina.

Materials and Methods

Oligonucleotides

WH427: 5' CCA AGA TCT GCC CAA GTT 3'. This is a sense primer, corresponding to bovine rod opsin upstream region –926 to –909.

WH425: 5' GAA GGC CCG AGG CCC ATC TG 3'. This is an antisense primer, corresponding to bovine rod opsin upstream region –842 to -825.

WH421: 5' CTG CCC CTT GCT CCT TCC 3'. This is a sense primer, corresponding to bovine rod opsin upstream region –1928 to –1911.

WH420: 5' CAG TTG CCT GGA GCC GCC 3'. This is an antisense primer, corresponding to bovine rod opsin upstream region –1599 to -1582.

WH419: 5' CCA TCC TCG AGT TCT CAG 3'. This is a sense primer, corresponding to bovine rod opsin upstream region –1629 to –1612.

WH418: 5' GCA CGA GCT CAG GGT GCG 3'. This is an antisense primer, corresponding to bovine rod opsin upstream region –1287 to -1270.

WH414: 5' CCC TTC CTC CAC CAT CGC TCC 3'. This is a sense primer, corresponding to bovine rod opsin upstream region –989 to –969.

WH413: 5' GGA GGG GTC TTC ACG ATC C 3'. This is a sense primer, corresponding to bovine rod opsin upstream region –1329 to –1311.

WH412: 5' CCC TAC AGG ATG AGC TG 3'. This is an antisense primer, corresponding to bovine rod opsin upstream region –967 to -949.

WH411: 5' GTG CAG GCC ACT GGG G 3'. This is an antisense primer, corresponding to bovine rod opsin upstream region –630 to -615.

WH396: 5' GCA GGG CTG CGT GCT CTG G 3'. This is a sense primer, corresponding to bovine rod opsin upstream region –2098 to –2080.

WH380: 5' GGG CCT AGA GCT AGG GG 3'. This is a sense primer, corresponding to bovine rod opsin upstream region –302 to –286.

WH365: 5' CCT GGT GGT AAG TGC TCT GGG 3'. This is an antisense primer, corresponding to bovine rod opsin upstream region –1909 to -1889.

WH364: 5' CCT CCT CAG CCC ATA AGC 3'. This is a sense primer, corresponding to bovine rod opsin upstream region –673 to –655.

WH363: 5' GCT TGC CCT GAG CCA GAG 3'. This is an antisense primer, corresponding to bovine rod opsin upstream region –326 to -309.

WH309: 5' GCT CTA GAA CTA GTG GAT 3'. This is a sense primer, corresponding to bovine rod opsin upstream region –357 to –339.

WH125: 5' TGG CTC CAA CTC CCC CCC C 3'. This is an antisense primer, corresponding to bovine rod opsin upstream region –19 to +1.

WH112: 5' CTC GAA GGG GCT GCG CAC CAC 3'. This is an antisense primer, corresponding to transcribed bovine rod opsin region +35 to +55.

WH62: 5' GGA TGC TTC TGA GGC CGG AG 3'. This is an antisense primer, corresponding to transcribed bovine rod opsin sequence +151 to +171.

Reverse primer: 5' GGA AAC AGC TAT GAC CAT G 3'. This primer contains sequences corresponding to the pBluescript II KS vector polylinker site.

T7 primer: 5' GTA ATA CGA CTC ACT ATA GGG C 3'. This primer contains sequences corresponding to the pBluescript II KS vector polylinker site.

T3 primer: 5' AAT TAA CCC TCA CTA AAG GG 3'. This primer contains sequences corresponding to the pBluescript KS vector polylinker site.

-20 primer: 5' GTA AAA CGA CGG CCA GT 3'. This primer contains sequences corresponding to the pBluescript KS vector polylinker site.

-40 primer: 5' GTT TTC CCA GTC ACG AC 3'. This primer contains sequences corresponding to the pBluescript KS vector polylinker site.

Plasmid Clone Construction

Rod opsin gene upstream region fragments were generated by PCR using the lambda phage BD1 insert (provided by J. Nathans) as the DNA template (Figure 2-1). Oligonucleotide primers were derived from the bovine opsin sequence (Nathans and Hogness, 1983). The PCR conditions were 10 pmole of upstream and downstream primer each, 20 mM Tris-HCl, pH 8.4, 50 mM KCl, 2 mM $MgCl_2$, 200 μM dNTPs. PCR fragments were filled in by 10 units of the large fragment of DNA polymerase I (GIBCO/BRL) with 1mM dNTPs, 1 X Reaction buffer 3 (BRL) at 37 °C for 1 hour. All fragments were then subcloned into the Sma I site of the pBluescript KS+ vector. The orientation and fidelity of opsin upstream fragment were determined by sequencing the region from miniprep DNA using either the T7 or T3 promoter primer. An opsin transcriptional start site in the clone close to the T7 promoter of the vector identified the clone as in the correct orientation for either the T7 or –40 primer to be used for primer extension analysis (see below). An opsin transcription start site in the clone close to T3 promoter of the vector identified the clone as being in the opposite orientation, then either the T3 or M13mp18 reverse primer was used for primer extension analysis.

Clone BU2.1 contains a 2.1 kb opsin upstream fragment (-2099 to +1) subcloned into Sma I site in the T7 promoter orientation. The opsin upstream fragment was produced by PCR using primers WH396 and WH125.

Clone BW2.1 contains a 2.1 kb opsin upstream fragment (-2099 to +1) subcloned into Sma I site in the T3 promoter orientation. The opsin upstream fragment was produced by PCR using primers WH396 and WH125.

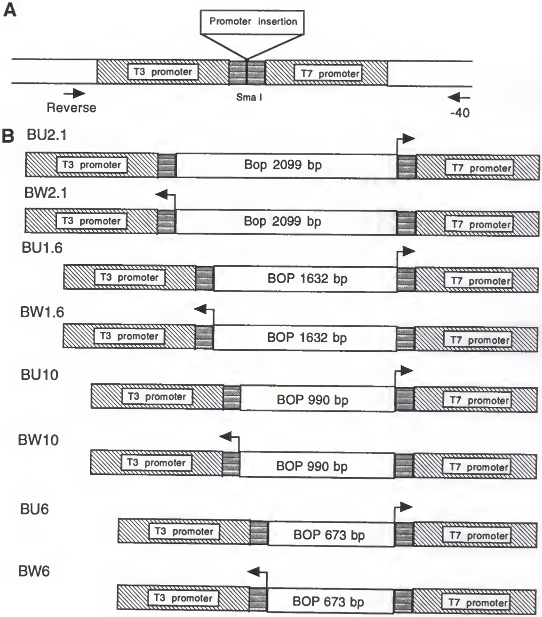

Figure 2-1: Structure of bovine rod opsin promoter-containing clones for *in vitro* transcription. A. The bovine rod opsin promoters were cloned into Sma I site in the pBluescript KS vector. B. The length and orientation of bovine rod opsin promoter sequence in each clone. The grey areas represent the pBluescript KS vector backbone. The arrow represents the transcription start site.

Clone BT1 contains an 874 bp opsin upstream fragment (-2099 to -1225) subcloned into Sma I site in the T3 promoter orientation.

Clone BU1.9 contains a 1.9 kb opsin upstream fragment (-1929 to +1) subcloned into Sma I site in the T7 promoter orientation. The opsin upstream fragment was produced by PCR using primers WH421 and WH125.

Clone BW1.9 contains a 1.9 kb opsin upstream fragment (-1929 to +1) subcloned into Sma I site in the T3 promoter orientation. The opsin upstream fragment was produced by PCR using primers WH421 and WH125.

Clone BU1.6 contains a 1.6 kb opsin upstream fragment (-1631 to +1) subcloned into Sma I site in the T7 promoter orientation. The opsin upstream fragment was produced by PCR using primers WH419 and WH125.

Clone BU1.3 contains a 1.3 kb opsin upstream fragment (-1330 to +1) subcloned into Sma I site in the T7 promoter orientation. The opsin upstream fragment was produced by PCR using primers WH413 and WH125.

Clone BW1.3 contains a 1.3 kb opsin upstream fragment (-1330 to +1) subcloned into Sma I site in the T3 promoter orientation. The opsin upstream fragment was produced by PCR using primers WH413 and WH125.

Clone BU10 contains a 1.0 kb opsin upstream fragment (-990 to +1) subcloned into Sma I site in the T7 promoter orientation. The opsin upstream fragment was produced by PCR using primers WH414 and WH125.

Clone BU6 contains a 600 bp opsin upstream fragment (-673 to +1) subcloned into Sma I site in the T7 promoter orientation. The opsin upstream fragment was produced by PCR using primers WH364 and WH125.

Clone BT2 contains a 200 bp opsin upstream fragment (-2099 to -1892) subcloned into Sma I site in the T7 promoter orientation. The opsin upstream fragment was produced by PCR using primers WH421 and WH125.

Clone BD1 contains a PCR fragment (bovine opsin upstream sequence -2099 to -1225) subcloned into the EcoR I site (filled in by Klenow DNA polymerase) of Clone BU6 (w/ Bop –673 to +1) in the T7 promoter orientation. The PCR fragment was produced by primer WH396 and WH364.

Clone BDW1 contains a PCR fragment (bovine opsin upstream -2099 to -1225) subcloned into the EcoR I site (filled in by Klenow DNA polymerase) of Clone BU6 (w/ Bop –673 to +1) in the T3 promoter orientation. The PCR fragment was produced by primer WH396 and WH364.

Clone BD2 contains a PCR fragment (bovine opsin upstream –2099 to –1892) subcloned into the EcoR I site (filled in by Klenow DNA polymerase) of Clone BU6 (w/ Bop –673 to +1) in the T7 promoter orientation. The PCR fragment was produced by primers WH365 and WH364.

Clone BI21 was made by digesting BU2.1 with Sac II and BamH I, deleting a 28 bp fragment from Bop –689 to –664. The linearized vector was than filled in by Klenow DNA polymerase, religated with T4 DNA ligase, and transformed into DH 5α cells by heat-shock. The deletion was verified by sequencing.

Bovine Retinal Nuclear Extract

Nuclear extracts were prepared by a modification of the method of Kodanaga (Kamakaka and Kadonaga, 1994). All reagents were kept at 4°C and all glassware was chilled on ice. The extraction was performed either at 4°C or on ice. 12 adult bovine retinas were pooled, washed with 5 volumes of phosphate buffered saline (137 mM NaCl, 2.7 mM KCl, 10mM Na_2HPO_4, 1.8 mM KH_2PO_4, pH7.4) once, and 5 volumes of buffer AB (15 mM HEPES, pH 7.6, 110 mM KCl, 5 mM $MgCl_2$, 0.1 mM EDTA, 2 mM DTT, 1 mM sodium metabisulfate, 0.2 mM PMSF, 1 mM benzamidine) once. The nuclei were collected by dounce homogenization in 8 ml buffer I' (15 mM HEPES pH 7.6, 10 mM KCl, 5 mM $MgCl_2$, 0.1 mM EDTA, 0.5 mM EGTA, 350 mM sucrose, 0.5% NP-40, 1 mM DTT, 1 mM sodium metabisulfate, 0.2 mM PMSF, 1 mM benzamidine) by 10 strokes of Dounce type B homogenizer. The homogenizer was then washed with another 2 ml of buffer I'. Nuclei were spun down in a Sorvall GSA rotor at 7000 x g for 15 minutes. After decanting the supernatant, lipid adhering to the wall of the centrifuge tube was wiped off using kimwipes. The pellet was resuspended in 10 ml buffer AB, and centrifuged at 8000 x g for 15 minutes. The nuclear pellet was weighed and resuspended in ½ volume (W/V) HEMG+0.1M KCl buffer (25 mM HEPES pH 7.6, 100 mM KCl, 12.5 mM $MgCl_2$, 0.1 mM EDTA, 20% glycerol, 1.5 mM DTT, 1 mM sodium metabisulfate, 0.1 mM PMSF, 1 mM benzamidine). The resuspension was incubated on ice for 60 minutes with occasionally swirling. The nuclear suspension was then centrifuged at 100,000 g for 1 hour at 4°C using a Beckman SW28 rotor. After the centrifugation, there were four distinct layers in the centrifuge tube. The top thin gray-white layer contained lipid. A yellow liquid layer contained the soluble nuclear fraction (SNF). The other two layers contain nucleic acid and nuclear debris. The SNF was collected and frozen in an ethanol/dry ice bath in 100 µl aliquots, and stored at -70°C. The total protein concentration of nuclear extract was measured by the Lowry assay.

Lowry Assay

Reagent A contains 2% Na_2CO_3, 0.4% NaOH, 0.16% sodium tartrate and 1% SDS. Reagent B contains 4% $CuSO_4{\cdot}5H_2O$. 5 μl of the SNF was diluted into 1 ml PBS, and 3 ml reagent C (Reagent A:B 100:1) was added to the sample. After incubation at room temperature for 1 hour, 0.3 ml phenol reagent (Folin Ciocalteu Phenol:H_2O 1:1) was added, and left at room temperature for another 1 hour. The OD_{660} was determined and compared with the standard curve of BSA to determine the protein concentration.

End-labeled Primers

A 5'-end labeling reaction was performed on 100 pmole of the indicated primer with 5X Forward buffer (BRL), 1 μl γ-^{32}pATP (6000 Ci/mmol, NEN Du Pont), 10 unit T4 polynucleotide kinase (BRL). The reaction mixture was incubated at 37°C for 30 minutes and then heat-deactivated at 65°C for 10 minutes. The end labeled primers were then ethanol precipitated twice, and resuspended in 50 μl dH_2O.

In Vitro Transcription with Retinal Nuclear Extract

A typical *in vitro* transcription was performed with 15 μl transcription buffer (12.5 mM HEPES pH 7.6, 50 mM KCl, 6.25 mM $MgCl_2$, 0.05 mM EDTA, 0.5 mM DTT, 5% glycerol), 5 μl soluble nuclear fraction (SNF), 1 μg DNA template, and 3 μl rNTPs (5mM each) in a final volume of 25 μl. For a titration of SNF(from 0.5 to 5 μl), the concentration of the reactants was maintained by adding a complementary amount of HEMG+0.1 M KCl buffer. The transcription reaction mixture was incubated at 21°C for

1 hour, and then stopped by adding 100 μl stop solution (20mM EDTA, 0.2 M NaCl, 1% SDS, 0.25 mg glycogen) and 300 μl 0.3 M sodium acetate, pH 5.3. The reaction mixture was extracted once with phenol:chloroform:isoamyl alcohol (25:24:1) and once with chloroform:isoamyl alcohol. The aqueous phase was then ethanol precipitated and resupspended in 10 μl RNase-free dH_2O.

Primer Extension

In vitro transcribed RNA was annealed with 5' labeled antisense primer (10 pmole) in 1X first strand buffer (50 mM Tris-HCl, pH 8.3, 75 mM KCl, 3 mM $MgCl_2$), 10 mM DTT, and 0.5 mM dNTPs. The annealing mix was heated at 75°C for 90 seconds, then annealed at 58°C for 20 minutes, and cooled at room temperature for 10 minutes. Then an extension mix containing 1X first strand buffer, 0.5 mM dNTPs, 10 mM DTT and 200 unit SuperScript II reverse transcriptase was added to start the reverse transcriptase (RT) extension. The extension proceeded at 37°C for 1 hour and then was stopped by adding 5 μl 0.3 M NaOAc, 2 μl tRNA (10mg/ml), and 150 μl ethanol. After incubation at -70°C for 15 minutes, the extension products were precipitated by centrifuged at 12,000 x g for 15 minutes, and washed with 70% ethanol. The pellet was then resuspended in 10 μl loading dye (98% formamide, 10 mM EDTA, 0.01% xylene cyanol, and 0.01% bromophenol blue). The extension products were then denatured at 90°C for 10 minutes, placed on ice for 5 minutes, and loaded on 6%, 8 M urea sequencing gels along with a sequencing reaction using the same primers and DNA template.

Detection of Nuclease

To detect the DNase activity in the retinal nuclear extract, 1 µg BU2.1 DNA was incubated with 10 µl SNF from each fraction of DEAE chromatography in 1X transcription buffer at 37°C for 30 minutes. Half of the incubated product was then separated on 1% agarose gel. The DNase levels were determined by the loss of BU2.1 DNA.

DEAE-Cellulose Chromatography

All chromatographic steps were performed at 4°C. A column containing 2 ml DEAE-cellulose was washed with wash buffer (50 mM Tris-HCl pH7.5, 50 mM KCl, 0.1 mM PNSF, 1 mM benzamidine). 1 ml retinal nuclear extract was loaded, and washed with the 4 bed volumes of wash buffer (0.05 M KCl) at a speed of 10 drops per minute. The flow-through was collected in 1 ml fractions. Nuclear protein was then eluted by a linear gradient (0.5 M to 2 M KCl), and collected in 1 ml fractions. The DNase activity of each fraction was then determined. Fractions from 0.5 M to 2 M KCl elution were pooled together and dialyzed against 300 ml HEMG+0.1 M KCl buffer twice. The protein concentration of 0.5 M KCl elution was determined by the Lowry assay.

Results

Clearly tissue and developmentally specific gene expression require the appropriate promoter. The rod opsin gene is expressed at very high levels in retinal rod cells, and to a lesser level in the pineal gland. Therefore, the minimal rhodopsin promoter capable of directing high level, photoreceptor –specific transcription would be very useful for obtaining photoreceptor-specific therapeutic gene expression. For retinal therapy, it is also important to express the target gene at an appropriate level since overexpression of wild type genes could also cause retinal degeneration (Olsson et al., 1992; Sung et al., 1994). Therefore, understanding the function of *cis*-elements in the rhodopsin promoter and identifying cognate *trans*-acting factors are essential to achieve this practical goal. DNA footprinting has already identified several DNA-protein interaction regions that appear to be involved in opsin regulation. Some overlap of these regions correspond with *cis*-elements for already identified factors, but most are still of unknown function in transcription.

To fulfill this goal, I developed an *in vitro* transcription system adapted to identify the role of these regions in transcription. Bovine retinal nuclear extracts were programmed with serially deleted bovine opsin promoter clones designed according to previous footprinting data (Figure 2-2). The transcriptional activity of each opsin promoter fragment was determined by primer extension. The transcriptional role of elements located on non-overlapping regions could thereby be identified by the relative levels of each promoter clone. The results suggest that a stable transcriptional extract from bovine retina will be difficult to make. However, results indicate that there is little, if any, difference between the proximal promoter region and larger region up to –2.0 kb with regard to supporting reasonable levels of correct rod opsin transcription.

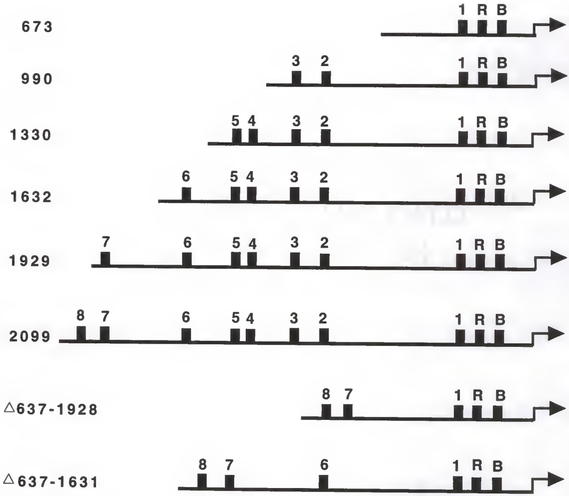

Figure 2-2: Footprinted *in vitro* by adult retinal nuclear extracts *Cis*-elements in the clones containing the bovine rod opsin upstream region. B, Bat-1; R, Ret-1; 1-8, CRS 1-8 (DesJardin & Hauswirth, 1996).

Retinal Nuclear Extract Directs Accurate Transcription from a Bovine Rod Opsin Promoter

Soluble nuclear fraction (SNF) extracts were isolated from pooled adult bovine retinas according to Kamakaka and Kadonaga (1994). As an initial estimate of the optimal conditions for a retinal nuclear extract capable of accurate transcription, several transcriptional conditions were tested. Buffers containing either 0.1 M KCl (low salt) or 0.4 M potassium glutamate (high salt) were used in the final high speed extraction of retinal nuclei. A DNA template (BW2.1) containing the 2.1 kb bovine rod opsin promoter was mixed with either high salt or low salt retinal extracts in a transcription reaction. A *Drosophila* RNA polymerase II extract (Promega) was added in some samples to determine the necessity of having exogenous RNA Pol II presence. 5'-end labeled reverse oligonucleotide primers were used in primer extension reactions to determine the approximate transcriptional level and the authenticity of transcription initiation. Figure 2-3 shows the results from the low salt extract. Without adding eukaryotic Pol II, this extract could produce transcription products detectable by primer extension. Pretreatment of products with RNase before primer extension nearly abolished the transcription signal. Therefore, these primer extension products were derived from an *in vitro* transcription rather than from pre-existing RNA or from a DNA template artifact. *In vitro* transcription initiated at two sites, one corresponded to the *in vivo* transcription start site, and the other initiated 10 bp upstream of the *in vivo* start site. The low salt extract generated about a 30:70 mix of +1 and +10 transcripts. However when mixed with a *Drosophila* Pol II extract, +10 transcripts were enhanced. *Drosophila* extract therefore appears to favor the incorrect transcription initiation site. The high salt

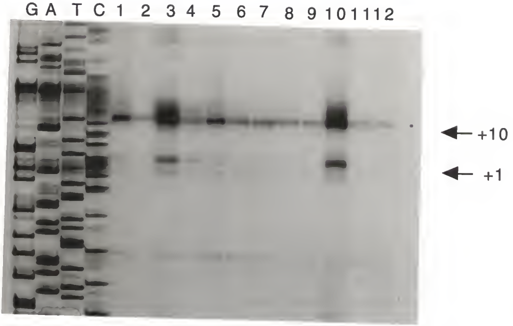

L(ul)	5	2.5	5	5						5			
H(ul)					15	10	5	2.5	5		5		
D(ul)	1	1			1	1	1	1				1	
RNase				+							+		

Figure 2-3: Primer extension of *in vitro* transcription products from the bovine rod opsin promoter. BW2.1 was used as the transcription template and a reverse primer was used to detect the transcripts in a primer extension assay. The amount of low salt bovine retinal extract (L), high salt bovine retinal extract (H) and *drosophila* extract (D) in the *in vitro* transcription is indicated below the figure. The *in vitro* transcripts from +1 and +10 site are indicated on the right site of the gel. The sequence ladder was created by using BW2.1 as a template for the reverse primer.

nuclear extract alone led to only low amounts of primer extension products. The addition of *Drosophila* Pol II further decreased this signal, suggesting that the *Drosophila* extract was inhibiting opsin promoter-derived transcription. More +10 transcripts than +1 transcripts were always generated. Therefore, the low salt retinal nuclear extract appears to contain its own RNA polymerase II and sufficient *trans*-acting factors to support reasonable transcription, a significant fraction of which is accurately initiated. Because addition of eukaryotic Pol II had no positive effect on the high salt extract, the low transcriptional level in this extract may not be due to lack of RNA polymerase, but rather caused by the inhibitory components or a lack of positive-acting regulatory factors.

Endogenous Nuclease Decreases *In Vitro* Transcription

Even though the low salt nuclear extract could produce a reasonable RNA initiation *in vitro*, this activity was not stable and the yield was inconsistent from preparation to preparation. One problem might have been contamination with nuclease in the extract. DNase in the extract could completely degrade target plasmid DNA in less than 30 minutes (Figure 2-4B). Clearly, loss of template during the *in vitro* reaction will lead to low levels of transcription. RNase was also present in the extract, and degraded input labeled RNA nearly 100% in 30 minutes at room temperature (data not shown). It was difficult to control levels of nuclease contamination in the extracts from one preparation to another. Titrated RNase inhibitor Ace (5 Prime to 3 Prime, Inc) was tested for its ability to inhibit RNase in the *in vitro* transcription reaction (Figure 2-4A). About 60% of a radiolabeled input RNA remained in the highest concentration (10 units) of RNase inhibitor. Added yeast total tRNA was also used to inhibit endogenous RNase by

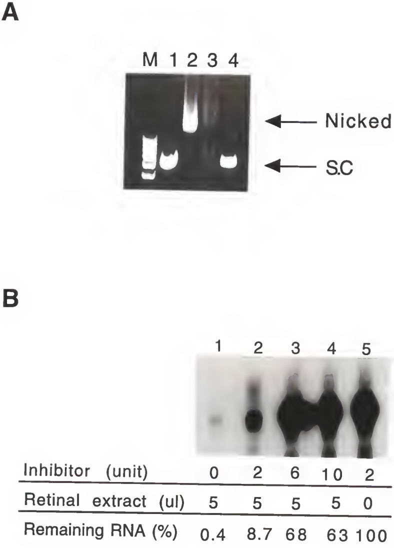

	1	2	3	4	5
Inhibitor (unit)	0	2	6	10	2
Retinal extract (ul)	5	5	5	5	0
Remaining RNA (%)	0.4	8.7	68	63	100

Figure 2-4: A. Detection of DNase in the retinal extract. 1 μg of BU2.1 plasmid DNA was incubated with 5 μl retinal extract in the same conditions as for the *in vitro* transcription for 30 minutes. Lane M. 1 kb DNA ladder (BRL). Lane 1 and 4. No retinal extract control. Lane 2. BU2.1 incubated with 0.5 M KCl DEAE fractionated retinal extract. Lane 3. BU2.1 incubated with unfractionated retinal extract. The position of supercoiled (S.C) and nicked (Nicked) plasmid DNA is indicated on the right of the figure. B. Effect of RNase inhibition in the bovine retinal transcription extract. Lane 1-4. The same amount α-P^{32} UTP labeled RNA was incubated with 5 μl retinal extract along with the RNase inhibitor (Inhibitor Ace). Lane 5. No retinal extract control. The amount of Inhibitor Ace and remaining RNA signal are indicated at the bottom of the gel.

competing as an RNase substrate (data not shown). At the highest concentration (5 mg/ml), RNase degradation of the tested input RNA was almost completely inhibited. The problem with high levels of tRNA is that it also inhibited transcription. The reason for this is unclear, but it may be due to a competition of transcription factors or Pol II between tRNA and the DNA template.

DEAE-Cellulose Chromatography to Remove Nucleases

DEAE-cellulose chromatography was used in an attempt to separate endogenous nucleases from transcriptional components in the retinal nuclear extract. After binding to the column at low salt, transcription factors and RNA polymerase were eluted with a 0.5 M to 2 M KCl gradient. Eluted fractions were tested for DNase activity (trace RNase was reasonably inhibited using RNase inhibitor). A majority of nuclease fractionated in the 0.05 M KCl wash (Figure 2-5). This also removed unbound proteins equivalent to about 50% of the extract protein. Fractions from 0.5 to 2 M contained no detectable level of DNase, and the majority of bound proteins were also eluted during this linear gradient.

After combining nuclear fractions from 0.5 M to 2 M (to avoid losing factors eluting at different salt concentration) and dialyzing against HEMG+0.1 M KCl buffer, BU2.1 was used as a template for *in vitro* transcription. Fractionated nuclear extract retained the ability to accurately transcribe from the bovine rod opsin promoter (Figure 2-6). However, the intensity of +10 and +1 initiated transcription products remained similar. Transcriptional products with this extract were low, even though nucleases had been separated or inhibited. A titration of nuclear extract did not improve the product yield, even at the highest amounts of protein. One possible explanation might be low protein

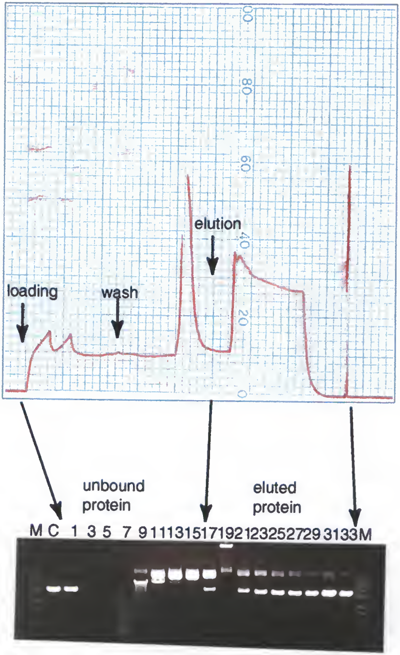

Figure 2-5: DEAE chromatography separates DNase from other bovine retinal proteins. The protein loading, wash and elution are indicated in the top panel. Every other fraction was tested for the DNase as in Figure 2-4. M: 1 kb BRL marker. C: no retinal extract incubation control.

concentration of the final fractionated extract. In a typical experiment, 5 mg retinal nuclear extract (from total 12 pooled adult retinas) was applied to the DEAE column. After salt elution, about 1 mg was recovered in the active fraction. Therefore at least 80% of the initial protein was lost during purification suggesting that critical transcription factors may have been lost or substantially diluted during the low salt wash.

Cis-elements for Rod Opsin Transcription

In spite of the inability to produce a highly active, stable transcriptional extract capable of accurate transcription on a rod opsin promoter template, there was sufficient activity available to gain a preliminary picture of the minimal promoter necessary for correct initiation. A DNA template containing 673 bp opsin promoter yielded transcription products similar in character and level to those using a 2.1 kb or 1.3 kb promoter in the *in vitro* transcription reaction (Figure 2-6), suggesting the proximal promoter contains sufficient *cis*-elements for bovine opsin transcription. This proximal bovine promoter, and analogous regions from other species, will form the basic promoter for obtaining therapeutic gene expression in rod PRs *in vivo*.

Discussion

A bovine nuclear extract is used to help identify functional *cis*-elements in the rod opsin promoter. Our major problem is to obtain a tissue-specific transcription extract. Several nuclear extract systems have been used by others for promoter studies from a variety of cell types, including Hela cell, muscle cell and liver cell. The basic principles

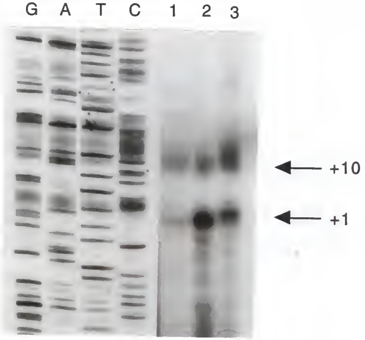

Figure 2-6: Primer extension for *in vitro* transcription products from the bovine rod opsin promoter with DEAE fractionated bovine retinal extracts. BU2.1 (-2099 to +1), BU1.6 (-1632 to +1) and BU6 (-673 to +1) were used as the *in vitro* transcription template and a -40 primer was used to detect the in vitro transcripts in the primer extension. Lane 1: BU2.1 as template. Lane 2: BU1.6 as template. Lane 3: BU6 as template. The *in vitro* transcripts from +1 and +10 site are indicated on the right site of the gel. The sequence ladder was created by using BU2.1 as a template for the -40 primer.

for preparation of nuclear extract are relatively invariant, but it is crucial to adopt specific modifications depending on the tissue and cell type of interest.

A method adapted from one standard protocol was chosen for preparing bovine retinal nuclear extract (Kamakaka and Kadonaga, 1994). A low salt (0.1 M KCl) buffer instead of high salt buffer (0.4 M potassium glutamate) was found to be best for the final step extraction because high salt retained more proteins, apparently inhibiting the *in vitro* transcription. Initial data showed that this high salt retinal extract processed only very low transcriptional activity, and that a commercial *Drosophila* Pol II extract added to the *in vitro* transcription provided no improvement. Primer extension revealed major transcription start sites at +10 and at +1 with or without *Drosophila* extract. Since there is a guanosine-rich tract between +15 to +1, RNA polymerase might initiate from this abnormal +10 start site during transcription because of difficulties in completely denaturing the template strands around +1. Another potential explanation is that some essential factors might have been lost during the preparation of the nuclear extract. Several factors, including TFIIB, have a role determining the transcription start site. In contrast, low salt nuclear extracts supported correctly initial transcription *in vitro* without adding *Drosophila* nuclear extract. Although the +10 transcripts were always present, this extract was able to yield transcripts from the *in vivo* start site with 50% intensity in some cases. Therefore, 0.1 M KCl low salt extraction produced a retinal extract for *in vitro* transcription most closely mimicking the *in vivo* situation.

One barrier to total success of low salt extract system was the inconsistency between preparations. Most preparations generated only relatively weak transcription products, difficult to detect even using primer extension. This modest transcriptional activity might not be caused by low levels of transcription factors and RNA polymerase, but rather by a high level of co-purified nuclease activity that degraded the DNA template and the nascent transcripts during the *in vitro* reaction. Nucleases in these extracts were found to degrade 100% of input DNA or RNA under *in vitro* transcription conditions in 30 minutes. Such nuclease activity might be intrinsic to photoreceptors owing to their extremely high rate of metabolism. To overcome this problem, RNase inhibitors, such as Vanadyl ribonucleotide complex and placental RNase inhibitor, were titrated into the transcription reaction. At the highest inhibitor concentration, RNase activity was decreased only about 30% , still insufficient for reproducible transcriptional analysis. High concentrations of yeast tRNA added to the transcription reaction did fully inhibit the RNase activity, but it also inhibited *in vitro* transcription. There was no inhibitor available to deal with the DNase activity in the retinal nuclear extract.

These problems forced a consideration of additional protein fractionation as a way to reduce the nuclease problem. DEAE column chromatography was tested in order to separate nucleases from the other nuclear proteins. A 0.05 M KCl wash of total soluble retinal nuclear proteins bound to the DEAE column was found to eliminate nuclease activity, and a subsequent fraction pooled from a 0.5 to 2 M KCl elution still directed the correctly initiated transcript from the opsin promoter. The amount of +1 transcripts was now similar to +10 transcripts, indicating that the factors determining the correct start site remained. The major problem with the DEAE fractionation was still the low recovery of the nuclear proteins. The possibility of factors being lost or inactivated during the low salt wash step also remained. Perhaps a larger scale of DEAE chromatography would provide sufficient proteins for reliable *in vitro* transcription, but this would require even more than the 12 bovine retinas used normally as starting material.

Recently, a similar nuclear extract system was used to determine promoter function by *in vitro* transcription (Chen and Zack, 1996). The bovine promoter (-573 to +70) was used in that study. These experiments found no transcriptional difference comparing a -573 bp to a -173 bp promoter. But the -173 to +70 bp promoter resulted in a much higher transcription level than the –38 to +70 bp promoter. In fact, several DNA-protein interaction sites have been located between –30 to –173 bp, including Ret 4 and Nr 1 binding sites. The transcriptional activity in this system was still low when compared to a general Hela cell nuclear extract. In our experiments, the -673 bp promoter showed similar transcriptional activity to the 2.1 kb and 1.3 kb promoter in some preparations, indicating that the transcription level might be dependent primarily on the proximal promoter. It appears that *in vitro* transcription will be useful for longer promoter analysis only if the transcription activity can be improved significantly.

CHAPTER 3
SELECTIVE DEGRADATION *IN VIVO* OF NONSENSE BETA PHOSPHODIESTERASE mRNA IN THE HETEROZYGOUS *RD* MOUSE

Introduction

The *rd* mouse is a classical model for autosomal recessive retinal degeneration. The original *rd* mice can be traced back to the rodless mice (gene sample, *r*) identified almost 75 years ago (Pittler et al., 1993). The homozygous *rd/rd* mouse exhibits an early onset retinal rod degeneration initiating at postnatal day 8, with nearly complete rod loss at postnatal day 30 (Bowes et al., 1989). Even though the heterozygous *rd*/+ mouse has no apparent anatomical abnormalities and does not undergo rod degeneration, the cyclic GMP level in the light adapted *rd*/+ mouse retina is 40% lower than that in the normal mouse (Ferrendelli et al., 1976; Doshi et al., 1985) and the ERG shows an altered sensitivity to light stimulation (Low, 1987).

A nonsense mutation at codon 347 and/or a retroviral insertion (Xmv-28) in the first intron of the β-subunit of cGMP phosphodiesterase (β-PDE) are the causes for this retinal degeneration (Bowes et al., 1989; Bowes et al., 1990; Pittler and Baehr, 1991; Bowes et al., 1993). Another similar nonsense mutation in β-PDE also causes retinal degeneration in the Irish setter dog with rod/cone dysplasia (Suber et al., 1993). The nonsense mutation in β-PDE will elevate the cGMP level in the retina (Farber et al., 1988), and dispose photoreceptors to apoptosis (Chang et al., 1993; Portera et al., 1994).

Cyclic GMP PDE is a key player in photoreceptor signal transduction and consists of 1 alpha subunit, 1 beta subunit, and 2 gamma subunits (Fung et al., 1990). When rhodopsin is excited by a photon, photoactivated rhodopsin activates the G-protein transducin which then binds the inhibitory gamma subunits of phosphodiesterase, revealing the cGMP phosphodiesterase activity of the alpha and beta subunits (Hargrave and McDowell, 1992). This serves to lower intracellular levels of cGMP leading to the closure of cation specific channels in the plasma membrane of rod outer segments, hyperpolarizing the plasma membrane and producing a neural signal (Stryer and Bourne, 1986).

The gene structure of the β-PDE gene is complex, consisting of at least 21 introns and 22 exons encoding an 853 amino acid protein with several functional domains (Baehr et al., 1991). A six amino acid domain (CAAX box) at the carboxyl terminus involved in membrane binding can be proteolyzed, methylated, and/or isoprenylated (Anant et al., 1992; Qin et al., 1992); a region conserved among several mammalian species (amino acids 554-750) is important for catalytic activity (Charbonneau et al. 1986); another region (amino acids 300-400) is the cGMP binding domain (Charbonneau et al. 1990); the N-terminus contains the gamma subunit-binding site. The nonsense mutation in codon 347 of the *rd* gene could produce a truncated protein which retains the inhibitory gamma subunit binding site. Thus far there is no evidence that the predicted truncated protein can be detected (Lee et al., 1988), and the mechanism relating the phenotype to the genotype remains unclear.

Several point mutations in the β-PDE have been related to autosomal recessive disease in humans (McLaughlin et al., 1993; McLaughlin et al., 1995). These mutations account for about 4% of Retinitis Pigmentosa cases in North America. A missense mutation in the rod β-PDE also causes autosomal dominant stationary night blindness (Gal et al., 1994). Recently, a point mutation in the PDE α subunit was found in an RP patient. Even though there have been no defects found in the PDE γ subunit so far (Hahn et al., 1994), a transgenic mouse line lacking the γ subunit also undergoes retinal degeneration, indicating mutations in this subunit might also cause retinal diseases in humans (Tsang et al., 1996).

Messenger RNA decay is important for gene regulation (Brawerman, 1990). Ordinarily, the secondary structure of the 3' end contributes to decay of mRNA in eukaryotes. Examples include the stem-loop in the histone H3 mRNA and the AU rich elements in c-*fos* and c-*myc* (Chen and Shyu, 1995). These structures appear to destabilize the poly A tail, and initiate mRNA decay. Destabilization elements might also be located within the reading frame; examples include yeast mRNAs for *MATα1*, *HIS3*, and *STE3* (Decker and Parker, 1994). mRNA degradation has been found to be linked to translation (Savant Bhonsale and Cleveland, 1992; Aharon and Schneider, 1993) because cycloheximide treatment can stabilize mRNAs with nonsense mutations, and a hairpin insertion in 5' UTR of triosephosphate isomerase mRNA not only inhibits the translation, but also prevents mRNA degradation (Belgrader et al., 1993). It is thought that the ribosomes need to bind to a messenger and to read through at least part of the coding region in order to initiate mRNA decay.

It is also possible the nucleases bound to ribosomes are responsible for the decay. A major example is a deadenylation-dependent pathway. If mRNAs contain specific sequence elements, they enter a deadenylation-independent degradation pathway, in which decapping is followed by 5' to3' endonucleolytic degradation (Decker and Parker, 1994).

A number of studies have shown that an altered stability of nonsense mRNA is important for a mutant phenotype. For example, in β-thalassamia, mammalian cells can specifically degrade a transcript containing a premature stop codon by a mechanism involving a ribosome-associated ribonuclease (Maquat et al., 1981; Lim et al., 1992). This degradation serves to protect the cell from the toxic effects of the mutant gene, and possibly from clinical disease in the heterozygous individual. Even though alternatively spliced transcripts of β-PDE have been found in the *rd* mouse retina (Bowes et al., 1989), ordinarily such misspliced RNAs are less than 15% of the normal transcripts, and are not likely to be the primary factor contributed to the retinal degeneration (Berget, 1995; Maquat, 1996).

Since specific levels of *rd* and wild type mRNA in the heterozygous *rd*/+ mouse have not been reported and the *rd* mutation is of the nonsense class, this chapter will test the hypothesis that the *rd* nonsense mRNA is specifically degraded *in vivo*.

Materials and Methods

Oligonucleotides

WH741: 5' GGCCGGGAAATTGTCTTCTAC 3'. This is a sense primer containing exon 5 and 6 sequences and corresponds to β-PDE cDNA sequence 921-943.

WH742: 5' CCCCAGGAACTGTGTCAG AGA 3'. This is an antisense primer containing exon 9 and 10 sequences and corresponds to β-PDE cDNA sequence 1258-1279.

WH770: 5' TCCTTCGACCTCTGTTCTTTTCCC 3'. This is a sense primer within β-PDE intron f (Pittler and Baehr, 1991).

WH769: 5' GGAGCTTCTAGCTGGGCAAAGTGA 3'. This is an antisense primer within β-PDE intron g (Pittler and Baehr, 1991).

Animals and Retinal Nucleic Acid Isolation from *rd*/+ Mouse

Three strains of 4 week old female heterozygous *rd* mice (B6C3xC3H f1, B6CBA/J f1, and CSJL/J f1) were purchased from the Jackson Laboratory. After sacrifice by CO_2 inhalation, 2-6 retinas from each strain mouse were dissected and pooled. Total RNA and genomic DNA were purified by Trizol extraction (Gibco BRL) according to the manufacturer's instructions. Total RNA and genomic DNA were then extracted with phenol/chloroform, ethanol precipitated with 0.3 M sodium acetate (pH 5.3) and resuspended in RNase-free H_2O. The concentration of total RNA and genomic DNA was determined spectrophotometrically, and the integrity of total RNA verified by electrophoresis on formamide / formaldehyde agarose (1%) gels.

RT-PCR and PCR for Detecting mRNA and Genomic Copies of β-PDE

To detect β-PDE mRNA, a 20 μl reaction was set up using 1 μg of total retinal RNA from the each mouse strain, 25 pmole primer WH742, Superscript first stand buffer (Gibco BRL), 10 mM DTT, and 200 μM dNTPs. The reaction mix was denatured at 80°C for 2 min and then annealed at 56°C for 20 min. 200 units of Superscript II reverse transcriptase (Gibco BRL) and 1 unit of RNase inhibitor-Ace (5 Prime to 3 Prime, Inc) were added to the mix and incubated at 37°C for 1 hour. For a negative control, no reverse transcriptase was added after the annealing step. Two microliters was removed from the reverse transcription reaction for PCR in a solution containing 20 mM Tris-HCl (pH 8.4), 50 mM KCl, 10 pmole WH741, 10 pmole WH742, 2 mM $MgCl_2$, 200 μM dNTPs, and 5 μCi of α-^{32}p dCTP (3000 Ci/mmol, NEN Du Pont). The PCR mix was denatured at 94°C for 5 minutes, and then run for 30 cycles of 94°C for 1 min, 55°C for 1 min and 72°C for 1 min. After the reaction, the PCR product was denatured at 94°C for 10 minutes and slowly cooled to room temperature for 3 hours. The PCR products were purified using a Wizard PCR purification kit (Promega) following the manufacturer's protocol, ethanol precipitated and resuspended in 20 μl H_2O.

To detect the β-PDE pre-mRNA, 1 μg of total retinal RNA was incubated with 2 units of RNase-free DNase (Ambion) and 1 unit RNase inhibitor in Superscript first strand buffer at 37°C for 15 min. The DNase was deactivated at 94°C for 5 min, and the DNase treated total RNA then used for RT-PCR as described above.

To detect the gene copy ratio between wild type and mutant β-PDE, 1 μg of genomic retinal DNA was used in a 50 μl PCR with 20 mM Tris-HCl (pH 8.4), 50 mM KCl, 10 pmole WH769, 10 pmole WH770, 2 mM $MgCl_2$ and 200 μM dNTP's. The PCR conditions were 94°C for 5 minutes, then 30 cycles of 94°C for 1 min, 57°C for 1 min and 72°C for 1 min. The PCR product was denatured, annealed and purified as above.

RFLP for Determining the Ratio of Wild Type and Mutant β-PDE

After each PCR reaction, 5 μl of 20 μl was used for restriction enzyme digestion. PCR products were digested with 10 units BsaA I (New England Biolabs, Beverly, Massachusetts) in NEB buffer 3 at 37°C overnight, then ethanol precipitated at – 70°C with one tenth volume 3M sodium acetate (pH 5.3) and 2.5 volume absolute ethanol for 30 minutes using 1 µl glycogen (5mg/ml) as a carrier. The precipitate was centrifuged at 14,000 g for 15 min, washed with 1 ml 70% ethanol, and resuspended in 10 µl H_2O. Half of the digestion product was mixed with 1 µl of 5 fold concentrated agarose dye (50% sucrose, 50 mM EDTA, 0.2% bromophenol blue and 0.2% xylene cyanol) and run on an 8% nondenaturing polyacrylamine gel at 600 volts for 3 hours. The digestion product bands were quantified by ImageQuant version 3.2 using a PhosphoImager (Molecular Dynamics). For Dde I digestion, 5 µl of each PCR product was incubated with 20 units Dde I (Gibco BRL) in BRL Restriction buffer 3 at 37 °C overnight, ethanol precipitated as for the BsaA I digestion, and quantified as above.

Results

Retinal degeneration in the *rd*/*rd* mouse starts at postnatal (PN) day 7 with nearly all the photoreceptors absent at PN day 21. In the *rd*/*rd* mouse there is about 10% mutant β-PDE mRNA left at PN 10. However, in the *rd*/+ retina the fraction of mutant versus wild type β-PDE mRNA has not been clearly defined. To quantify these levels and determine whether mutant mRNA levels are equivalent to the wild type, we analyzed a series of *rd*/+ mice in which the wild type transcript can be used as an internal control for quantitation. The strategies for using RT-PCR to determine the ratio between the wild type and mutant mRNA, pre-mRNA and gene copy are shown in Figure 3-1. The nonsense point mutation in codon 347 creates a Dde I restriction site, and removes a BsaA I site from the wild type sequence. Digesting β-PDE mRNA RT-PCR products with BsaA I or Dde I therefore yields three diagnostic fragments of 120 bp, 239 bp, and

359 bp. PCR products of genomic DNA or pre-mRNA (middle and right columns of Figure 3-1) contain a second Dde I site common to all products as well as the polymorphic Dde I site in the mutant PCR product and the BsaA I site in the wild type PCR product. Dde I digestion for these PCR products yields four fragments: 182 bp, 110 bp, 72 bp, and 30 bp. The BsaA I digestion yields three fragments: 212 bp, 140 bp, and 72 bp.

Heteroduplex products form during PCR amplification when one strand has the wild type sequence while the other has the mutant sequence, thus creating a single base mismatch at nucleotide 1047. These heteroduplexes are not cleaved by either BsaA I or Dde I, but can be accounted for by adopting the simple correction method of Apostolakos (Apostolakos et al., 1993). After the PCR, all products are heat-denatured, and then slowly reannealed to duplex DNA. In this process, all the wild type (W) and mutant (M) product stands will randomly anneal with W and M complementary strands giving duplex wild type (WW), mutant (MM) and heteroduplex (WM) forms. Only the WW products will be cut by BsaA I and only the MM products will be cut by Dde I. Therefore, by measuring the fraction of cleavage products for these two digestions, the fraction of WW and MM in the PCR products can be easily calculated according to the equation, $W^2+2MW+M^2=1$, where W and M are the fractions of wild type and mutant strands, respectively. Since W+M must be equal to 1, it is also possible to confirm that both the digestions have been complete. This method eliminates an incomplete restriction enzyme digestion as a variable experimental factor.

To determine the ratio between the wild type and mutant transcripts we used a quantitative RT-PCR (Gilliland et al., 1990; Siebert and Larrick, 1992). Primer pairs

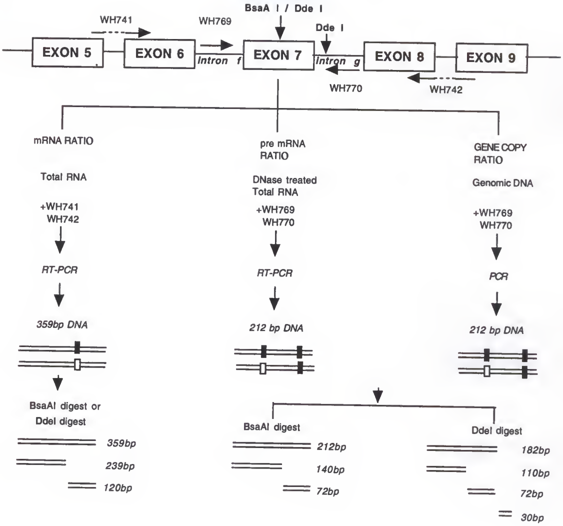

Figure 3-1. Strategy for using RT-PCR and PCR to determine the ratio of wild type to mutant β-PDE for mRNA, pre-mRNA, and gene copies. For the mRNA ratio (left column), total RNA from *rd*/+ retinas was used as the RT-PCR template with the exon-specific primers WH741, WH742. The PCR product was 359 bp for either the homoduplex wild type or mutant and heteroduplex (not shown). Black rectangles (▮) represent Dde I restriction sites; Open rectangles (▯) represent the BsaA I restriction site. For pre-mRNA or gene copy ratios (middle and right columns), DNase-treated total RNA or genomic DNA was used as the RT-PCR or PCR template respectively, exploying the intron specific primers WH769 and WH770. The RT-PCR product is 212 bp, including homoduplexes for wild type or mutant strands and heteroduplex (not shown). There are two Dde I restriction sites in the PCR products, one is a site common to all the PCR products, the other is the polymorphic site distinguishing the wild type (BsaA I site) and mutant sequence (Dde I site). The digestion fragments are shown diagramatically (not to scale).

flanking the mutation site were used to amplify product from total RNA from the heterozygous *rd*/+ retinas. The primers are specific for exons 5 and 6 (5' primer) and for exons 8 and 9 (3' primer). Using primers that span 2 exons largely avoids interference from unspliced pre-mRNA template in the RT-PCR. The equivalent fraction of PCR product from different cycles was run on agarose gel, and plotted versus the cycle number. The linear range for this PCR amplification was from cycle 15 to 30 (Figure 3-2). The yield of PCR products saturated after cycle 30 due to loss of Taq polymerase activity, limiting amounts of dNTPs or inhibition by side products. Since there is just one nucleotide difference between the wild type and mutant transcript and the same primers are used in both RT-PCR reactions, the amplification efficiency of the wild type and mutant mRNA should be identical. To confirm this, we set up a RT-PCR cycle titration series in which products from different numbers of PCR cycles were purified and digested with BsaA I (Figure 3-2). If the amplification efficiency for the wild type and the mutant transcript is identical (Pannetier et al., 1993; Souaze et al., 1996), their ratio should remain unaffected by PCR cycle number under conditions in which the amount of product is proportional to the number of the cycles completed. This ratio was essentially constant between 25 and 40 cycles (Figure 3-2). Between 15 and 20 cycles, the wild type transcript amount was only slightly higher, possibly because the amplification had not progressed sufficiently to accurately quantitate PCR products or because the effect of background signal was too high for an accurate ratio to be determined. The linear range of this RT-PCR reaction was therefore from 15 to 40 cycles, and we chose 30 cycles as our standard condition in all experiments. In this initial experiment, we found that *rd* mutant mRNA bearing the nonsense mutation was significantly underrepresented relative

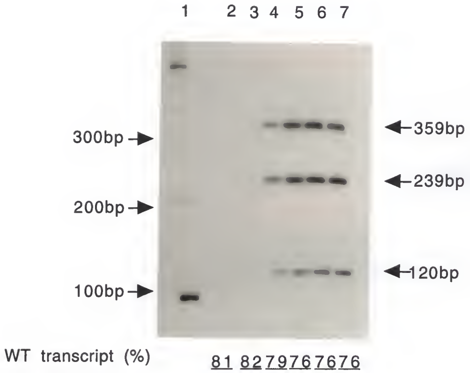

Figure 3-2. RT-PCR cycle titration. RT-PCR products of β-PDE mRNA using increasing cycle numbers were digested with BsaA I and separated by electrophoresis in an 8% polyacylamide gel. Lane 1: 100 bp marker. The sizes of the marker are indicated on the left side of the gel. Lanes 2-7: digested products from 15, 20, 25, 30, 35 and 40 cycles. The sizes of the digested fragments are indicated on the right side of the gel. The percentages of wild type products in the total PCR products are shown at the bottom of each lane.

to the wild type. As a fraction of the total β-PDE transcript in the heterozygous *rd*/+ mouse retina, about 24% was derived from the mutant gene, the remaining 76% was the wild type sequence, a wild type to *rd* ratio of 3.2.

The β-PDE mRNA *rd*/+ Ratio is Unequal and Unchanged in 3 Strains of Heterozygous *rd*/+ Mice

To make sure that this unequal ratio between the wild type and mutant mRNA was not due to the genetic background of the strain of the mouse tested (i.e. due to a non β-PDE gene effect), the same RT-PCR was performed using total RNA from three different heterozygous *rd*/+ mouse strains as template (Figure 3-3). These three strains have different genetic backgrounds for either or both the wild type allele and the *rd* allele. We found that the unequal mRNA ratio is maintained in all three strains (Table 3-1). In each, the ratios of wild type to mutant is 3-4:1. Therefore, this appears to be a general phenomenon intrinsic to mutant β-PDE expression and metabolism in the heterozygous *rd*/+ mouse, not an effect of the genetic background of the mouse strain carrying the mutant allele.

The β-PDE *rd*/+ Gene Copy Ratio is Equal in 3 Strains of Heterozygous *rd*/+ Mice

Even though we used the total RNA of heterozygous *rd* /+mouse retinas as RT-PCR templates, it is worth formally excluding the possibility that the unequal gene expression ratio is due to unequal gene copy numbers between the wild type and mutant β-PDE's. To confirm that *rd*/+ mice have equal copy numbers of each β-PDE allele, a pair of intron specific primers flanking exon 7 were designed and *rd*/+ retinal genomic DNA was used

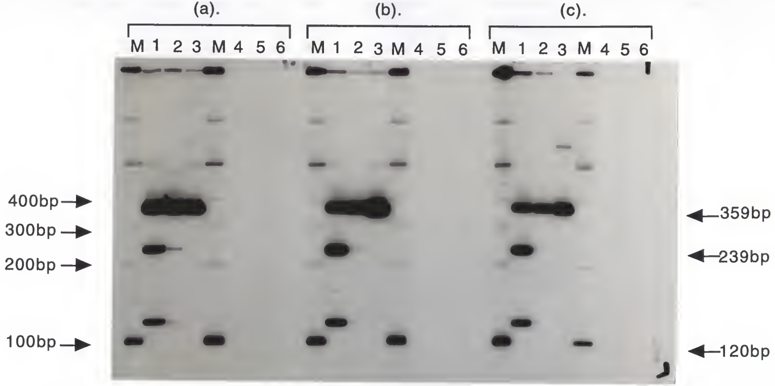

Figure 3-3. Levels of wild type and mutant β-PDE mRNAs in three strains of *rd*/+ mouse. (a) B6C3xC3H f1 rd/+ strain. The RT-PCR products were digested with BsaA I or Dde I. Lane M: 100bp marker. The sizes of the markers are indicated on the left side of the gel. Lane 1: BsaA I digestion (indicating wild type transcripts). Lane 2: Dde I digestion (indicating *rd* transcripts). Lane 3: uncut control. Lane 4: no reverse transcriptase added control products digested with BsaA I. Lane 5: no reverse transcriptase added control products digested with Dde I. Lane 6: no reverse transcriptase added control products without digestion. (b). B6CBA/J f1 *rd*/+ strain. The lane arrangement is the same as (a). (c). CSJL/J f1 *rd*/+ strain. The lane arrangement is the same as (a). The sizes of the digestion fragments are indicated on the right side of the gel (refer to Fig 1).

as the PCR template. The PCR products were then digested with BsaA I or Dde I (Figure 3-4) to distinguish *rd* from wild type gene sequences. In all three strains, wild type gene sequences comprised about 50% of the total PCR products determined either by BsaA I or Dde I digestion (Table 3-1). The wild type fraction from BsaA I digestion plus the mutant fraction from Dde I digestion was always close to 100%. Therefore both digestions were complete and since the same digestion conditions were used in the RT-PCR assay for mRNAs, our estimates of mRNA fraction are not compromised by incomplete restriction enzyme digestions. We conclude that the gene copy number of the wild type β-PDE is the same as that of the mutant gene and that the unequal ratio of mRNAs is not due to a corresponding difference in gene copy number.

The Pre-mRNA *rd*/+ Ratio is Equal in 3 Strains Heterozygous *rd*/+ Mice

To help determine more precisely how expression of wild type and mutant β-PDEs differ, we determined whether the unequal transcript ratio is also present at the pre-mRNA level. Using the same intron specific primers as for PCR assessment of gene copy number, we amplified the total RNA by RT-PCR. To avoid PCR product interference from template genomic DNA, we treated total RNA with RNase-free DNase before starting the RT reaction. The RT-PCR products were then digested with either BsaA I or Dde I (Fig 3-5) as previously. The pre-mRNA ratio between the mutant and wild type was also close to 1:1 in all three mouse strains (Table 3-1). To ensure that this protocol detected products only from pre-mRNA, a control RT-PCR reaction containing no reverse transcriptase was run for each sample. In each case, no product was

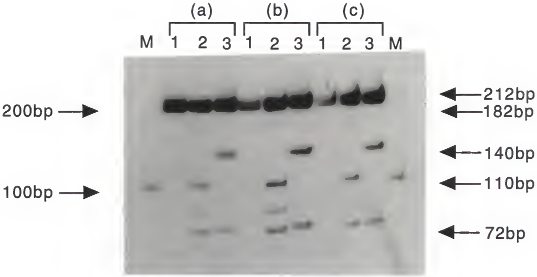

Figure 3-4. Levels of genomic wild type and mutant β-PDE gene copies in three rd/+ strains. Lane M: 100 bp marker. The sizes of the markers are indicated on the left side of the gel (refer to Fig 1). (a). B6C3xC3H fl *rd*/+ strain. Lane 1: PCR products digested with BsaA I. Lane 2: PCR products digested with Dde I. Lane 3: Uncut PCR products. (b). B6CBA/J fl *rd*/+ strain. The lane arrangement is the same as (a). (c). CSJL/J fl *rd*/+ strain. The lane arrangement is the same as (a).

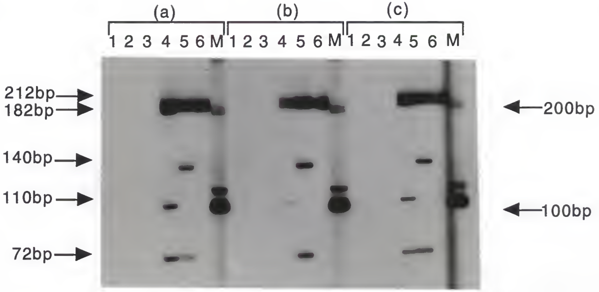

Figure 3-5. Pre-mRNA levels of wild type and mutant β-PDE in three strains of *rd*/+ mouse. (a). CSJL/J f1 *rd*/+ strain. Lane M: 100bp marker. The sizes of the markers are indicated on the right side of the gel. Lane 1: no reverse transcriptase added control digested with Dde I. Lane 2: no reverse transcriptase added control digested with BsaA I. Lane 3: no reverse transcriptase added control without digestion. Lane 4: RT-PCR products digested with Dde I. Lane 5: RT-PCR products digested with BsaA I. Lane 6: uncut RT-PCR products. The sizes of the digestion fragments are indicated on the left site of the gel (refer to Fig 1). (b). B6CBA/J f1 *rd*/+ strain. The lane arrangement is the same as (a). (c). B6C3xC3H f1 *rd*/+ strain. The lane arrangement is the same as (a).

TABLE 3-1

	β-PDE gene			β-PDE pre-mRNA			β-PDE mRNA		
rd/+ strains	B6C3 xC3H f1	B6CBA f1	CSJL/J f1	B6C3 xC3H f1	B6CBA f1	CSJL/J f1	B6C3 xC3H f1	B6CBA f1	CSJL/J f1
BsaAI cleavage (%)	22.1± 3.2	22.2± 1.4	22.0± 1.0	24.4 ± 3.6	33.5± 5.3	25.5± 4.6	58.1± 0.4	61.2± 1.1	62.9± 1.9
Wild type amount (%)	46.9± 3.5	47.2± 1.4	47.0± 1.0	49.3± 3.8	57.7± 4.9	50.3± 4.7	76.2± 0.3	78.2± 0.7	79.3± 1.2
Wild type/ Mutant ratio	0.87± 0.20	0.90± 0.07	0.89± 0.03	0.98± 0.21	1.40± 0.39	1.03± 0.27	3.2± 0.10	3.59± 0.21	3.85± 0.40

Table 3-1. Amounts of wild type and mutant *rd* β-PDE genomic DNA, mRNA and pre-mRNA in the rd/+ mouse retina. BsaA I cleavage (%) represents the fraction of total PCR products appearing in the BsaA I cleavage products. Wild type amount (%) represents the wild type fraction in the total PCR products corrected by the method of Apostolakos (Apotsolakos et al, 1990). The wild type to mutant ratio represents the value from the cleavage data corrected by the method of Apostolakos. The values given are the average ± the standard deviation from three independent experiments.

detectable, confirming that the DNase pretreatment had already removed all β-PDE DNA templates.

Discussion

Here I tested the hypothesis that the specific degradation of nonsense mRNA occurs. The ratios of wild type vs. *rd* gene copy number, pre-mRNA copy number and mRNA copy number averaged over three strains *rd*/+ mice are 0.90±0.10, 1.14±0.29 and 3.55±0.24 respectively. The unequal mRNA ratio between the wild type and mutant gene can be caused by either unequal transcription or by specific degradation of nonsense *rd* transcript. Since pre-mRNA levels are equivalent, transcription from the wild type and mutant β-PDE alleles must be the same. This suggests that the retroviral insertion in the first intron does not affect transcription of the mutant β-PDE gene. I can not exclude the possibility, however, that the retroviral insertion may interfere with the splicing of β-PDE pre mRNA. Since most alternatively spliced mRNA is less than 15% of total mRNA, it is more likely that specific degradation of the nonsense mRNA is the cause of the unequal mRNA ratio between the wild type and mutant gene.

A nonsense mutation in codon 347 and/or a retroviral insertion in first intron of the β-PDE gene are the cause of retinal degeneration in the homozygous *rd*/+ mouse. Even though the mutant gene is well characterized, the molecular mechanism relating phenotype to genotype remains unclear. One reason for this uncertainty is the enigmatic results of attempts to rescue *rd*/*rd* retinal degeneration by creating a transgenic *rd*/*rd* mouse with an extra normal copy of the β-PDE cDNA (Lem et al., 1992). In that experiment, a wild type copy of the β-PDE gene, driven by a 4.4 kb mouse opsin promoter, was added to the *rd*/*rd* mouse. This mouse line exhibited rescue of photoreceptors for 3 months. However, after that point, photoreceptor degeneration ensued. At four months, the majority of photoreceptors had been lost. Introduction of wild type copy of the β-PDE gene by viral mediated gene delivery also failed to rescue photoreceptors permanently (Bennett et al., 1996).

There are several possibilities for the failure of permanent rescue of photoreceptor in the transgenic *rd* mouse. Possibilities include inactivation of the transgene by methylation or by neighboring gene effects. Another explanation might be the semi-dominant effect of *rd* mRNA in the transgenic mouse. My results suggest that even though the *rd*/+ heterozygate has no apparent retinal phenotype, the *rd* gene may not be totally recessive. Implied in this scenario is the co-existence of both wild type and *rd* mRNAs. Since there are two copies of the mutant β-PDE gene in the *rd*/*rd*/+ transgenic mouse, the level of mutant transcript is likely to be higher than in the heterozygous *rd*/+ mouse, and this might interfere with the correct functioning of the wild type transgene product. Since the rod cGMP phosphodiesterase is a heterotetramer, expression levels of the three subunits might be critical for normal PDE activity. In the transgenic mouse line lacking the PDE γ subunit, the PDE has lower activity than in wild type mice instead of the expected higher activity (Tsang et al., 1996). Disruption of the γ subunit leads to a decrease in the amount of the α and β subunits, indicating that levels of these three subunits is co-regulated. One possible mechanism for this coordination is through the protein degradation pathway in the endoplasmic reticulum (ER). If newly synthesized proteins cannot form a proteinase-resistant complex, the free proteins might be re-localized from the ER to proteosomes, where they would be degraded (Wiertz et al., 1996; Kopito, 1997). This is true for the CD3 γ chain (Bonifacino et al., 1989) and the α, β subunits for human TCR (Wileman et al., 1990). Therefore the proper ratio of different subunits might be necessary for the integrity of photoreceptors and correct expression of PDE activity *in vivo*.

The fact here that mRNA levels do not reflect gene or pre-mRNA levels is unexpected but not unprecedented. Studies with the yeast *Saccharomyces cerevisiae* have shown that transcripts with nonsense mutations can be specifically recognized by a translation-linked RNA degradation system (Beelman and Parker, 1995). Upon translation initiation, ribosomes scan the mRNA and trigger transcript degradation when a nonsense mutation is encountered. This is accomplished by first shortening the 3' poly A tail and then decapping the mRNA (Tuite, 1996). The exonuclease Xrnl then degrades the decapped mRNA in the 5' to 3' direction. For mRNA containing a premature translational termination signal, a deadenylation-independent pathway might be more important. The mRNA becomes decapped and is then degraded by a 5' to 3' exonuclease (Muhlrad and Parker, 1994). The mRNA degradation might also be initiated by endonucleolytic cleavage within the 3' UTR, and degraded by a 3' to 5' exonuclease (Decker and Parker, 1994).

Although the mRNA structure of yeast is somewhat different from that in mammalian cells, for example, the 3' end poly A signal in yeast appears to be unique (Guo and Sherman, 1996), an analogous mechanism of nonsense mRNA degradation is likely to exist in mammalian cells. Maquat and coworkers have shown that nonsense mutations lead to nucleus-associated degradation of transcripts following splicing in mammalian cells (Belgrader et al., 1994a; Belgrader et al., 1994b; Maquat, 1995; Zhang and Maquat, 1996), and this degradation is also related to translation initiation (Belgrader et al., 1993;

Zhang and Maquat, 1997). The specific degradation of nonsense mRNA conserves the cellular energy and eliminates deleterious proteins by inhibiting their synthesis.

Human β-thalassaemia is an autosomal recessive disease of red blood cells (Kugler et al., 1995). Nonsense or frameshift mutations that cause the premature termination of translation in exon I or exon II of the β-globin gene are responsible for about half of the defects. It has been shown that specific degradation of the mutant mRNA dramatically decreases the mutant β globin transcript level (Lim et al., 1992), and that this may well protect the heterozygous carrier. It therefore appears that degradation of nonsense mRNA is important for this protection. In some cases of β-thalassaemia, if the nonsense mutant and wild type mRNA levels are equivalent in the heterozygote, individuals will be symptomatic, formally exhibiting dominant disease (Thein et al., 1990; Kazazian et al., 1992; Hall and Thein, 1994). Another similar example is recessive myosin heavy chain mutants in *Caenorhabditis elegans*, where a normally recessive mutation becomes dominant if the cells lose the ability to eliminate nonsense mRNAs (Pulak and Anderson, 1993). We have shown a similar specific mRNA degradation for a nonsense β-PDE allele that might have an analogous protective effect for the *rd*/+ heterozygous mouse.

A variety of mutations are known to be responsible for degenerative retinal diseases such as Retinitis Pigmentosa (Lindsay et al., 1992). Changes in the rod opsin coding region are a major cause, accounting for approximately one-fourth of RP. Nonsense mutations are an important subclass of such rod opsin gene mutations (Daiger et al., 1995). Some mutant alleles such as E249Ter, a glutamic acid 247 to stop codon change, cause an autosomal recessive phenotype (Rosenfeld et al., 1992b), while others, such as Q344Ter, a glutamine 344 to stop codon change, lead to autosomal dominant RP

(Jacobon et al., 1991). Why one nonsense mutation leads to dominant disease and another causes recessive disease remains unclear (Sung et al., 1991; Sung et al., 1993). One possibility is that the nonsense gene protein product may interfere with the wild type protein, either by producing a dominant negative truncated protein or by interfering at the RNA level with mRNA metabolism. In these cases, nonsense codon induced mRNA degradation pathways could play an important role in determining retinal phenotype. It has been shown that the degradation efficiency of a nonsense mRNA will increase if the mutation is close to 5' end of the message (Cooper, 1993). This boundary effect is true for most of mRNAs containing a premature termination signal. Therefore, it might be expected that a short nonsense mRNA would be degraded efficiently, thus limiting its interference with the normal gene. This should lead to little or no phenotype in the heterozygous carrier and hence to a "recessive" designation. This may explain why the E247Ter mutation is autosomal recessive. On the other hand, if degradation of the nonsense mRNA is inefficient, the mutant transcript level would remain sufficiently high to cause dominant disease, such as for the Q344Ter mutation.

The *rd* β-PDE mutation fits this boundary hypothesis well. Since the point mutation is at codon 347, located at a site only 40% through the coding sequence, mRNA degradation in the retinal photoreceptor might be quite efficient. In fact, depending on the specific kinetics of formation and decay of β-PDE mRNA, a small increase in nonsense-specific mRNA degradation could easily lead to the observed 3-4:1 ratio. The remaining mutant mRNA might not be sufficient to cause disease in the heterozygous *rd*/+ mouse, even though it may be capable of interfering with mRNA metabolism or reducing PDE activity. This effect of a truncated mRNA may also explain the *rd*/*rd*/transgenic β-PDE phenotype. Since the residual undegraded *rd* transcript in the *rd*/*rd*/+ animal should be twice that in the *rd* /+ heterozygote, the dominant nature of this 347Ter mutation when two gene copies are present may be manifested as a slow retinal degeneration, thus explaining the lack of permanent photoreceptor rescue.

Here I have shown that a β-PDE nonsense mRNA is specifically degraded in heterozygous *rd*/+ mouse retinas. Such targeted message degradation appears to be a general mechanism for protecting heterozygous carriers from the dominant effects of nonsense mutations. Nonsense mutants thereby might have a semidominant effect that becomes apparent only if overexpressed. Such degradation of nonsense mutant mRNA, if sufficiently general, might be an important factor in determining whether such mutations will cause dominant or recessive disease in photoreceptors.

CHAPTER 4

IN VITRO ANALYSIS OF HAMMERHEAD RIBOZYMES SPECIFIC TO THE mRNA OF CGMP PHOSPHODIESTERASE BETA SUBUNIT

Introduction

The *rd* mouse is one of the most studied models for autosomal recessive retinal degeneration. A nonsense mutation at codon 347 and /or a retrovirus insertion (Xmv-28) in the first intron of the β-subunit of cGMP phophosdiesterase (β-PDE) are its cause(s) (Pittler and Baehr, 1991; Bowes et al., 1993). The retinal degeneration starts at postnatal (PN) day 8, with most of the rod cells lost by PN 30. Cone cells survive until PN 30 but are eventually lost by 2-4 months. Even though the genetic basis of this retinal degeneration is known, the precise biochemical mechanism remains unclear. Since the phenotype of the *rd* mouse is autosomal recessive, a transgenic mouse line was created to test whether a wild type gene copy of β-PDE could rescue degeneration in *rd/rd* mouse. This was accomplished by introducing a wild type copy β-PDE driven by a 4.4 kb mouse opsin promoter into a line of *rd* mouse (Lem et al., 1992). This line exhibited rescue for 3 months, however photoreceptor loss still ensued after this point. By four months, the majority of the photoreceptors were lost. The reason why a wild type copy β-PDE did not fully rescue the retinal degeneration of *rd* mouse remains speculative. Perhaps the site of transgene integration or the use of a nonhomologous promoter lead to inappropriate levels of β-PDE for permanent rescue. Alternatively, the nonsense transcripts of β-PDE might interfere with the metabolism of normal β-PDE mRNA during transcript processing or translation. Supporting this, I found that specific degradation of nonsense mutant β-PDE transcript took place during or after pre-mRNA splicing in the retinas of heterozygous *rd*/+ mouse. Allele-specific degradation reduces the mutant β-PDE mRNA level dramatically in all *rd*/+ strains tested, and might lead to photoreceptor protection in heterozygotes. Therefore, the relative accumulation of nonsense β-PDE mRNA in the *rd*/*rd*/+ transgenic mice might have deleterious effects on photoreceptors in contrast to the *rd*/+ mouse.

To test this idea, I designed ribozymes to specifically target and cleave *rd* mRNA in *rd*/+ and *rd*/*rd*/+ animals. Ribozymes are catalytic RNA molecules that can specifically cleave another RNA molecule based on sequence complementary to the target RNA and short consensus sequences. Hammerhead and hairpin ribozymes are alternative structural motifs for catalytic RNA (Long and Uhlenbeck, 1993). Hammerhead ribozymes were first identified in the positive strand of satellite RNA of tobacco ringspot virus, where they intramolecularly cleave to produce monomer viral RNA from rolling circle viral RNA replication intermediates. Cleavage of substrate RNAs results in products with 5' hydroxyl and 2', 3' cyclic phosphate termini. Mutagenesis has identified 11 conserved residues in the catalytic domain of hammerhead ribozymes (Ruffner et al., 1990). An important feature for design of a synthetic ribozyme is that helix arms I and III can be adjusted to base pair with different substrate RNA sequences. The flexibility of helix I and III means that a wide variety of RNA, including many RNAs containing single base changes from the wild type, can be targeted.

Because ribozymes can specifically inhibit gene expression, they can be used for studying gene expression or suppressing pathogenic genes. Ribozymes against HIV dramatically reduce virus production (Yu et al., 1993a). Another hammerhead ribozyme suppresses EB virus gene (EBNA-1) mRNA and protein expression (Huang et al., 1997). Ribozymes are also used for cancer therapy by destroying the expression of oncogenes, such as *ras*, *bcl-abl* etc. Recently, adenovirus-mediated ribozyme expression resulted in a 96% reduction of mRNA for human growth hormone in transgenic hGH mouse liver (Lieber and Kay, 1996).

Both hammerhead and hairpin ribozymes require specific sequence motifs for the substrate RNA. For the hammerhead ribozyme, the required sequence at the cleavage site is 5' NUX↓N 3' (N is any nucleotide, X is A, C or U) (Ruffner et al., 1990). The required cleavage sequence for the hairpin ribozyme is 5' NBN↓GUC 3'(N is any nucleotide, B is G, U or C) (Anderson et al., 1994). Since the recognition sequence for hammerheads is less stringent than that of hairpin ribozymes, it is usually easier to find a matching target for hammerhead ribozymes.

A GUA target cleavage sequence exists 3 nucleotides downstream of the nonsense mutation at codon 347 of β-PDE. Therefore I designed a hammerhead ribozyme to target nonsense β-PDE transcripts using GUA as the cleavage site. My aim was to obtain a ribozyme that could specifically recognize the nonsense β-PDE transcript but not the wild type counterpart, and thereby possibly reduce the amount of nonsense β-PDE transcripts in photoreceptors without affecting the wild type β-PDE transcript level.

A hammerhead ribozyme specific to the wild type β-PDE mRNA was also designed and tested *in vitro*. The target site of this ribozyme is also located on the GUA sequence upstream of the nonsense mutation site. This ribozyme should specifically cleave the wild type β-PDE mRNA but not the mutant transcript. *In vivo* expression of this "antiwild type" ribozyme in the photoreceptor of heterozygous *rd*/+ mice should decrease levels of wild type β-PDE transcript accentuating effect of the mutant mRNA. This might negatively affect formation of active PDE, and induce retinal degeneration in heterozygous *rd*/+ mouse. This new phenotype might provide insight into the importance of the balance between the wild type and mutant transcripts in determining retinal degeneration in the *rd* mouse.

Here I characterize these two hammerhead ribozymes against β-PDE *in vitro*. The ribozyme Rz636 can specifically cleave a synthetic RNA substrate with a nonsense β-PDE sequence but not the wild type counterpart. It can also cleave full length β-PDE transcripts in presence of all retinal RNAs. The ribozyme Rz838 can specifically cleave synthetic and the full length wild type β-PDE transcripts *in vitro*. The kinetic constants of those two ribozymes were also determined using synthetic RNA substrates of several different lengths.

Materials and Methods

Oligonucleotides

WH636: 5'-GCC ACG CGT CTA AGT TTC GGC CTT TCG GCC TCA TCA GGC AGA AGA ATT CCT ATA GTG AGT CGT ATT A- 3'. This antisense primer contains a T7 promoter and an active hammer ribozyme sequence for mutant β-PDE flanked with EcoR I and Mlu I restriction sites.

WH707: 5'-GCC ACG CGT CTA AGT TTC TGC CTT TCG GCG TCA ACA GGC AGA AGA ATT CCT ATA GTG AGT CGT ATT A- 3'. This primer contains an inactive hammer ribozyme sequence for the mutant β-PDE flanked with EcoR I and Mlu

I restriction sites. Underlined nucleotides were changed from the WH636 sequence to create an inactive ribozyme as an antisense control.

WH709: 5' -GGC GGA TCC GAA TTC CGG CTG ATC ACT GGG CCC TGG CCA GTG GCC TTC CAA CCT AAG TAG CAG AAA G- 3'. This is a 5' sense overlapping primer for the mutant β-PDE substrate. The underlined nucleotide denotes the position corresponding to the nonsense mutation in β-PDE sequence.

WH708: 5' -GCG AAG CTT ACG CGT AGC ATT CAT GAT GTT ACA GAT AAA GCC ACT TTC TGC TAC TTA GGT TGG AAG G- 3'. This is a 3' antisense overlapping primer for the mutant β-PDE substrate. The underlined nucleotide denotes the position corresponding to the nonsense mutation in β-PDE sequence.

WH710: 5' -GGC GGA TCC GAA TTC CGG CTG ATC ACT GGG CCC TGG CCA GTG GCC TTC CAA CCT ACG TAG CAG AAA G- 3'. This is a 5' sense overlapping primer for the wild type β-PDE substrate. The underlined nucleotide denotes the position corresponding to the nonsense mutation in β-PDE sequence.

WH711: 5' - GCG AAG CTT ACG CGT AGC ATT CAT GAT GTT ACA GAT AAA GCC ACT TTC TGC TAC GTA GGT TGG AAG G- 3'. This is a 3' antisense overlapping primer for the wild type β-PDE substrate. The underlined nucleotide denotes the position corresponding to the nonsense mutation in β-PDE sequence.

WH789: 5'-AUG CUA AGU AGC AGA A-3'. This is an RNA oligonucleotide containing the mutant β-PDE mRNA sequence (+1034 to +1049). The underlined nucleotide denotes the position corresponding to the nonsense mutation in β-PDE sequence.

WH790: 5'-AUG CUA CGU AGC AGA A-3'. This is an RNA oligonucleotide containing wild type β-PDE mRNA sequence (+1034 to +1049). The underlined nucleotide denotes the position corresponding to the nonsense mutation in β-PDE sequence.

WH838: 5'-GCC ACG CGT CTA CGT TTC GGC CTT TCG GCC TCA TCA GGC AGA AGA ATT CCA TA- 3'. This is an antisense primer containing an active hammer ribozyme sequence for the wild type β-PDE mRNA flanked with EcoR I and Mlu I restriction sites. The outlined nucleotide is the site corresponding to the mutated position of β-PDE in the *rd* mouse.

WH839: 5'-TAT GGA ATT CTT CTG CCT GAT GAG GCC GAA AGG CCG AAA CGT AGA CGC GTG GC -3'. This is a sense primer containing an active hammer ribozyme sequence for the wild type β-PDE mRNA flanked with EcoR I and Mlu I restriction sites. The outlined nucleotide is the site corresponding to the mutated nucleotide of β-PDE in the *rd* mouse.

WH840: 5'-TAT GGA ATT CTT CTG CCT GTT GAC GCC GAA AGG CAG AAA CGT AGA CGC GTG GC -3'. This is a sense primer containing an inactive hammer ribozyme sequence for the wild type β-PDE mRNA flanked with EcoR I and Mlu restriction sites. The underlined nucleotides were changed from the WH839 sequence to create an inactive ribozyme as an antisense control.

WH841: 5'-GCC ACG CGT CTA CGT TTC TGC CTT TCG GCG TCA ACA GGC AGA AGA ATT CCA TA- 3'. This is an antisense primer containing an inactive hammer ribozyme sequence for the mutant β-PDE mRNA flanked with EcoR I and Mlu I restriction sites. The underlined nucleotides were changed from the WH838 sequence to create an inactive ribozyme as an antisense control.

Plasmid Construction for Substrate and Ribozyme RNAs

Clone pMT contained the *rd* mutant β-PDE substrate sequence (95 nucleotides), which was subcloned into the EcoR I and Mlu I sites of plasmid pHC (Altschuler et al., 1992). Two overlapping oligonucleotides (WH708, WH709, 200 pmole each) were annealed by heating at 94°C for 2 minutes in 20 mM Tris-HCl pH 7.5, 50 mM NaCl, then incubated at 55°C for 15 minutes and shifted to ice for another 5 minutes. The annealed oligonucleotides were ethanol precipitated, resuspended in dH_2O and the single stranded regions filled in using 10 units of the large fragment of DNA polymerase I (GIBCO/BRL) in 1mM dNTP, Reaction buffer 3 (BRL) at 37°C for 1 hour. After heat inactivating the polymerase at 65°C for 15 minutes, the filled-in oligonucleotides were ethanol precipitated and digested with 30 units each of EcoR I and Mlu I overnight at 37°C. The digested oligonucleotides were then ethanol precipitated again and ligated into the EcoR I and Mlu I sites of the plasmid pHC downstream of a T7 RNA polymerase promoter sequence. Ligated plasmid DNA was used to transform competent *E. coli* DH5-α cells by heat shock at 42°C for 90 seconds. Colonies were screened by ampicillin resistance and restriction digestion and verified by sequencing.

Clone pWT containing the wild type β-PDE substrate sequence (95 nucleotides) was constructed similarly to pMT using two overlapping oligonucleotides (WH710, WH711).

Clone pRz636 containing a hammerhead ribozyme specific to nonsense β-PDE transcript was constructed similarly to pMT. An oligonucleotide (WH 636) was annealed with T7 top strand primer, filled in with Klenow DNA polymerase and then digested with EcoR I and Mlu I. The digested oligonucleotides were ligated into EcoR I and Mlu I sites of plasmid pHC.

Clone pWRz containing an inactive hammerhead ribozyme specific to nonsense β-PDE transcript was constructed similarly to pRz636. This clone served as an antisense control for hammerhead ribozyme Rz636. An oligonucleotide (WH707) with three point mutations in the conserved catalytic domain sequence of the hammerhead ribozyme Rz636 was used to construct this clone.

Clone pRz838 contained an active hammerhead ribozyme specific to the wild type β-PDE transcript. This clone was constructed similarly to clone pMT. Two complete overlapping oligonucleotides (WH838 and WH839) were annealed, digested with EcoR I and Mlu I, then ligated into the EcoR I and Mlu I sites of vector pHC.

Clone pRz840 contained an inactive hammerhead ribozyme specific to the wild type β-PDE transcript. This cloned was constructed similarly to clone pRz838 using two complete overlapping oligonucleotides (WH840 and WH841).

In Vitro Synthesis of Ribozyme and Substrate RNAs

Plasmids pMT, pRz636 and pWRz were linearized with Mlu I, and pWT was linearized with Hinc III. All synthetic RNAs were generated by *in vitro* transcription using 10 units T7 RNA polymerase (Stratagene, La Jolla, CA). 1 μg linearized DNA template was used in the transcription reaction with 20 mM sodium phosphate buffer (pH 7.7), 8 mM $MgCl_2$, 2 mM spermidine, 2.6 mM each GTP,ATP, CTP, 0.6 mM UTP, and 10 μCi α-^{32}P UTP (NEN Du Pont) at 37°C for 2 hours. The transcription products were filtered through a Sephadex G-25 spin column, extracted with phenol:chloroform:isoamyl alcohol (25:24:1) once, chloroform once, and then ethanol precipitated with 1 μg glycogen carrier, washed with 70% ethanol and resuspended in water. The yield of each transcription reaction was determined by the specific activity of the transcription products after TCA precipitation.

TCA Precipitation

After ethanol precipitation, 5 μl of the 500 μl of *in vitro* transcription product was mixed with 5 μl tRNA (10mg/ml), and 95 μl dH_2O. This mix was added to 2 ml ice-cold 5% TCA, and incubated on ice for another 5 minutes. The precipitate was filtered on Whatman nitrocellulose membrane (BA85), and washed with 5 ml 5% TCA. The radioactivity of the precipitate was determined by liquid scintillation counting.

RNA Oligonucleotide Substrates

To determine the efficiency of the ribozyme as a function of different length RNA substrates, two short RNA oligonulceotides were synthesized directly by the University of Florida DNA Synthesis Core. WH789 (5'-AUG CUA AGU AGC AGA A-3') contains the mutant β-PDE sequence, and WH790 (5'-AUG CUA CGU AGC AGA A-3') contains the wild type β-PDE sequence (the altered nucleotide is underlined in each sequence). 50 μl of each RNA oligonucleotides was deprotected after synthesis by addition of 100 μl fresh triethylamine trihydrofluoride and mixed at room temperature for 24 hours. The reaction was quenched by adding 20 μl dH_2O and 1 ml 1-butanol. After incubation at -20°C for 45 minutes, the RNA oligonucleotides were centrifuged (12,000 x g) at 4°C for 10 minutes. The pellets were washed with 500 μl absolute ethanol, and dried under vacuum for 15 minutes. Each pellet was then resuspended in 100 μl dH_2O, and the amount of recovered RNA was determined spectrometrically by OD at 260 and 280 nm. The deprotected RNA oligonucleotides were labeled at their 5' ends by T4 polynucleotide kinase with γ-^{32}P ATP (6000mCi/mmol, NEN Du Pont). One microliter of the 50 μl kinase reaction was diluted 1:1000, and the amount of incorporated radioactivity determined by TCA precipitation. The 5' end labeled RNA oligonucleotides were gel purified on 20%, 8 M urea polyacrylamide gels to isolate the full length 16 nt RNA oligonucleotides. The band corresponding to the full length product was excised from the gel and incubated with 20 mM EDTA, 500 mM ammonium acetate (pH 5.3) at 37°C for 2 hours. The eluates were extracted once with phenol:chloroform:isoamyl alcohol (25:24:1), once with chloroform, and then ethanol precipitated and resuspended in 50 μl RNase-free dH_2O. The amount of purified oligonucleotide was determined by specific activity after TCA precipitation of an aliquot as above.

Retinal RNA Extraction

Total RNA was purified from the retinas of heterozygous *rd*/+ mice (B6C3H f1 strain, Jackson Laboratory) by Trizol extraction (Gibco BRL) according to the manufacturer's instructions. RNA was then extracted with phenol/chloroform, ethanol precipitated with 0.3 M sodium acetate (pH 5.3) and resuspended in RNase-free H_2O to obtain approximately 1 μg/μl. The RNA concentration was determined spectrophotometrically, and its integrity verified by electrophoresis on formamide / formaldehyde agarose (1.2%) gels. Typically, one retina yielded 6-10 μg of total RNA.

Ribozyme Cleavage Reaction Conditions

Standard 15 μl cleavage reactions were performed with 20 mM Tris-HCl (pH 7.5), 20 mM $MgCl_2$, 100 nM substrate RNA and 100 nM ribozyme, with incubation at 37°C. Each ribozyme was renatured in 20 mM Tris-HCl (pH 7.5), 10 mM $MgCl_2$ at 37°C for 3 hours before the cleavage reaction. Cleavage reactions were stopped by RNA dye (50 mM EDTA, 10 M urea, 0.02% Bromophenol blue, and 0.02% xylene cyanol) and separated by 6%, 8 M urea polyacrylamide gel electrophoresis. For cleavage of full length β-PDE RNA, 1 μg total retinal RNA from *rd*/+ mice was used in the reaction, and incubated with different amounts of ribozyme (from 6.6 μM to 6.6nM) for 12 hours at 37°C.

Magnesium Titration of the Cleavage Reaction

Ribozyme cleavage reactions (15 μl) were performed with different magnesium concentrations (from 5 mM to 200 mM). 3 μl of the reaction mix were taken out at designated time points and quenched with 10 μl stop solution (100 mM EDTA, 100 mM NaOAc, 50 mM Tris-HCl, pH 7.5, 1 μg tRNA). The reaction mix was then ethanol precipitated in10 μl RNase-free dH_2O and mixed with 5 μl RNA loading dye. For the 95 nt long substrate, the cleavage products were separated on 6%, 8 M urea sequencing gels. For the 16 nt RNA oligonucleotide substrate, the cleavage products were separated on 10%, 8 M urea gels.

Time Course of the Cleavage Reaction

Three microliters were taken out of the 15 μl reaction sample at designated time points and the reaction was stopped by adding 3 μl RNA loading dye. Products of the reaction were then separated on either 6% (for 95 nt substrate) or 10% (for 16 nt RNA oligonucleotide), 8 M urea polyacrylamide gel.

Kinetic Analysis

Internally-labeled *in vitro* transcripts or end-labeled synthetic RNA oligonucleotides were used as substrates for kinetic analysis. To determine the single turnover kinetic constants of Rz636 with the 95 nt RNA target, cleavage was performed with 20 mM Tris-HCl (pH 7.5), 20 mM $MgCl_2$, at 37°C for 30 minutes. The reaction samples contained a fixed amount ribozyme (100 nM) and increasing amounts of RNA substrate. For single turnover kinetic constants of Rz636 or Rz838 with the 16 nt RNA oligonucleotide target, a fixed amount ribozyme (200 nM) and increasing amounts of substrate were used in the cleavage reaction. For multi-turnover kinetic constants of either Rz636 or Rz838 with the 16 nt RNA substrate, 20 nM of ribozyme and increasing amounts of substrate were used in the reaction. Values of V_{max}, K_M and k_{cat} were determined by double reciprocal plots of velocity versus substrate concentration.

RT-PCR for Detecting Full Length β-PDE mRNA Cleavage by Ribozymes

The cleavage of the nonsense or wild type full length β-PDE mRNA by Rz636 or Rz838 was determined by RT-PCR and RFLP. The amount of nonsense β-PDE mRNA was determined by comparison with the wild type β-PDE mRNA amount. After ribozyme cleavage, retinal RNA was reverse transcribed into cDNA with 25 pmole WH742, then amplified by PCR using 10 pmole of primers WH741, WH742. PCR conditions were denaturation at 94°C for 5 minutes, and then 30 cycles of 94°C for 1 min, 55°C for 1 min and 72°C for 1 min. After the reaction, the PCR product was denatured at 94°C for 15 minutes and slowly cooled to room temperature over 3 hours. The PCR products were purified using a wizard PCR purification kit (Promega) following the manufacturer's protocol, ethanol precipitated and resuspended in 20 μl H_2O. 5 μl of PCR products were digested with 10 units BsaA I (New England Biolabs) in NEB buffer 3 at 37°C overnight, then ethanol precipitated using 1 μl glycogen (5mg/ml) as a carrier. Half of the digestion product was mixed with 1 μl of 5 fold concentrated agarose dye (50% sucrose, 50 mM EDTA, 0.2% bromophenol blue and 0.2% xylene cyanol) and run on an 8% nondenaturing polyacrylamide gel at 600 volts for 3 hours. The digestion product bands were quantified by ImageQuant version 3.2 using a PhosphoImager (Molecular Dynamics). For Dde I digestion, 5 μl of each PCR product was incubated with 20 units Dde I (Gibco BRL) in BRL Restriction buffer 3 at 37°C overnight, ethanol precipitated as for the BsaA I digestion, and quantified as above. The amount of wild type or mutant β-PDE was corrected by the method of Apostolakos (Apostolakos et al., 1993).

Results

Ribozyme Rz636 Specifically Cleaves the Mutant β-PDE Transcript

To cleave nonsense β-PDE transcript, I designed a hammerhead ribozyme (Rz636) specific to nonsense β-PDE transcripts (Figure 4-1A). I substituted the A:T base pair with a G:C base pair in helix II to increase the stability of ribozyme structure. I also changed 3 conserved nucleotides in the catalytic domain to create an inactive ribozyme, WRz, and used it as a control for determining whether ribozyme binding to target without cleavage had any effect on the measured level of each substrate (antisense effect). Since there is only one nucleotide difference between the mutant and wild type substrates (at site 15.2), I first needed to determine the specificity of the active ribozyme for the mutant substrate. For Rz636, the cleavage reaction with the 95 nt mutant target RNA resulted in two products, the predicted 55nt long 5' fragment and 40nt long 3' fragment (Figure 4-2). In contrast, incubation with 120 nt wild type RNA substrate did not produce any cleavage products (Figure 4-2). Therefore, Rz636 specifically recognizes the mutant substrate and cleaves it. The inactive ribozyme WRz cannot cleave either wild type or mutant substrate. Since WRz has the same annealing sequence as Rz636 but lacks catalytic activity, it is a proper control for any antisense effect in *in vivo*.

Ribozyme Rz838 Specifically Cleaves the Wild Type β-PDE Transcript

To determine the specificity of Rz838, mutant or wild type RNA oligonucleotides were incubated with either Rz838 or Rz840 (Figure 4-3). Ribozyme Rz838 cleaved only the wild type oligonucleotides, not the mutant counterpart. Control inactive ribozyme could not cleave either wild type or mutant RNA oligonucleotides. Ribozyme Rz838 also could cleave a longer wild type β-PDE RNA (120 nt) produced by *in vitro* transcription, but with a lower efficiency (data not shown). This is consistent with the hypothesis that local secondary structure of RNA can adversely affect the ribozyme cleavage reaction.

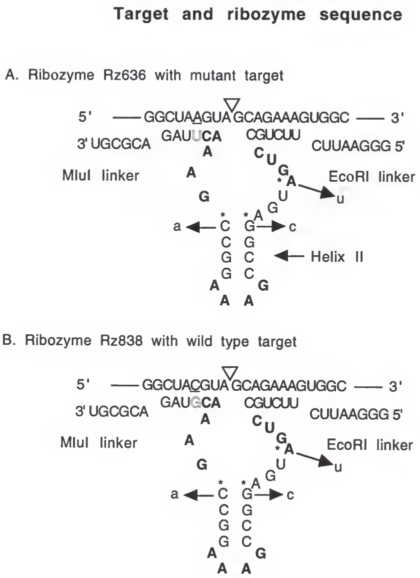
Target and ribozyme sequence
A. Ribozyme Rz636 with mutant target
5' —— GGCUAAGUA GCAGAAAGUGGC —— 3'
3' UGCGCA GAUUCA CGUCUU CUUAAGGG 5'
A C U G *A U G
MluI linker
EcoRI linker
u
a
c
A G * * C G C G G C G C A G A A
Helix II
B. Ribozyme Rz838 with wild type target
5' —— GGCUACGUA GCAGAAAGUGGC —— 3'
3' UGCGCA GAUGCA CGUCUU CUUAAGGG 5'
A C U G *A U G
MluI linker
EcoRI linker
u
a
c
A G * * C G C G G C G C A G A A

Figure 4-1: Schematic diagram of the ribozymes specific to β-PDE mRNAs. (A). Ribozyme Rz636 with its mutant β-PDE substrate. (B). Ribozyme Rz838 with its wild type β-PDE substrate. Conserved sequences necessary for ribozyme activity are shown as bold letters. The nucleotides with asterisks in the catalytic core were mutated to the indicated nucleotides in the individual control ribozymes. The underlined nucleotide represents the C to A mutation in cGMP β-PDE mRNA of *rd* mice. The open triangle shows the ribozyme cleavage site. EcoR I and Mlu I sequences were linked to the ribozyme sequence for cloning.

Lane	1	2	3	4	5	6	7
Active Rz	+	+	+	+		+	
Control Rz					+		+
Wt target						+	+
Mutant target	+	+	+	+	+		

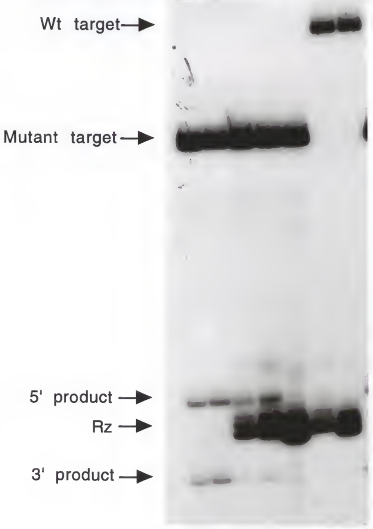

Figure 4-2: Specificity of ribozyme Rz636. Unlabeled (lane 1-2) or α-^{32}P UTP labeled (lane 3-7) active ribozyme Rz636 or control ribozyme WRz were incubated with either the 96 nt mutant β-PDE substrate (lane 1-5) or the 122 nt wild type β-PDE substrate (lane 6-7) at 37°C for 30 minutes. The sizes of ribozymes, substrates and cleavage products are indicated on the left side of the figure.

Magnesium Concentration Affects the Rz636 Cleavage Reaction

Magnesium is required in the breakage of the phosphodiester bond in the RNA substrate by hammerhead ribozyme (Long and Uhlenbeck, 1992). It may also help the ribozyme-substrate complex fold into an active conformation (Long and Uhlenbeck, 1992). A properly functioning ribozyme is therefore typically quite sensitive to the level of magnesium in the reaction. Therefore, we determined Rz636 activity on the 95 nt target as a function of magnesium concentration (Figure 4-4A). In 20 mM magnesium, Rz636 cleaves about 15% mutant substrate in 30 minutes, but in 200 mM magnesium, it cleaves about 60% in the same period (Figure 4-4B). Ribozyme Rz636 is also active in 10 mM magnesium (the lowest magnesium concentration tested). Since more mutant substrate can be cleaved as a function of increasing magnesium concentration, Rz636 appears to exhibit typical ribozyme behavior. The concentration of magnesium for catalysis in the reaction is in the nanomolar range (2 moles of magnesium per mole of ribozyme). Consequently, the increased activity observed on the increased magnesium concentration up to 200 mM affects the stabilization of the active RNA structures. Because magnesium is critical for either or both activity and ribozyme conformation, we also tested Rz636 activity against the wild type substrate at the highest magnesium concentration, and found no cleavage products (data not shown). Therefore, the specificity of Rz636 is maintained even at very high, nonphysiological magnesium concentrations. The inactive ribozyme WRz also cleaved neither the wild type nor the mutant substrate at high magnesium concentration (data not shown).

Figure 4-3. Specificity of β-PDE ribozymes with RNA oligonucleotide substrates. Analysis of riobozyme Rz636 (specific to mutant β-PDE mRNA), Rz838 (specific to wild type β-PDE mRNA) and Rz840 (inactive control ribozyme for Rz838) is indicated above the gel. The ribozyme, substrate and cleavage products are indicated on the left side of the figure.

Lane:	1	2	3	4	5	6	7	8
Rz (WT control)	+	+						
Rz (WT)			+	+				
Rz (mutant)					+	+		
Target (WT)	+		+		+		+	
Target (mutant)		+		+		+		+

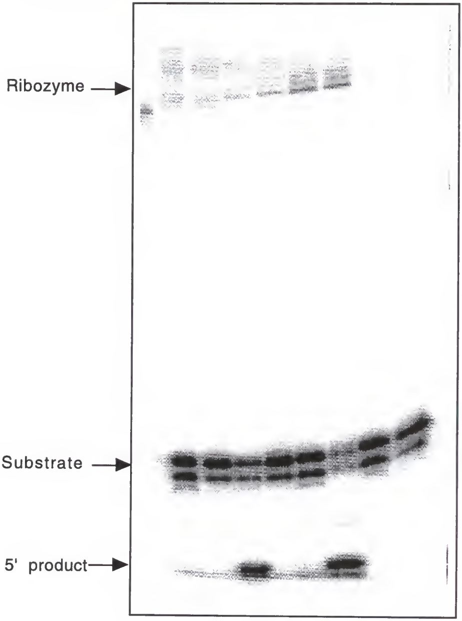

Figure 4-4: Magnesium titration for ribozyme Rz636. α-^{32}P UTP labeled ribozyme Rz636 was incubated with 96 nt mutant β-PDE substrate with increasing magnesium concentration. (A). Lane 1: 10 mM magnesium. Lane 2: 25 mM magnesium. Lane 3: 50 mM magnesium. Lane 4: 75 mM magnesium. Lane 5: 100 mM magnesium. Lane 6: 150 mM magnesium. Lane 7: 200 mM magnesium. Lane 8 and 10: 96 nt substrate alone with 10 mM magnesium. Lane 9: 96 nt substrate alone with 150 mM magnesium. The sizes of ribozyme (Rz), target (T) and cleavage products (5' product and 3' product) are indicated on the left side of the figure. (B). Graph of magnesium titration for ribozyme Rz636. The cleavage percentage given is the average for three experiments, and error bars represent the standard deviation.

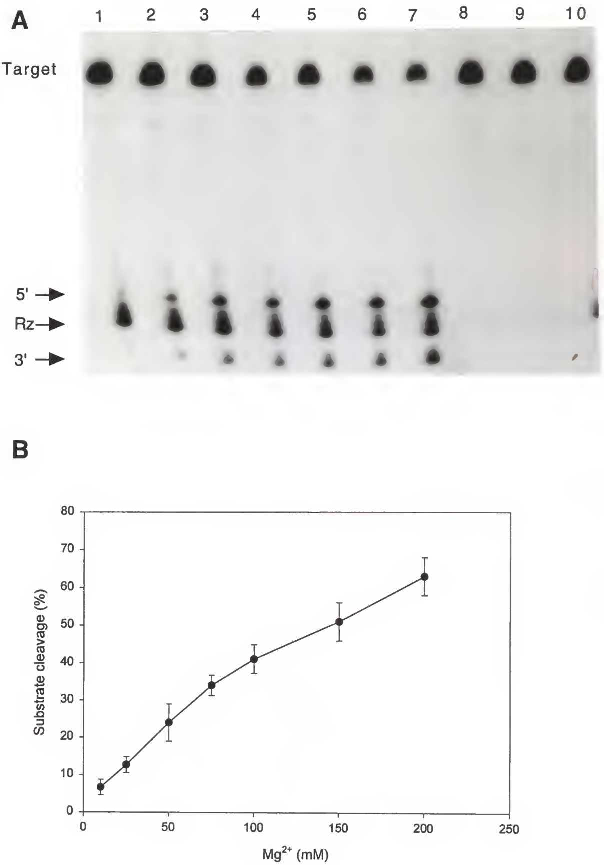
A
1
2
3
4
5
6
7
8
9
10
Target
5'
Rz
3'
B
Substrate cleavage (%)
0
10
20
30
40
50
60
70
80
0
50
100
150
200
250
Mg^{2+} (mM)

Magnesium Concentration Affects the Cleavage Reaction of Rz838

A similar magnesium titration experiment was set up for ribozyme Rz838 (Figure 4-5). The maximum amount of cleavage for substrate WH789 at 10 hours was about 38% (see the time course of Rz838 (Figure 4-7)). The cleavage product percentage was set to 100% on the assumption that the remaining target is folded and inaccessible for cleavage. In 5 mM magnesium, about 5% substrate was cleaved in 15 minutes, with 28% cleaved after a 1 hour incubation. The cleavage increased with increasing magnesium concentration. About 43% of the substrate was cleaved in 1 hour at 20 mM magnesium, while almost 62% was cleaved after 2 hours in 200 mM magnesium (Figure 4-5). Therefore, this ribozyme can cleave its substrate very efficiently under the optimal conditions. It can also function at physiological magnesium concentration.

Cleavage Time Course for Rz636

To determine activity of Rz636 during a cleavage reaction with the 95 nt target RNA, we performed a time course experiment for Rz636 (Figure 4-6A). The cleavage products increased with the reaction time. About 60% of the mutant substrate was digested after 10 hours incubation at 20 mM magnesium. Almost 100% of the substrate was cleaved after 21 hours (Figure 4-6B). Essentially all the substrate was cleavable since no plateau in level of products was seen during the reaction. No cleavage products were detected when the wild type target was incubated with Rz636 after 10 hours incubation (data not shown). The inactive ribozyme also did not digest either wild type or mutant substrate after 10 hours incubation (data not shown). This sort of quantitative analysis of ribozyme

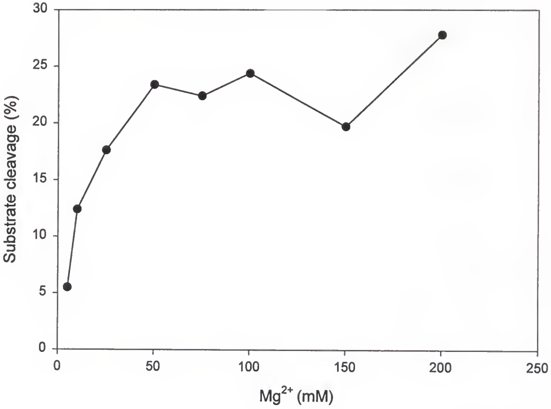

Figure 4-5: Graph of magnesium titration of Rz838 cleavage of RNA oligonucleotides. Ribozyme Rz838 was incubated with wild type β-PDE oligonucleotide substrate WH790 in increasing magnesium concentration at 37°C for 15 minutes

Figure 4-6: Time course for ribozyme Rz636 cleavage. Unlabeled ribozyme Rz636 was incubated with the 96 nt mutant β-PDE substrate. Aliquots were analyzed at the time points indicated. (A). Lane 1: 30 minutes. Lane 2: 1 hour. Lane 3: 2 hours. Lane 4: 3 hours. Lane 5: 4 hours. Lane 6: 6 hours. Lane 7: 8 hours. Lane 8: 10 hours. Lane 9: 21 hours. Lane 10: 22 hours. The target substrate and ribozyme products are indicated on the left side of the figure. (B). Graph of the time course for Rz636. The cleavage percentage given is the average for three experiments, and error bars represent the standard deviation.

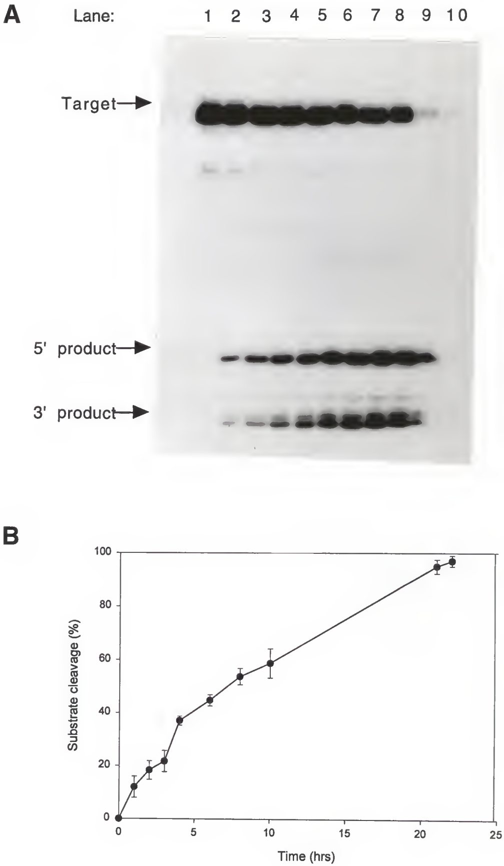
A
Lane:
1
2
3
4
5
6
7
8
9
10
Target
5' product
3' product
B
100
80
60
40
20
0
Substrate cleavage (%)
0
5
10
15
20
25
Time (hrs)

activity allowed a choice of reaction conditions to be made for the subsequent kinetic analysis (below).

Cleavage Time Course for Rz838

The time course of Rz838 was determined like that for Rz636 (Figure 4-7A). The reaction plateaued after 30 minutes with about 38% of the target cleaved (Figure 4-7B). Since the rest of substrate could not be consumed even after long incubation, it appears that this RNA substrate contained a substantial fraction of uncleavable RNA. This may mean that some RNA was in an unproductive conformation or that the RNA was incompletely deprotected. Since uncleaved RNA would not be expected to affect the actual cleavage, all the cleavage rates were calculated assuming 38% cleavage was the complete reaction. Cleavage was very efficient for Rz838, and practically finished in 15 minutes (about 90% of the target was cleaved in 15 minutes).

Cleavage of a Short Synthetic RNA Oligonucleotides Substrate

The substrates used in the previous experiments were *in vitro* transcription products 95-122 nt long. Typically, however, relatively short substrate RNAs (15-30 nt) are used for initial ribozyme characterization. An advantage in using longer RNA substrates is that any secondary structure is likely to be closer to that of the full length transcript, since the secondary structure of the annealing site is primarily determined by immediate neighboring RNA sequences. Ribozyme cleavage reactions can be separated into three steps: annealing, cleavage and dissociation. The annealing and dissociation steps are the most important factors affecting the velocity of the cleavage reaction. The enhanced

Figure 4-7. Time course for ribozyme Rz838 and Rz636 cleavage of RNA oligonucleotides. (A). Ribozyme Rz838 was incubated with wild type β-PDE substrate WH790. Aliquots were analyzed at different time points. Lane 1: 5 minutes. Lane 2: 15 minutes. Lane 3: 30 minutes. Lane 4: 1 hours. Lane 5: 2 hours. Lane 6: 4 hours. Lane 7: 8 hours. Lane 8: 10 hours. (B). Ribozyme pRz636 was incubated with mutant β-PDE substrate WH789. The lane arrangement is the same as (A). The sizes of substrate (S) and 5' cleavage products (5') are indicated on the left side of the figure. (C). Graph of the time course of Rz838 and Rz636 cleavage.

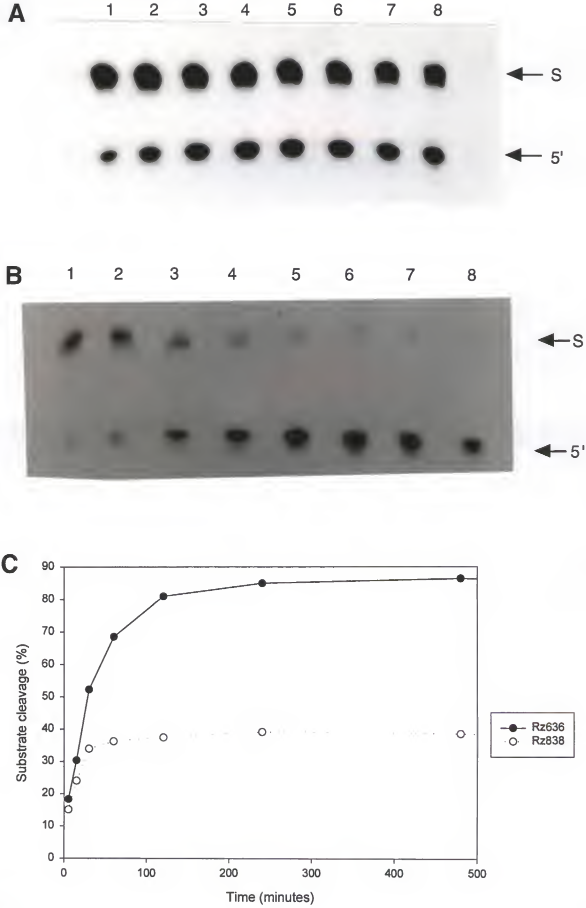
A
1
2
3
4
5
6
7
8
S
5'
B
1
2
3
4
5
6
7
8
S
5'
C
Substrate cleavage (%)
0
10
20
30
40
50
60
70
80
90
0
100
200
300
400
500
Time (minutes)
Rz636
Rz838

secondary structure in a long RNA substrate could dramatically affect the annealing and dissociation between ribozyme and substrate, thus slowing the cleavage rate. It has been reported that a 4-log difference in the velocity for the same ribozyme can exist between 950 nt and 15 nt substrates. Since kinetic data for most well characterized ribozymes have been determined using short RNA oligonucleotides, we synthesized such RNA oligonucleotides as substrates for a reliable comparison. The active ribozyme Rz636 can specifically cleave mutant RNA oligonucleotide targets but not the wild type counterpart (Figure 4-3). As expected, the cleavage reaction is much faster than that with the longer RNA substrate. About 70% of the 16 nt substrate was cleaved in 2 hours compared to 30% of the 95 nt long substrate. Therefore, Rz636 retains its specificity with the short oligonucleotide substrates but has a higher reaction rate.

Kinetic Analysis of Rz636

To determine the catalytic efficiency of Rz636, I performed single turnover (ribozyme excess) and multiple turnover kinetic analysis using fixed amount ribozyme Rz636 and increasing amounts of substrate (either the 16 nt RNA oligonucleotide or the 95 nt *in vitro* transcript) (Figure 4-8). The values for V_{max}, K_M and k_{cat}/K_M were determined by double reciprocal plot of velocity against substrate concentration (Table 4-1). The K_M of Rz636 is about 30 nM, and is comparable to that of the native hammerhead ribozyme. Since the dissociation rate might also affect Km values, especially with long annealing arms, we determined the k_{cat}/K_M, which may represent a more accurate enzymatic activity under physiological conditions. The k_{cat} for reaction with the 95 nt substrate reaction is about 0.014 min^{-1}, and k_{cat}/K_M is $4x10^5 M^{-1}min^{-1}$ (data not shown). The k_{cat} from 16nt

Figure 4-8. Kinetics of ribozyme Rz636 cleavage with a mutant β-PDE RNA oligonucleotide substrate. (A). Single turnover reaction for ribozyme Rz636 (Substrate concentration rate limiting). A fixed amount of Rz636 was incubated with increasing amounts of mutant β-PDE substrate WH789 at 37°C for 15 minutes. Lane 1: 1 nM. Lane 2: 10 nM. Lane 3: 25 nM. Lane 4: 50 nM. Lane 5: 100 nM. Lane 6: 200 nM. (B). Multiple turnover reaction for ribozyme Rz838 (Ribozyme concentration rate limiting). A fixed amount of Rz838 was incubated with increasing amounts of mutant PDE substrate WH789 at 37°C for 15 minutes. Lane 1: 20 nM. Lane 2: 40 nM. Lane 3: 80 nM. Lane 4: 120 nM. Lane 5: 160 nM. Lane 6: 200 nM. (C). The double reciprocal kinetic curve for the Rz636 multiple turnover reaction.

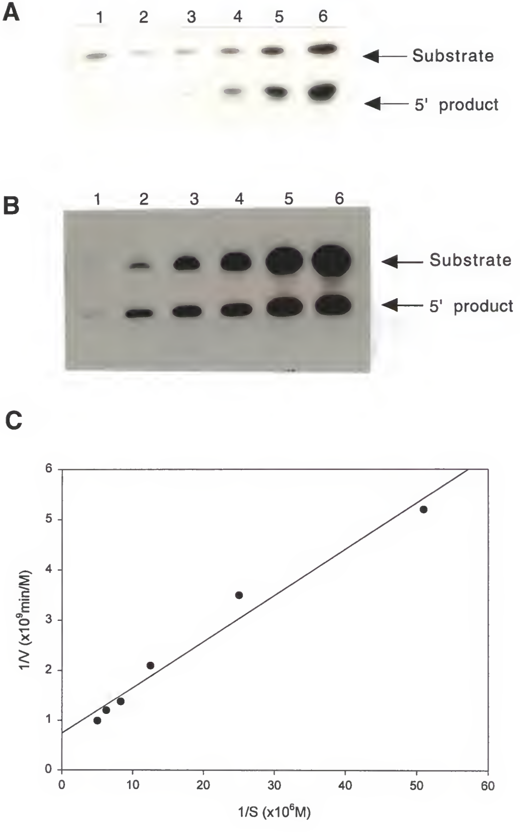
A
1
2
3
4
5
6
Substrate
5' product
B
1
2
3
4
5
6
Substrate
5' product
C
1/V (x10^{9}min/M)
0
1
2
3
4
5
6
1/S (x10^{6}M)
0
10
20
30
40
50
60

substrate is 0.17 min^{-1}, which give a k_{cat}/K_M value about $1.4x10^6$ $M^{-1}min^{-1}$ (Table 4-1). This k_{cat} value is about 13 fold higher than for the 95nt substrate, and again, it is more comparable to the natural ribozyme.

Kinetic Analysis of Rz838

Kinetic constants of single turnover and multi-turnover (target excess) reactions were determined for Rz838 similar to Rz636 using synthetic RNA oligonucleotide WH790 as the substrate (Figure 4-9). The Km of Rz838 is about 125 nM, the k_{cat} is 0.12 min^{-1}. The k_{cat}/K_M is $1x10^6$ $M^{-1}Min^{-1}$, which is similar to Rz636, and in the range of natural ribozymes (Table 4-1).

Cleavage of Full Length Mutant β-PDE mRNA by Rz636

Even though Rz636 can cleave an RNA substrate 95 nt in length at a reasonable rate, it is important to test its activity on the full length β-PDE mRNA because of the possibility of additional secondary structure in full length mRNA. If Rz636 can cleave the full length β-PDE mRNA *in vitro*, it is most likely to function within photoreceptor cells as well. Total retinal RNA was extracted from heterozygous *rd*/+ mouse retinas, and incubated with different amount of Rz636. The cleavage products were then amplified by RT-PCR using one pair exon specific primers. Since the nonsense mutation in β-PDE codon 347 creates a restriction site polymorphism (the wild type has BasA I site, and the mutant has Dde I site), I digested the RT-PCR products with either BsaA I or Dde I to determine the amount of nonsense full length β-PDE mRNA relative to wild type β-PDE mRNA. The amount of nonsense transcript before and after the cleavage

Figure 4-9. Kinetics of ribozyme Rz838 cleavage. (A). Single turnover reaction for ribozyme Rz838 (Substrate concentration rate limiting). A fixed amount of Rz838 (200 nM) was incubated with increasing amounts of wild type β-PDE substrate WH790 at 37°C for 15 minutes. Lane 1: 1 nM. Lane 2: 10 nM. Lane 3: 25 nM. Lane 4: 50 nM. Lane 5: 100 nM. Lane 6: 200 nM. (B). Multiple turnover reaction for ribozyme Rz838 (Ribozyme concentration rate limiting). A fixed amount pRz838 was incubated with increasing amount of wild type β-PDE substrate WH790 at 37°C for 15 minutes. Lane 1: 20 nM. Lane 2: 40 nM. Lane 3: 80 nM. Lane 4: 120 nM. Lane 5: 160 nM. Lane 6: 200 nM. (C). The double reciprocal kinetic curve for the Rz838 multiple turnover reaction.

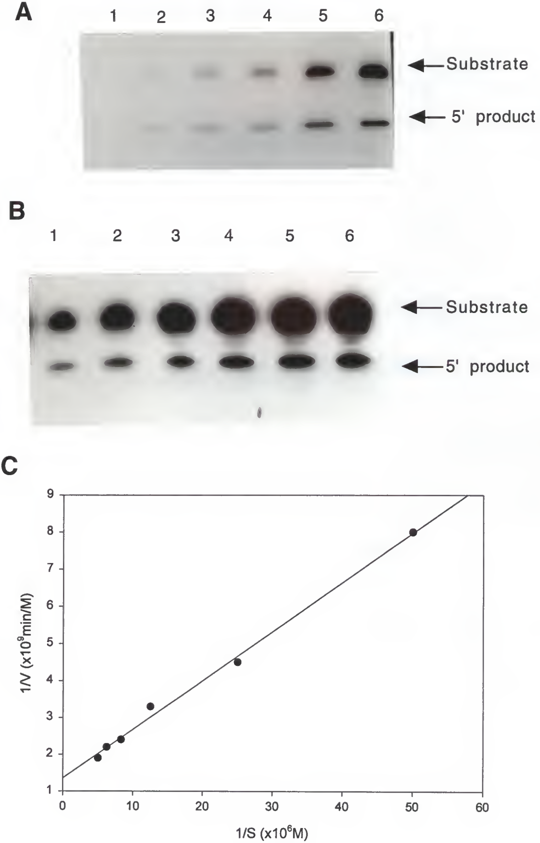
A
1
2
3
4
5
6
Substrate
5' product
B
1
2
3
4
5
6
Substrate
5' product
C
1/V (x10^{9}min/M)
1/S (x10^{6}M)
0
10
20
30
40
50
60
1
2
3
4
5
6
7
8
9

Table 4-1

Ribozyme	Target	K_{cat} (min^{-1})	K_M (nM)	K_{cat}/K_M ($M^{-1}min^{-1}$)
Rz636	96 nt β-PDE transcript	0.014	35	4×10^5
	16 nt β-PDE oligonucleotides	0.17	120	1.4×10^6
Rz838	16 nt β-PDE oligonucleotides	0.12	114	1.0×10^6

Table 4-1: Summary of kinetic constants of ribozyme Rz636 and Rz838.

(normalized to the wild type levels in each case) was compared to determine how much of nonsense full length β-PDE mRNA had been cleaved by Rz636 (Figure 4-10A). When 6.7 μM Rz636 was used in the cleavage reaction, about 65% nonsense full length β-PDE mRNA was cleaved after 12 hours incubation (Figure 4-10B). Even when 1000 fold less Rz636 was used, about 20% nonsense full length β-PDE mRNA was cleaved. Interestingly, the inactive ribozyme WRz can also decrease nonsense β-PDE mRNA by about 15% at the highest concentration of ribozyme (Figure 4-10B). This might represent an antisense effect of WRz, since ribozyme mRNA complex might interfere with the RT reaction. Alternatively, there may be non-specific degradation of mRNA during the 12 hours incubation in 20 mM magnesium. In summary, Rz636 can cleave nonsense full length β-PDE mRNA under protein-free *in vitro* conditions.

Cleavage of Full Length Wild Type β-PDE mRNA by Rz838

Total retinal RNA extracted from heterozygous *rd*/+ mice was incubated with 1000 nM Rz838. The cleavage of wild type β-PDE was determined as for Rz636. Inactive ribozyme Rz840 was incubated with the same amount of retinal RNA as a control. Active ribozyme Rz838 (1000 nM) cleaved over 40% of the wild type mRNA target after an overnight incubation. 100 nM Rz836 cleaved about 16% of the wild type mRNA under the same conditions. Control ribozyme Rz840 led to a slight decrease the level of wild type mRNA (about 2-5%), similar to that for the inactive ribozyme Rz636.

Figure 4-10. Ribozyme Rz636 cleaves full-length mutant β-PDE *in vitro*. Ribozyme Rz636 was incubated with total retinal RNA from an *rd*/+ mice retina overnight. The products were amplified by RT-PCR using primers WH699 and WH700, and digested with BsaA I which cleaves only PCR products from wild type β-PDE templates (For explanation of fragment sizes see Figure 3-1). (A). Lane M: 100 bp marker. Lane 1: Uncut RT-PCR products. Lane 2: No ribozyme incubation control. Lane 3: Total *rd*/+ retinal RNA incubated with 6.6 uM Rz636. Lane 4: Total rd/+ retinal RNA incubated with 660 pM Rz636. Lane 5: Total *rd*/+ retinal RNA incubated with 66 pM Rz636. Lane 6: Total *rd*/+ retinal RNA incubated with 6.6 pM Rz636. The sizes of RT-PCR products are indicated on the right size of the figure. (B). Graph of full-length mutant β-PDE cleavage with ribozyme Rz636 and WRz. The cleavage percentage given is the average for three experiments, and error bars represent the standard deviation.

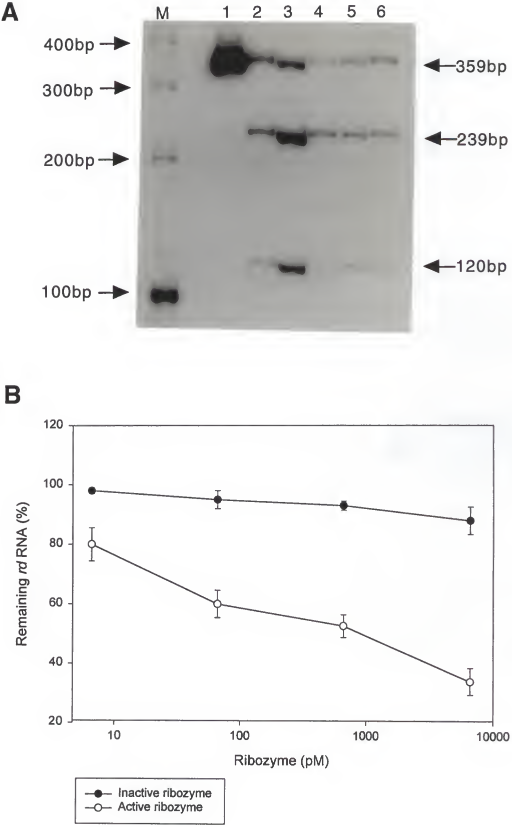
A
M
1
2
3
4
5
6
400bp
300bp
200bp
100bp
359bp
239bp
120bp
B
120
100
80
60
40
20
Remaining *rd* RNA (%)
10
100
1000
10000
Ribozyme (pM)
Inactive ribozyme
Active ribozyme

Discussion

The mutation responsible for retinal degeneration in *rd* mouse has been identified (Pittler and Baehr, 1991). Since the phenotype of *rd* mouse is autosomal recessive, a transgenic mouse line was constructed to rescue the retinal degeneration by introducing a wild type copy of β-PDE into the *rd* mouse background (Lem et al., 1992). The transgenic mouse exhibited a delay in retinal degeneration from 3 weeks to about 3 months. However, after 3 months, the retinal degeneration re-initiated. A wild type copy β-PDE delivered into the *rd* mouse retina by an recombinant adenovirus also only transiently rescued the degeneration (Bennett et al., 1996). It is important to determine why a wild type copy β-PDE cannot fully rescue the *rd* phenotype. This problem raises the question of whether retinal degeneration in the *rd* mouse is fully autosomal recessive or semi-dominant. Here, I tested the hypothesis that a properly designed ribozyme could specifically and efficiently degrade β-PDE mRNA.

It has been found that eukaryotic cells can specifically degrade some nonsense mRNAs by a translation-linked mechanism, and that this will protect cells from the deleterious effect of the mutant transcript. Alternatively, inefficient degradation of nonsense transcripts can lead to abnormal metabolism of the cells by either producing toxic truncated protein or interference with mRNA translation. Either process might produce a disease phenotype in these cases. β-thalassemia is one of the best characterized examples. Ordinarily, nonsense mutations occurring in β-globin result in an autosomal recessive phenotype. In these cases, the level of nonsense transcripts is much lower than that of its wild type counterpart due to mRNA degradation. Since cells recognize the 5' nonsense mutations more efficiently than those closer to the 3' end, a 3' mutation is often more harmful to the cell. In β-thalassemia, some nonsense mutations, especially those occurring in the last exon of β-globin, cause an autosomal dominant phenotype. Consistent with this principle, these nonsense transcript levels are much closer to the wild type. This is also true in the recessive myosin heavy chain mutants in *Caenorhabditis elegans,* which can become dominant if cells lose the ability to eliminate nonsense mRNAs (Pulak and Anderson, 1993). We found that a similar mechanism may exist in the photoreceptors, suggesting that high level of nonsense β-PDE transcript might interfere with expression from the normal transcript (Chapter 3). This might provide an explanation for the dilemma of delayed retinal degeneration in the transgenic *rd/rd*/+ mouse. Since there are two mutant β-PDE copies in the transgenic *rd* mouse background, more nonsense transcripts are made and possible expressed, and these higher levels of deleterious transcripts (and/or protein) might have a harmful effect on photoreceptors, leading to a late onset degeneration.

To experimentally test this hypothesis, hammerhead ribozymes were designed to specifically target nonsense or wild type transcripts. The specificity, activity and kinetic constants of these ribozymes were characterized *in vitro*. Since there was a GUA sequence nearby and downstream of the nonsense mutation, it was chosen as the ribozyme cleavage site. Although GUC is the most common site for hammerhead ribozyme cleavage and is expected to have a faster cleavage rate than a GUA site, GUA is the natural site of cleavage in the minus strand of sLTSV. Thus the GUA cleavage site sequence is a viable alternative, suggesting that sequence is not the only factor determining the cleavage rate. Neighboring nucleotides also greatly affect ribozyme efficiency (Fedor and Uhlenbeck, 1990), and GUA and GUC targets were reported to have equivalent rates of cleavage in some instances (Koizumi et al., 1988; Perriman et al., 1992).

The ribozyme Rz636 can specifically cleave a synthetic nonsense β-PDE substrate, and it is active at low (near physiological) magnesium concentrations. It can also cleave full length nonsense β-PDE mRNA in presence of other retinal RNAs *in vitro*. The ribozyme Rz838 has similar features against wild type β-PDE substrates. The catalytic rates of Rz636 and Rz838 are within the range of natural ribozymes. It is interesting to note that the catalytic rate of Rz636 is 10 fold less with the 95 nt long substrate than with 16 nt synthetic RNA. Since the multiple turnover velocity is lower than single turnover velocity, this indicates that the product dissociation step is rate limiting. Bertrand (1994) has shown similar 5 to 10 fold catalytic differences between 950 nt and 60 nt target Pit transcripts. Another group also found three orders of magnitude difference between full length 985 nt HIV LTR and 19 nt synthetic RNA substrates (Heidenreich and Eckstein, 1992). The most probable explanation is secondary and tertiary structures within longer RNA targets inhibit the accessibility and/or dissociation of the ribozyme. Ordinarily, shorter RNAs are less likely to adopt stable double stranded conformations, and they are therefore better targets for ribozymes. For comparison with existing data on natural ribozymes, it seems more reliable to use the short synthetic RNA targets even though longer targets are closer to the natural conformation of *in vivo* transcripts.

Since protein-free *in vitro* conditions are clearly different from the *in vivo* environment, the true catalytic rate for any ribozyme might be very different inside the cell. It has been shown that some RNA binding proteins will accelerate the ribozyme cleavage reaction by either increasing annealing affinity or aiding dissociation after cleavage. In the next chapter, I will test the effect of hnRNP A1 to assist the ribozyme reaction *in vitro*, in order to determine whether RNA binding proteins can accelerate cleavage.

In the final chapter, I will discuss experiments in which ribozyme Rz636 was delivered to transgenic *rd/rd*/+ mouse retina by recombinant adeno-associated virus. *In vivo* expression of this ribozyme should decrease the amount of nonsense β-PDE transcripts. If our hypothesis is correct, we should be able to extend the rescue of transgenic *rd/rd*/+ mouse. In a complementary experiment, ribozyme Rz838 will be delivered into heterozygous *rd*/+ mouse to determine whether it can induce retinal degeneration in the normally asymptotic *rd*/+ mouse by reducing the level of wild type transcripts.

The targeting sequence of ribozymes can be adjusted to match different substrates, and target transcripts with mutations. Therefore ribozymes can be adapted for suppressing genetic or acquired diseases. Several ribozymes were designed to target regions of HIV mRNA (Heidenreich and Eckstein, 1992), and decreases in virus expression was observed. This high specificity property of ribozymes can lead to elimination of mutant transcripts without affecting wild type levels, and may prove to be a very useful way to prevent retinal degeneration caused by dominant negative mutations. Since the intracellular environment is quite different from normal *in vitro* conditions, *in vivo* experiments will be necessary to determine whether such a system will function in photoreceptors. Setting up this system for the photoreceptors will help us establish whether delivery of other ribozymes specific to other mutations in different photoreceptor genes can help cure genetic retinal diseases.

CHAPTER 5
THE EFFECT OF hnRNP A1 ON THE CLEAVAGE REACTION OF HAMMERHEAD RIBOZYME RZ636

Introduction

Ribozyme cleavage reactions can be carried out in a protein-free environment *in vitro* (see chapter 4). However, since there is a very different environment inside the cell, prediction of *in vivo* behavior based on *in vitro* results is still a challenge. The protein concentration and ionic environment in the cell can affect every step of ribozyme cleavage. Pre-mRNA, a potential ribozyme target, is associated with hnRNPs in the nucleus, and some hnRNPs shuttle with mature mRNA during export out of the nucleus to the cytoplasm (Pinol Roma and Dreyfuss, 1992; Dreyfuss et al., 1993). Once in the cytoplasm, other proteins bind to mRNA along with some original hnRNP proteins to aid in RNA stability and translation. Whether hnRNPs and other cytoplasmic RNA binding proteins inhibit or enhance the accessibility of a ribozyme to its target remains unclear. Many hnRNPs are RNA binding proteins, some of which function in pre-mRNA splicing, polyadenylation, and mRNA transport . RNA binding proteins might also act as chaperones to help RNA assume its correct conformation. Since RNA is composed of only four nucleotides, the chances of alternative misfolding are high compared with proteins (Herschlag, 1995). Some RNA binding protein chaperones help RNAs form a correctly folded structure or resolve misfolded RNAs. Such RNA chaperones lower the free energy required for correct RNA folding, and might also stabilize the correct RNA structure. Some examples are *E. coli* phage T4 gap protein, retrovirus nucleocapsid proteins (NCp7) and human hnRNP A1 protein. Each has an affinity for single stranded nucleic acid, and a single strand exchange activity. Since RNAs are also localized to different cytoplasmic compartments, this geographic preference might also alter the accessibility of a ribozyme to its substrate. It has been shown that ribozyme cleavage efficiency will dramatically increase if the ribozyme and target substrate are colocalized in the same subcellular compartment (Sullenger and Cech, 1993).

To obtain efficient cleavage *in vivo*, it is necessary to use a relative long targeting arm for some ribozymes, thus stabilizing the hybrid between ribozyme and target. However, the dissociation rate is dramatically decreased with such long arms on a ribozyme *in vitro*, and target specificity is decreased. Therefore, for reagents against point mutation substrates, "long armed" ribozymes often cleave not only the mutant substrate but also the wild type counterpart with approximately equivalent efficiency. Since RNA chaperon proteins can increase single strand exchange, they might be able to accelerate the ribozyme cleavage rate by increase the annealing of ribozyme to target and/or help the dissociation after cleavage. The resultant potential increase in ribozyme turnover rates means that a therapeutic effect can, in theory, be obtained with lower concentrations of ribozyme. It has been found that the HIV NCp7 protein can increase the cleavage rate of some slow acting ribozymes 5-fold *in vitro* (Tsuchihashi et al., 1993). This effect is dependent on the length of the helix arm between the ribozyme and substrate. For ribozyme gene therapy, it may be desirable to coexpress these proteins with the ribozyme in the cell to enhance cleavage rates. Recently, hnRNP A1 was found to have an acceleration function to ribozyme cleavage (Bertrand and Rossi, 1994). The relatively nonspecific RNA binding activity of hnRNP A1 might contribute to this function and it may therefore be a reasonable candidate for a general ribozyme enhancing RNP *in vivo*.

hnRNP A1 is an abundant protein in heterogeneous nuclear ribonucleoprotein particles (hnRNP). HnRNP proteins coat nascent heterogeneous nuclear RNAs (hnRNAs), and are involved in pre-mRNA splicing, mRNA transportation and polyadenylation. HnRNP A1 binds preferentially to 5' and 3' splicing sites (Swanson and Dreyfuss, 1988; Buvoli et al., 1990; Burd and Dreyfuss, 1994). It can enhance the annealing of antisense RNA to the pre-mRNA 3' splice site (Portman and Dreyfuss, 1994), and influences 5' splice site selection and exon skipping *in vitro*. The interaction of A1 with pre-mRNA is influenced by both U1 and U2 snRNPs (Mayeda and Krainer, 1992; Mayeda et al., 1993; Mayrand et al., 1993). It is believed that A1 can promote U1 and U2 annealing to either the 5' splice site or a branch point through its RNA annealing activity. A1 may also participate in the nucleo-cytoplasmic transport of mRNA (Pinol Roma and Dreyfuss, 1992).

As for most hnRNPs, hnRNP A1 is an RNA binding protein (34kd, 320 amino acids). It has features common to many RNA binding proteins. A1 belongs to a large family of RNA binding proteins that contain RNA recognition motifs (RRM) (Kenan et al., 1991). Proteins in this family function at different levels of RNA biosynthesis and processing. The RRM motif (or RNA binding domain, RBD) typically contains about 80 residues. Conserved amino acid domains (such as RNP-1 and RNP-2) appear to be responsible for general RNA affinity. The non-conserved portions in RRMs probably are involved in sequence-specific RNA binding, or protein-protein interaction (Kenan et al., 1991). There are three such RNA binding domains in the A1 protein. Two copies of RRM (or

RNP-CS) reside near the N-terminus. Another motif containing several repeats of a glycine-rich RGG box (Kiledjian and Dreyfuss, 1992) is located near the C-terminus. A nuclear localization sequence is located downstream of the RGG box, and this sequence might interact with other proteins in the cytoplasm (Cartegni et al., 1996). A1 also interacts with different RNA-binding proteins through its glycine-rich RGG box to form homo- or hetero-complexes. It binds to single stranded nucleic acid preferentially and nonspecifically, and it has moderate cooperativity for this binding. The annealing activity of A1 is very efficient, and involves protein-protein interaction to stabilize the RNP complex, thus allowing RNA-RNA interaction to form double stranded RNA (Pontius, 1993).

If A1 can enhance the ribozyme activity *in vivo*, we might not need to overexpress the ribozyme in order to obtain an efficient cleavage rate. Here, I will test the effect of hnRNP A1 on ribozyme Rz636 activity. Recently, a specific binding site for hnRNP A1 was determined by *in vitro* selection (Burd and Dreyfuss, 1994). A1 can bind very tightly to this site. Theoretically, A1 function improves with its RNA affinity. To test this idea, the A1 binding site was cloned into the ribozyme vector adjacent to the ribozyme Rz636 targeting sequence (Figure 5-1). To increase the affinity even further, two copies of A1 binding site were used as the binding unit. Since we do not know whether the relative position of the A1 binding site sequence adjacent to the ribozyme affects ribozyme cleavage, A1 binding sites were linked either in front of or behind the ribozyme sequence or in both positions. GST-A1 was purified over a GST-Sepharose column, and tested in the *in vitro* cleavage reaction. By analyzing each modified ribozyme, I hoped to assess whether the A1 protein and A1 binding site sequence enhance the cleavage reaction of Rz636. If A1 can enhance the cleavage reaction, we can introduce this binding site into other ribozymes and perhaps improve the cleavage efficiency of a wide range of ribozymes *in vivo*.

Materials and Methods

Oligonucleotides

Al305: 5' CAG GCG AAT TCT ATG ATA GGG ACT TAG GGT GCT CGG TAT GAT AG 3'. This oligonucleotide is a 5' overlapping primer for the hnRNP A1 binding site. There is an EcoR I site near the 5' end.

WH786: 5' GGC GTG AAT TCC ACC CTA AGT CCC TAT CAT ACC GAG CAC CCT A 3'. This oligonucleotide is a 3' overlapping primer for the hnRNP A1 binding site. There is an EcoR I site near the 3' end.

Plasmid Clone Construction

RzAE2: One copy of hnRNP A1 binding site was subcloned into the EcoR I site of clone pRz636. The A1 binding site precedes the ribozyme sequence and is in the same orientation as the ribozyme (Figure 5-1). To construct clone RzAE2, two primers (A1305 and WH786, 1000 pmole each) were denatured in 20 mM Tris-HCl, pH 7.5 and 50 mM NaCl at 94°C for 2 minutes, annealed at 62°C for 10 minutes, and placed on ice for another 5 minutes. The annealed products were ethanol precipitated and suspended into 20 μl dH_2O, and the ends filled-in with 5 units of Klenow Pol I (NEB) in 1X NEB Klenow buffer, 200 μM dNTPs at 37°C for 1 hour. After heat deactivating the DNA polymerase, the filled-in product was ethanol precipitate again, and digested with EcoR I overnight. The products were then ligated into the EcoR I site of pRz636. Transformants were screened by colony blotting, and verified by sequencing using the WH602 primer.

RzAE10: Two copies of the hnRNP A1 binding unit were subcloned in tandem into the EcoR I site of clone pRz636. These two binding sites preceded the ribozyme sequence, and both were in the same orientation as the ribozyme sequence (Fig 5-1). Construction of this clone was analogous to RzA1E2, and the two-copies of the A1 binding site sequence was confirmed by PCR and DNA sequencing.

RzAM1: One copy of the hnRNP A1 binding unit was subcloned into the Mlu I site of clone pRz636. The A1 binding site followed the ribozyme sequence, and was in the same orientation as the ribozyme (Figure 5-1). To construct this clone, oligonucleotides Al305 and WH786 were 5'-phosphorylated by DNA kinase, annealed, and filled in as for RzAE2. Clone pRz636 was linearized with Mlu I and blunt-ended by Klenow DNA polymerase (Gibco BRL). The filled-in A1 binding sites were ligated into the blunt-ended Mlu I site of pRz636. Transformants were screened by PCR, and confirmed by sequencing.

RzAEM: One copy of the hnRNP A1 binding unit was subcloned in the EcoR I site of clone RzAM1. This yields a ribozyme sequence with one A1 binding site in front of ribozyme and another A1 binding site behind the ribozyme. Both binding sites were in the same orientation as the ribozyme (Figure 5-1). Construction of this clone was similar to RzAM1. Clone RzA1M was linearized by EcoR I and then blunt-ended by Klenow Pol I. Primers Al305 and WH786 were 5'-phosphorylated by polynucleotide kinase, filled in and ligated into the blunt-ended EcoR I site of RzAM1. Clones were confirmed by DNA sequencing.

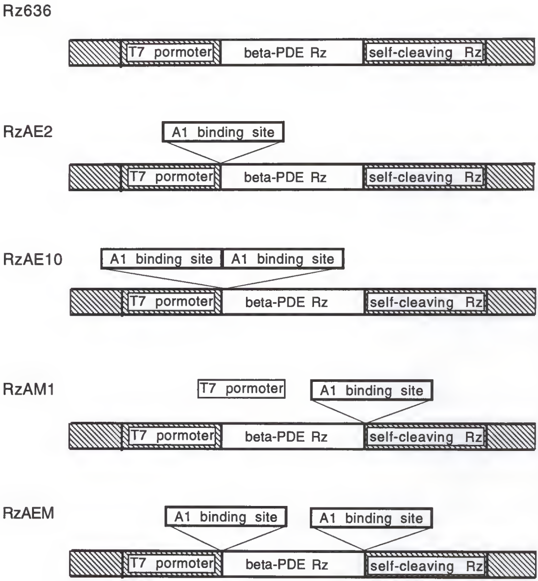

Figure 5-1: Structure of ribozyme clones containing hnRNP A1 binding site sequence (A1W). The gray rectangle represents the pHC vector backbone.

GST-A1 Colony Screen

Glutathione S-transferase (GST) - A1 fusion protein was purified by GST column chromatography (Pharmacia). The plasmid GST-A1 (kindly provided by Dr. Silvano Riva, University of Pavia) was first screened on a small scale to obtain the most vigorously growing colony. Plasmid GST-A1 DNA from this colony was transformed into DH5α cells by heat shock. Three colonies were picked and inoculated into 5 ml each of 2YT-G+Amp (1.6% tryptone, 1% yeast extract, 0.5% NaCl, 2% glucose and 100 μg/ml Ampicillin). After shaking at 37°C for 4 hours, 20% glycerol stocks were made by adding 1ml of each culture to 1 ml 40% glycerol with storage at -70°C. 2 ml 2YT-G+Amp was inoculated with 10 μl of the glycerol stock for each colony, and grown overnight. 10 ml 2YT-G+Amp culture was then inoculated with 10 μl of the overnight culture of each colony, and grown for another 4 hours until the OD_{260} reached 0.6-0.8. 2 ml was put into another tube for a non-induced control. 130 μl of 100 mM IPTG was added into the remaining 8 ml cultures at 37°C and induced for another 1-2 hours. The pellets were spun down and stored at -70°C.

GST-A1 Protein Purification

GST-A1 purification followed Promega's instructions with minor modifications. All the steps were performed at 4°C or on ice except where noted. 6.7 ml of GST-sepharose 4B (75% aqueous slurry) was spun at 500 g for 5 minutes, and washed with 50 ml ice-cold PBS. The beads were spun down again, and resuspended in 5 ml PBS. For the small scale screen, 2ml of 2YT-glucose –AMP media was inoculated with 10 μl of the glycerol stock, and grown overnight. 15 ml of 2YT-glucose-Amp media was inoculated with 10 μl of the overnight culture, and grown until the A_{600} reached 0.6 to 0.8 (3-5 hrs). 1.5 ml of this culture was spun down as an uninduced control. 130 μl 100mm IPTG was added to the remaining 13 ml culture, and grown for another 2 hrs as the induced portion. 1.5 ml of the induced culture was centrifuged at 4°C for 2 minutes and the pellet stored at – 70°C for the next step. To purify GST-A1, the pellet was resuspended in 300 μl ice-cold 1X PBS, and the cells disrupted using a sonicator equipped with an appropriate probe. After sonicating at a setting of 4 for 10 seconds, the cells were placed on the ice for 1 min. This step repeated until the cell suspension became transparent. Broken cells were pelleted for 5 min at 5,000 g in a cold room to remove insoluble material. 20 μl of a 50% PBS slurry of the GST-4B was added to each supernatant and mixed gently for 5 min at room temperature. 100 μl PBS was then added, vortexed briefly, and spun for 2 min at 5,000 x g to sediment the beads. The pellet was washed with 1X PBS twice for a total of three washes. The fusion protein was eluted by the addition of 10 μl glutathione elution buffer (10 mM reduced glutathione, 50 mM Tris-HCl, pH8.0) and incubated at room temperature for 5 minutes. The beads were spun for 5 minutes and the supernatant transferred to fresh tubes and analyzed on 10% SDS-PAGE gels.

For large scale purification, a GST-sepharose 4B column was set up. 5 ml of GST-sepharose 4B was loaded onto a 10 ml disposable column. The induced cell pellet from 500 ml culture was broken in a French press, and loaded onto the column. 50 ml of PBS (10 bed volumes) was used to elute unbound protein, and then 25 ml (5 bed volumes) of high salt buffer (50 mM Tris-HCl, pH 7.0, 1 M NaCl) was loaded to elute nucleases. The high salt buffer was then washed off by another 25 ml of PBS. The GST-A1 was then eluted with 25 ml of elution buffer (10 mM reduced glutathione, 50 mM Tris-HCl, pH8.0) and collected in 5 ml fractions. Ten microliters each of the wash fraction, high salt fraction, and eluted fraction were loaded onto 10% SDS PAGE gel. The eluted fraction containing GST-A1 based on to apparent molecular weight was dialyzed against 1000 ml of dialysis buffer I (10 mM Tris-HCl, pH7.5, 1 mM EDTA, 20% glycerol) twice for one hour each, and dialyzed against 1000 ml of dialysis buffer II (10 mM Tris-HCl, pH7.5, 1 mM EDTA, 50% glycerol) overnight. GST-A1 was then stored in -70°C. A standard curve of protein was determined by densitomitry of BSA protein standards on a 10% SDS gel stained with Coomassie Blue. The GST-A1 concentration was determined by comparing staining density with BSA standards. About 2000 μl GST-A1 protein (2 μg/μl) was obtained from a 500 ml culture.

Ribozyme Cleavage with GST-A1

The ribozyme cleavage conditions were 20 mM Tris-HCl, pH7.5, 20 mM $MgCl_2$, 1 μl RNase inhibitor (BRL). The ribozyme concentration was about 500 nM and the cleavage substrate MT RNA was about 60 nM. Different amounts of GST-A1 were added in a GST-A1 titration experiment, with the dialysis buffer II (10 mM Tris-HCl, pH7.5, 1 mM EDTA, 50% glycerol) used to dilute the GST-A1 protein.

Gel Mobility Shift

Gel mobility shift experiments were performed in 20 mM Tris-HCl, pH7.5, 20 mM $MgCl_2$, 140 mM KCl, and 10 units of RNase inhibitor (BRL). 30 nM of α-^{32}p UTP internally labeled substrate transcript was used as the target in each gel mobility shift reaction. For each transcript, a titration of GST-A1 (diluted in dialysis buffer II) was used in the 15 μl reaction. The final GST-A1 volume was 5 μl in each case. The reaction mixes were incubated at 37°C for 15 minutes, then run on a 4% native Tris/glycine polyacrylamide gel (polyacrylamide: bisacrylamide 30:0.8) at 12 volts/cm for 1 hour.

UV Crosslinking

The RNA mixture contained 0.34 μl 100 mM $MgCl_2$, 0.5 μl 1 M HEPES (pH7.6), 3 μl internally labeled RNA (about 1 x 10^5 cpm), 2 μl RNasin and 6 μl dH_2O. The RNA was then mixed with 2 μl ATP (final concentration of 18.75 mM), 1 μl creatine phosphate, 11 μl Hela nuclear extract, and then incubated at 30°C for 10 minutes and placed on ice for another 5 minutes. 0.5 μl tRNA (10 mg/ml) was then added into the reaction mix and uv-crosslinked for 5 minutes in a Stratagene Crosslinker set on the autocrosslink setting. 2.5 μl of RNase A (10 mg/ml) was added and incubated at 37°C for 30 minutes. Finally, an equal amount 2X SDS loading buffer was added and the samples analyzed on 10% SDS polyacrylamide gels.

Results

To determine whether RNA binding by hnRNP A1 can accelerate the ribozyme cleavage reaction *in vitro*, the A1 binding site was linked to the ribozyme Rz636. Previous experiments in other labs have shown that hnRNP A1 alone can accelerate the ribozyme cleavage reaction *in vitro*, especially for intrinsically slow ribozymes (Bertrand and Rossi, 1994). Introducing a binding site should increase the affinity of A1 for the ribozyme, and might improve reaction parameters. Since the binding site might also affect the secondary structure of the ribozyme, A1 binding site sequences were also placed both in front of and behind the ribozyme or on both sides. I also constructed one clone with two copies of A1 binding site in front of Rz636. By testing the *in vitro* cleavage reaction of all constructs, I hoped to determine the effect of hnRNP A1 and A1 binding site sequence on the ribozyme reaction.

Removal of RNase from the GST-A1 Protein Preparation

GST-A1 was first purified by the batch-binding method. This procedure was found to yield high amounts of co-purifying RNases along with the fusion protein. Another preparation of GST-A1 was purified by GST-Sepharose 4B column chromatography. A high salt (1 M NaCl) elution was used to remove nucleases before A1 elution. The fusion protein in this case did not have significant RNase contamination (data not shown). The 95 nt MT transcripts were intact, even after 4 hours of incubation under cleavage conditions. This high salt wash also eliminated endogenous RNA that could nonspecifically bind with A1.

GST-A1 Binds Rz636 containing the A1 Binding Site Sequence but not Rz636 Alone

Since the preferred A1 binding site was determined by *in vitro* selection using native hnRNP A1, it is important to know whether the GST tag affects the RNA binding properties of hnRNP A1. A gel mobility shift experiment was set up using identical amounts of ribozyme transcript, 95nt long ribozyme substrate RNA and a titrated series of hnRNP A1 concentrations (Figure 5-2). The binding conditions included 140 mM KCl, a salt concentration that allows optimal binding of hnRNP to RNA substrates

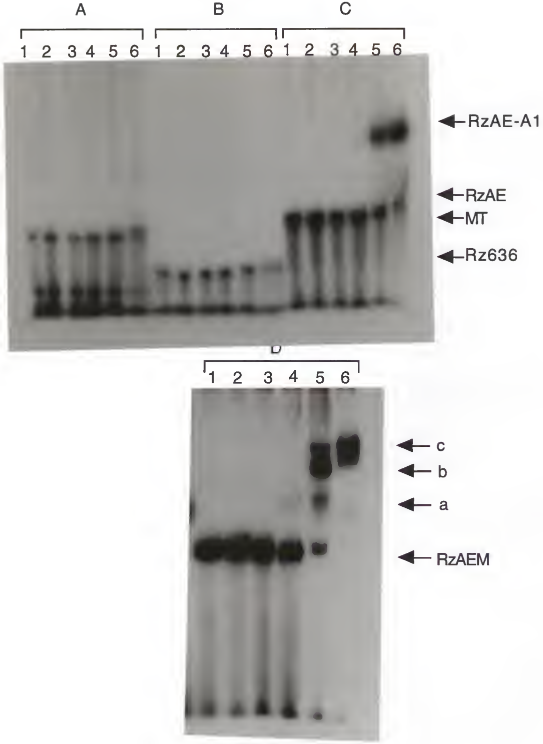

Figure 5-2: Gel mobility shift for GST-A1 with α-^{32}P labeled β-PDE ribozyme or target. A. PMT target substrate with hnRNP A1. Lane 1: no GST-A1 control. Lane 2: 0.77 ng GST-A1. Lane 3: 3.9 ng GST-A1. Lane 4: 7.7 ng GST-A1. Lane 5: 77 ng GST-A1. Lane 6: 390 ng GST-A1. B. Ribozyme Rz636 with GST-A1. C. Ribozyme RzAE2 with GST-A1. D. Ribozyme RzAEM with GST-A1. The lane arrangements in B, C and D are the same as in A.

(Nadler et al., 1991). GST-A1 did not bind the RNA substrates lacking a binding site (MT transcripts), even at very high concentrations (390 ng/μl). GST-A1 also did not bind the parental ribozyme, Rz636 transcripts, also lacking the A1 binding site. However, all ribozymes containing the A1 binding site could bind GST-A1 at 77 ng/μl. The optimal concentration of GST-A1 in previous experiments was reported as 50 ng/μl (Bertrand and Rossi, 1994) and our data are generally consistent with this protein concentration. When 390 ng/μl GST-A1 was used in the gel shift experiment, virtually all the ribozyme that had an A1 binding site was shifted. There were three complexes forming between RzAEM and A1. Each might represent one, two or three A1 binding sites bound to GST-A1. Therefore, the glutathione S-transferase tag did not affect the ability of hnRNP A1 to bind ribozymes as long as an A1 binding site sequence was present. Additionally, this fusion protein clearly retained its activity after purification, allowing functional experiments to be carried out.

Effect of hnRNP A1 on the Ribozyme Cleavage Reaction

Varying amounts of GST-A1 (0-666 ng/μl) were added to the ribozyme reaction and rates of substrate cleavage determined. Instead of accelerating the reaction, GST-A1 appeared to inhibit formation of cleavage products (Figure 5-3). One possible reason for loss of cleavage might be residual RNase in the GST-A1, even though the activity of RNase was very low when MT transcript was the substrate. Since MT does not bind A1, a trace nuclease effect might not have be seen in RNase control experiment. However, since GST-A1 does bind ribozyme, presumably at the A1 binding sites, residual RNase might dramatically decrease the ribozyme amount if bound A1 mediates RNA

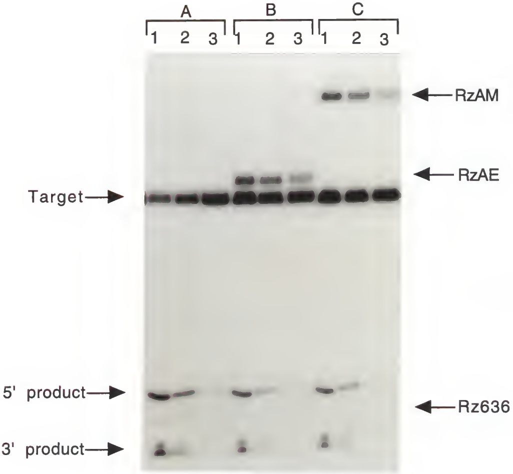

Figure 5-3: Cleavage of mutant β-PDE RNA with ribozymes containing the hnRNP A1 binding site. Substrate was incubated with ribozymes at 37°C for 1 hour. A. Cleavage with Rz636. Lane 1: no GST-A1 control. Lane 2: 166 ng/μl GST-A1 in the reaction. Lane 3: 666 ng/μl GST-A1 in the reaction. B. Cleavage with RzAE2. The lane arrangement is the same as A. C. Cleavage with RzAM. The lane arrangement is the same as A. The substrate and cleavage products are indicated on the left of the figure. The ribozymes are indicated on the right of the figure.

degradation. In this experiment, the level of GST-A1 was correlated with levels of ribozyme inhibition. This effect was clearly more dramatic for ribozymes with A1 binding site sequences than for Rz636 alone, consistent with a potential role for A1 or its binding sequence in mediating ribozyme activity loss. Another possibility is that GST-A1 affects adversely formation of a complex between ribozyme and target. Previous experiments have shown that ribozyme length might also affect cleavage efficiency (Bertrand and Rossi, 1994). hnRNP A1 accelerates the cleavage reaction only if helix arms are between 6 and 7 bp without an A1 binding site.

Even though this result is disappointing, a positive role for A1 binding to ribozyme cannot be ruled out completely based on just this *in vitro* cleavage assay. *In vivo* experiments need to be carried out to reach a definitive conclusion.

UV Crosslinking of Nuclear Protein and Ribozyme Rz636

Even though hnRNP A1 did not accelerate the cleavage reaction of modified Rz636 ribozymes *in vitro*, it is possible that other RNA binding proteins would affect the cleavage reaction inside cells. RNA binding proteins are abundant in the nucleus, and many are important for pre-mRNA processing. Therefore, UV-crosslinking was used to determine whether any nuclear proteins have an affinity for the Rz636 ribozyme (Figure 5-4). Hela nuclear extract was UV-crosslinked with either Rz636 or RzAEM transcripts. As a positive control, RzAEM transcripts, containing the A1 binding site, were crosslinked to GST-A1. RzAEM and Rz636 both crosslinked with several nuclear proteins. Some of these proteins were common to both Rz636 and RzAEM and some were unique to one or the other ribozyme. This indicates that the A1 binding site in

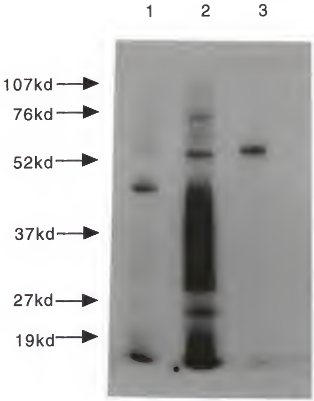

Figure 5-4: Gel of UV-crosslinking of the radiolabeled β-PDE ribozymes to hnRNP A1 or Hela nuclear extract. Lane 1. Ribozyme Rz636 UV-crosslinked with Hela nuclear extract. Lane 2. RzAE2 UV-crosslinked to Hela nuclear extract. Lane 3. RzAE2 UV-crossing with hnRNP A1. The sizes of the protein marker are indicated on the left of the figure.

RzAEM affects the binding to some proteins, but RzAEM still binds some proteins in common with Rz636. It is interesting that Rz636 binds primarily two proteins (45 kd and 65 kd) whereas RzAEM binds a large family of proteins of different sizes. Perhaps the A1 binding site in RzAEM mediates this enhanced binding. Another possibility is the size difference between these two ribozymes. RzAEM is 80 bp longer than Rz636, thus allowing RzAEM to bind more proteins per molecule in a nonspecific manner.

Discussion

In this chapter, I tested whether hnRNP A1 and its cognate binding site can affect the cleavage rate of ribozyme Rz636. GST-A1 binds to the ribozyme as long as an A1 binding site is present, but does not bind the basic ribozyme or the target with high enough efficiency. The A1 binding site functions within the ribozyme without an obvious preference for its position relative to ribozyme active site. Additionally, the A1 portion of the GST-A1 fusion protein appears to retain most of its RNA binding activity. Previous experiments in other laboratories have shown that A1 has non-specific RNA binding activity, with one hnRNP A1 binding with every 15 nt of RNA in substrates without the A1 binding sequence (Cobianchi et al., 1988; Nadler et al., 1991). When 100 ng/µl of A1 was used in the gel-shift experiment with a 60 nt long target RNA, 4 gel-shifted bands were found (Bertrand and Rossi, 1994). However, no GST-A1 was found binding with either target MT transcript or ribozyme Rz636 alone even with 390 ng/µl A1 present in the gel shift assay. Thus, in experiments reported here there appeared to be an absolute requirement for at least one A1 binding site in the target RNA. One possibility for the difference between my results and most of Bertand ans Rossi (1994) is that there is often significant secondary structure in the target RNA, and A1 has a much lower binding affinity for double stranded RNA. RNA can assume secondary and tertiary structures easily through interaction between the 2'-hydroxyl group, and phosphorus and metal ions (Herschlag, 1995). Ordinarily, these structures are quite stable, and there is little tendency for such folded RNA to denature and refold correctly. This is easy to understand for Rz636 RNA since this hammerhead ribozyme has significant double stranded secondary structure stabilized by base pairing. However for MT, it is more difficult to explain. An alternative possibility is that the GST tag in the GST-A1 fusion protein partially disrupts the structure of hnRNP A1, and weakens the nonspecific RNA binding activity. Since A1 has an extremely high binding affinity to its A1 binding site sequence, GST-A1 may bind to RNA containing this binding site in spite of the GST tag. This would explain why somewhat higher than expected concentrations of GST-A1 (70 ng/μl) are needed to create a gel-shifted ribozyme band when the A1 binding site is present.

Previous experiments had shown that hnRNP-A1 enhances the ribozyme cleavage reaction (Bertrand and Rossi, 1994). Since the N-terminus of A1 has a helix-destabilizing activity, it may disrupt RNA helices and promote rapid dissociation of the ribozyme-target complex before cleavage occurs. A1 might also promote the annealing step in the ribozyme reaction, since A1 can stabilize transient RNA double stranded structures by lowering the energy required for transitions between duplex structures. The level of enhancement is dependent on the length of the hybrid formed between the ribozyme and its substrate. No enhancement was found for helix arms less than 6 bp or longer than 8 bp. The effect of A1 on the single turnover reaction was found to be not as pronounced as that on the multi-turnover reaction. This small window for enhancement might due to nonspecific binding activity or to the *in vitro* conditions, or both.

Although including the A1 binding site in the ribozyme was expected to increase the binding affinity of A1 for the ribozyme, it might decrease the ribozyme cleavage rate. Since A1 needs specific salt conditions to function, ribozyme cleavage was performed in 140 mM NaCl, optimal for A1-RNA efficient binding. However, independent of the salt concentration, we obtained the similar depression of ribozyme cleavage with A1. Another variable factor may be the GST-A1 concentration. Since GST-A1 has strong single strand RNA binding and exchange activities, a high concentration of A1 might serve to disrupt the single stranded catalytic core of hammerhead ribozyme (Nadler et al., 1991). However, GST-A1 was shown to not alter ribozyme cleavage between 10 ng/µl and 666 ng/µl. Since ribozyme Rz636 contains 12 bp in its helix arms, A1 probably does not have a major effect. An alternative explanation is that GST-A1 may not have the equivalent function as A1 alone due to the interference of the GST tag. This we have not tested.

Another possible explanation for our *in vitro* data is that there may be a trace of nuclease in the GST-A1 fusion protein preparation. We did find that the amount of ribozyme decreased with the increasing amounts of GST-A1. It is also possible that the complex between ribozyme and A1 is not functional in the cleavage reaction. The loss of ribozyme might well be a major factor contributing to the low observed *in vitro* cleavage. Even though GST-A1 protein was purified by affinity chromatography, and the high salt wash eliminated the majority of RNases, residual nuclease contamination might remain, at a level not detectable with the 95 nt MT substrate. Since GST-A1 did not bind to MT transcript, a trace of nuclease might not be apparent when using MT RNA as the substrate. Since A1 can bind the ribozyme very well, low levels of RNases might be enhanced if A1-bound ribozyme was the substrate. Alternatively, A1 might function in coordination with other RNA binding proteins *in vivo*, whereas A1 alone *in vitro* is insufficient to enhance the cleavage reaction. Most RNA binding proteins with RRM domains first interact modestly with RNA ligands through the conserved aromatic and basic residues in the RNP-1 and RNP-2 elements, and then, via protein-protein interactions through glycine-rich RGG boxes, to further stabilize the initial protein-RNA association. It has been shown that other RNA binding proteins interact with hnRNP-A1 *in vivo* (Cartegni et al., 1996). We have not tested whether ribozymes with the A1 binding site would work better than those without this site *in vivo*. The RNA unwinding activity of A1 is more pronounced for full length transcript than short synthetic substrates *in vitro*, and hnRNP A1 is very abundant in the nucleus. The concentration of A1 is about 10 μM in the nucleus, a much higher concentration than we used *in vitro* (about 1.5 μM). Finally, RNA inside the cell is likely to be associated with other RNA binding proteins, thus reducing any nuclease effect. Therefore, it might be worth comparing the cleavage enhancement between ribozymes with and without the A1 binding site under *in vivo* conditions.

It is known that other RNA binding proteins inside the cells besides A1 can enhance the ribozyme reaction. The CYT-18 protein (mitochondrial tyrosyl-tRNA synthetase) promotes RNA splicing of group I introns by stabilizing the active conformation (Mohr et al., 1992). Recently, it has been found that the newt ribozyme can form an RNA-protein complex in the oocytes of *Triturus* and that several 31 to 65 kd polypeptides can crosslink with the newt ribozyme (Luzi et al., 1997). This RNP form of the newt ribozyme retains its cleavage activity *in vitro*. Most RNA binding proteins are quite conserved in eukaryotic cells, implying that nuclear proteins in mammalian cells might have the equivalent function. UV crosslinking experiments shown here demonstrate that the hammerhead ribozyme Rz636 can bind several proteins in a Hela cell nuclear extract. These proteins might act as cofactors for ribozyme activity and enhance its catalytic reaction *in vivo*. It would be interesting to isolate these proteins, and test their effects on the ribozyme reaction.

In summary, the effect of GST-A1 fusion protein and A1 binding site containing ribozyme was tested *in vitro*. GST-A1 bound to A1 binding site tagged ribozymes but did not enhance the cleavage reaction of Rz636 in the test tube. However, these *in vitro* results might not directly extend to the *in vivo* situation. It will be necessary to test this idea *in vivo* in order to draw solid conclusions about effects of hnRNP A1 proteins on ribozyme function.

CHAPTER 6

IN VIVO CHARACTERIZATION OF A HAMMERHEAD RIBOZYME SPECIFIC TO A NONSENSE TRANSCRIPT OF THE MOUSE cGMP PHOSPHODIESTERASE BETA SUBUNIT

Introduction

A ribozyme (Rz636) specific to the nonsense β-PDE transcript was shown to specifically cleave *in vitro*. To test whether this ribozyme can function *in vivo* and possibly extend the rescue of retinal degeneration in the transgenic *rd/rd/*+ mouse, it is necessary to express Rz636 in photoreceptors and determine its *in vivo* effect.

To deliver Rz636 to the retina, the ribozyme was subcloned into an adeno-associated virus package vector, and packaged into recombinant AAV (rAAV). Expression of this ribozyme was controlled by a 472 bp proximal mouse rod opsin promoter. A green fluorescence protein reporter gene driven by the same promoter resulted in photoreceptor-specific expression also using rAAV as the vector (Flannery et al., 1997). To obtain efficient gene expression, it is critical to choose the correct promoter and delivery method. The rhodopsin promoter is a powerful, cell-type specific promoter that should produce high levels of ribozyme expression. To obtain a therapeutic effect, such high levels of ribozyme expression in the cells may be needed. The opsin promoter also gives the photoreceptor-specific expression, even though it might support expression in both rod and cone photoreceptors.

We chose adeno-associated virus 2 as our delivery vector. AAV is a nonpathogenic virus with about 80-90% of the human population sero-positive without any symptoms.

This nonpathogenic feature gives recombinant AAV a safety advantage over other commonly used virus vectors. AAV is a single stranded DNA virus, belonging to the family parvoviridae (Muzyczka, 1992). There are two phases of its life cycle: the latent and lytic phases. In cells infected with a high MOI, AAV alone establishes a latent infection in which low levels of viral *Rep* protein promote AAV DNA integration into human chromosome 19 at q13.3-qter (Kotin et al., 1990; Samulski et al., 1991). The sequence of the integration site appears to be important for integration efficiency (Giraud et al., 1994). Latent AAV can be reactivated and rescued by superinfection with adenovirus, herpes simplex virus or vaccinia virus. The AAV inverted terminal repeats (ITRs) are necessary for replication, packaging and integration. Recently, a 165 bp terminal repeat consisting of a single ITR flanked by 2 copies of the ITR D element exhibited the equivalent function (Xiao et al., 1997).

AAV can infect both dividing and non-dividing cells. This feature is important for delivery of genes to terminally differentiated somatic cells. Since the adult photoreceptor is post-mitotic, this is a good target for infection with rAAV. A *lacZ* reporter gene regulated by a CMV promoter and delivered by rAAV was found to express in an occasional photoreceptor as well as in other cells of the retina (Ali et al., 1996). In a more relevant study, a green fluorescence protein driven by mouse opsin proximal promoter exhibited photoreceptor specific expression after rAAV transfer (Flannery et al., 1997).

rAAV does not appear to elicit a significant inflammatory reaction. rAAV containing a Factor IX gene can express in immunocompetent mice for over half a year (Snyder et al., 1997). *lacZ* reporter expression can persist for over 240 days in normal mouse muscle cells (Fisher et al., 1997). This rAAV did not stimulate CTLs, but could activate $CD4^+$ T cells of the T_{H1} subset. However, the antibody response did not block readministration of AAV vector. Since the eye is an isolated, relatively immune-privileged organ, this muted immune response should be helpful for gene expression in photoreceptors.

A 470-bp mouse opsin promoter is sufficient for photoreceptor specific gene expression (Flannery et al., 1997). However both rods and cones appeared to be transduced. Since the size of either the hammerhead or hairpin ribozyme is about 100 nucleotides long, larger promoter fragments could be used if tissue specific expression is found to be a problem. Verma's lab recently used a 2.1-Kb mouse opsin promoter for a similar study with a lentiviral vector, and obtained an apparently similar level of gene expression (Miyoshi et al., 1997).

Since more than 90% of rodent photoreceptors are rods, it might not be necessary to achieve truly rod specific expression to ultimately obtain a rod phenotypic change. For these reasons, ribozyme Rz636 was cloned into either Mop 500 UF2 (472 bp proximal rod opsin promoter) or Mop 1700 UF2 (1633 bp rod opsin promoter), in order to test any promoter effects on ribozymes *in vivo*. Ribozymes with their own 472 bp mouse rod opsin promoters were also cloned into the backbone of an AAV vector already containing an opsin promoter-regulated GFP. Thus, a reporter gene (GFP) and ribozyme could be co-expressed in the same vector, each with its own promoter. With this vector, we can monitor injection efficiency by determining the expression levels of GFP in the same mouse retinas expressing ribozymes.

Materials and Methods

Oligonucleotides

WH696: 5’ CCC AGC GGC CGC GGA ATT CTT CTG CCT GAT GAG 3’. This sense primer corresponds to the 5’ ribozyme sequence of clone pRz636. There are Not I and an EcoR I sites near the 5’ end.

WH721: 5’ CCC AGC GGC CGC GGA ATT CTT CTG CCT GTT GAC 3’. This sense primer corresponds to the 5’ ribozyme sequence of clone WRz. There are Not I and an EcoR I sites near the 5’ end. The underlined nucleotides denote those changes in the catalytic core of the hammerhead ribozyme Rz636.

WH602: 5’ CCC AGC GGC CGC GCT TGC ATG CCT GCA GGT CG 3’. This is an antisense primer corresponding to the sequence downstream of the self-cleaving hairpin in vector pHC.

WH603: 5’ CCC AGC GGC CGC GGA AAC AGG ACT GTC ACG CG 3’. This is an antisense primer corresponding to the sequence upstream of the self-cleaving hairpin in vector pHC.

WH784: 5’ GCA TGT GTC GAC CCT CCT CAG CCC ATA AGC TCC T 3’. This sense primer corresponds to the bovine opsin upstream sequence, –673 to –653, with a Sal I site near the 5’ end.

WH785: 5’ TCA GTT GTC GAC GTC AAG TGA GCC ATT GTC AGG C 3’. This sense primer corresponds to the mouse opsin upstream sequence, –385 to –365, with a Sal I site near the 5’ end.

Plasmid Clone Construction

NMLRz: This clone contains an active hammerhead ribozyme Rz636 sequence and a self-cleaving hairpin driven by the mouse opsin proximal promoter (-385 to +85 bp). Plasmid Mop500 UF2 was digested with Not I to release the GFP gene sequence, and the vector fragments dephosphorylated with alkaline phosphatase. Primers WH696 and WH602 were used for a PCR reaction with Rz636 as template. The 200 bp PCR product was digested with Not I, and subcloned into the Not I site of Mop500 UF2. Transformants were screened by EcoR I digestion, and the integrity of the terminal repeats was determined by Pst I and Xho I digestion.

NMWLRz: This clone contains an inactive ribozyme WRz sequence and a self-cleaving hairpin driven by mouse opsin proximal promoter. The construction of this clone was similar to NMLRz, except that primers WH721, WH602 and template pWRz were used in the PCR reaction.

NMSRz: This clone contains an active ribozyme Rz636 sequence driven by mouse opsin proximal promoter. The construction of this clone is similar to NMLRz, except that primers WH696 and WH603 were used in the PCR reaction.

NMWSRz: This clone contains an inactive ribozyme WRz sequence driven by the mouse opsin proximal promoter. Construction of this clone is similar to NMLRz, except that primers WH721, WH603 and template pWRz were used in the PCR reaction.

UFRz18: This clone contains both an active ribozyme Rz636 sequence driven by the mouse opsin proximal promoter and a GFP gene driven by an identical promoter. Plasmid Mop500 UF2 was digested with Sal I and dephosphorylated by alkaline phosphatase. Primers WH785 and WH602 were used for a PCR reaction with NMLRz as template. The 850 bp PCR product was digested with Sal I, and subcloned into the Sal I site of Mop500 UF2. The transformants were screened by Sal I digestion. The integrity of the terminal repeats and the orientation of the ribozyme insert were determined by Pst I and EcoR I digestions. The ribozyme with its Mop500 promoter is in the opposite orientation relative to the GFP cassette.

AAV838: This clone contains an active ribozyme Rz838 sequence and a self-cleaving hairpin driven by the mouse opsin proximal promoter. Construction of this clone is similar to NMLRz, except that primers WH696, WH602 and template pRz838 were used in the PCR reaction.

AAV848: This clone contains an inactive ribozyme Rz840 sequence and a self-cleaving hairpin driven by the mouse opsin proximal promoter. Construction of this clone is similar to NMLRz, except that primers WH721, WH602 and template pRz840 were used in the PCR reaction.

GFP838: This clone contains both an active ribozyme Rz838 sequence driven by the mouse opsin proximal promoter and GFP driven by an identical promoter. Construction of this clone is similar to UFRz18 except that primers WH785, WH602 and template AAV 838 were used in the PCR. The ribozyme with its Mop500 promoter is in the same orientation as the GFP cassette.

GFP840: This clone contains both an inactive ribozyme Rz840 sequence driven by the mouse opsin proximal promoter (472 bp) and GFP driven by another Mop500 promoter. Construction of this clone is similar to UFRz18 except that primers WH785, WH602 and template AAV 840 were used in the PCR. The ribozyme with its Mop500 promoter is in the opposite orientation as the GFP cassette.

ΔMop500: This clone contains a 60 bp deletion in the normal 472 bp mouse opsin promoter and is used as a competitive template for QC-PCR to determine rAAV titers. The 1.7 Kb mouse opsin promoter (-1700 to +85) was cloned between the Kpn I (blunt-ended) and Xho I sites of pBluescript KS. This plasmid was then digested with EcoR I and EcoR V to delete 60 bp nucleotides. After blunt-ending with Klenow DNA polymerase I, this plasmid was religated to obtain clone ΔMop500.

Maintenance of Host Tissue Culture Cells

DMEM media was purchased from Cellgro. Complete DMEM media was prepared by adding 50 ml FBS (Fetal bovine serum, Hyclone), and 5 ml of penicillin/streptomycin (10000 units/10000 μg/ ml, BRL) into 500 ml DMEM media to obtain 10% FBS, 1X Penstrep. All media was prewarmed to 37°C before adding to cells. Human embryonic kidney cells (293 cells) were grown in 15 cm dishes in complete DMEM media at 37°C/5% CO_2 until confluence. After 1 day, the old media was removed, and the cells were washed with 5 ml PBS. 2 ml of 25 mM Trypsin-EDTA (BRL) was added and the dish gently swirled ensure total contact with the cells, followed by incubation at 37°C/5% CO_2 for 10 minutes. Another 4 ml of complete DMEM was then added, and 2 ml of cell suspension was plated onto each new dish (15 cm) containing 20 ml of fresh, complete DMEM. Typically, 4 dishes (15 cm) are sufficient for one transformation.

For preparing a cell stock, 1 plate (15 cm dish) was trypsinized as before. 8 ml of complete DMEM was then added to dislodge the cells, and cells were placed in a 15 ml sterile tube. The cells were spun at 1,500 g for 10 minutes. The cell pellet was resuspended in 9 ml of complete DMEM/1 ml DMSO, and split into 1 ml samples in orange cap sterile plastic tubes. The cells were slowly frozen by incubation at -20°C for 2 hours, -80°C overnight, and then in liquid nitrogen. To restart the cell line, 10 ml of complete DMEM was added to 1 ml of frozen cells, plated on 10 cm dish, and the media changed the next day.

Production of Recombinant AAV

DNA transfection: For each 15 cm dish, 100 µg of CsCl gradient purified recombinant plasmid DNA was added to obtain an efficient transfection. PDG is a helper plasmid containing wild type AAV *rep* and capsid genes and the adenovirus genes required for AAV particle assembly. Recombinant DNA and pDG (at proximately 1:3 ratio W/W) were resuspended in 875 µl 0.1X TE (10 mM Tris, pH 7.5, 1 mM EDTA), then mixed with 0.125 ml 2 M $CaCl_2$, 1 ml 2X Hepes Buffered Saline (273 mM $NaCl_2$, 10 mM KCl, 1.5 mM Na_2HPO_4, 0.2% Dextrose (w/v), 1% HEPES (w/v), pH 7.05) to obtain 2 ml of transfection solution. The transfection solution was incubated at room temperature for 5 to 10 minutes until a hazy precipitate formed. After the old media was removed, 3 ml of DMEM/10% FBS was added to the transfection solution and the mix plated onto a 15 cm plate. The cells were incubated at 37°C/5% CO_2 overnight, and the media changed the next morning. The cells were harvested on the third day after transfection.

Virus harvest: Cells on the dish were removed using a cell scraper, and collected into centrifuge tubes. The cells were pelleted at 1,500 rpm for 15 minutes, then suspended in lysis buffer (1 ml/dish, 150 mM NaCl, 50 mM Tris-HCl, pH 8.4). The pellet can be stored at -70°C until the next step. To harvest recombinant virus, the cells were frozen and thawed 3 times, then spun at 3,000 g for 5 minutes at 4°C. The supernatant was transferred to 50 ml OakRidge tubes, and cold saturated ammonium sulfate (1/3 volume of lysis buffer, pH 7.0) added to the supernatant. The precipitate was incubated on ice for 10 minutes, and then spun at 8,000 rpm in a JA-20 rotor for 10 minutes at 4°C. The supernatant was collected and transferred to fresh 50 ml OakRidge tubes. Cold saturated ammonium sulfate (2/3 volume of lysis buffer, pH 7.0) was added to the supernatant, and put on ice for 20 minutes for a second precipitation. The solution was spun at 12,000 rpm in a JA-20 rotor for 20 minutes at 4°C. The virus pellet was resuspended in 39 ml CsCl solution (1.37 g/ml in PBS), and put into Beckman Quick-seal tubes (39 ml). After the tubes were sealed, the CsCl solution was spun in a 60Ti rotor at 60,000 rpm for 20 hrs at 15°C. Using a 20 gauge needle, the middle third of the gradient was collected as 1000 µl aliquots into 1.5 ml eppendorf tubes. The fractions were stored at -20°C until the next step.

PCR determination of recombinant virus fraction: 1 µl of a 1:100 dilution of each gradient fraction was used as a template for PCR with primers specific to the input recombinant DNA. Positive fractions were pool together and concentrated by spinning through Centricon filters (#15 centrifugal filter, 50k MWC, Millipore), washed with Ringer's lactated solution 3 times, then resuspended in 200 µl of Ringer's lactated solution.

Quantitative competitive PCR to determine recombinant virus titer: 1 µl of the virus stock was incubated with 10 µl DNase I (BRL) in 100 µl reaction mix (50 mM Tris-HCl, pH 7.5, 10 mM $MgCl_2$) at 37°C for 1 hour. This step eliminates contamination by recombinant DNA on the outside of rAAV virions. Then 10 µl of 10X Proteinase K buffer was added (100 mM Tris-HCl, pH8.0, 100 mM EDTA, 10% SDS), followed by 1 μl proteinase K (18.6 mg/ml, Boehringer). The mixture was incubated at 37°C for 1 hour. Viral DNA was then purified by phenol/chloroform extraction twice, followed by chloroform extraction and ethanol precipitation using 10 μg glycogen as a carrier. The DNA pellet was resuspended in 20 μl of H_2O.

To determine the physical titer of rAAV, a series of competitive PCR reactions were set up using a deleted GFP DNA template as competitor. For rAAV containing the mouse opsin promoter, ΔMop500 was used as competitive template. A series of concentrations of ΔMop500 (100, 50, 10, 1, 0.2 pg) with 2 μl viral DNA was used in each PCR reaction. 5 μl of each PCR reaction was loaded onto a 1.5% agarose gel and the intensities of the viral DNA product and competitor DNA PCR product were determined by densitometry and plotted versus the concentration of ΔMop500. The concentration of rAAV DNA was derived from the point of equal density between the two PCR products. Theoretically, 1 pg viral DNA is equivalent to 4×10^5 recombinant AAV particles.

Subretinal Injection of rAAV

1 month old *rd*/+ mice (CSJL/f1, Jackson lab) were anesthetized by injecting 150 μl ketamine-HCl/xylazine(20 mg/ml) (1:1 and diluted to 1:5) intraperitoneally. The eyes were swabbed with 2.5% Mydfrin (Phenylephrine HCl), Tropicamide ophthalmic solution, and 0.5% Proparacaine HCl. Before injecting the virus, one drop of 2.5% Hydroxyl propyl methylcellulose was placed on the eye. The animals were housed for another 5 weeks after injection before the transgene effect was determined (Figure 6-1).

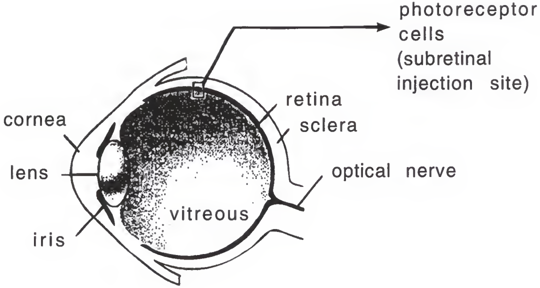

Figure 6-1: Schematic diagram of the subretinal injection (modified from Miyoshi *et al*, 1996)

RFLP for Determining β PDE mRNA Levels

The retinas of *rd*/+ mice were taken 30 days after injection. Each retina was put into one tube. Retinal RNA of each retina was prepared by the Trizol method following manufacture's instruction (BRL). RT-PCR and RFLP were performed as described in Chapter 4.

Results

Subretinal Injection

It is critical to deliver the transgene-containing rAAV to the subretinal space. Subretinal injection is the most direct route for gene delivery to photoreceptor since all inner segments are accessible here (Figure 6-1). Although an intravitreous injection might be less damaging, rAAV must diffuse through the inner retina before reaching photoreceptor bodies, and this severely reduces the transduction efficiency (Zolotukhin., et al, 1996). Since mouse eyes are small, it is necessary to attempt to monitor the injection. Visible dyes or fluorescent dyes can be coinjected to determine the site of injection. Alternatively, an rAAV containing both GFP and ribozymes can be used for this purpose. By determining retinal expression of GFP, it should be possible to determine whether the injection is successful or not. As a test, fluorescent dyes were injected into 5 mice by subretinal injection. The dyes were detected in the subretinal space in 6 out of 10 eyes, indicating that about a 60% injection success rate can be expected.

Ribozyme Rz636 Lowers Rod *rd* mutant β-PDE mRNA Levels

The nonsense β-PDE mRNA level in heterozygous *rd*/+ mice was determined 8 weeks after the injection of rAAV containing a gene for the Rz636 ribozyme. By RFLP analysis of RT-PCR products (see chapter 4), Rz636 can decrease nonsense mRNA transcripts from 7 to 15% (Figure 6-2). This decrease of nonsense transcripts suggests that ribozyme Rz636 can function within the photoreceptor, and can be used for the transgenic *rd* mouse study. The control ribozyme, WRz, did not show significant effects in the *rd*/+ mouse, implying that any antisense effect might not be measurable in photoreceptors of the *rd*/+ mouse. I plan to inject those two ribozymes into the transgenic mouse retina, and assay whether either can delay the retinal degeneration of transgenic *rd* mouse. The aim is to reduce the level of the *rd* transcript to levels near that seen in the *rd*/+ animal, which does not exhibit photoreceptor cell death and retinal degeneration.

Discussion

We have found that ribozyme Rz636 can decrease by up to 15% the β-PDE nonsense transcript level in the heterozygous *rd*/+ mouse. The inactive control ribozyme, WRz, had essentially no effect on nonsense β-PDE transcripts. This result shows that ribozymes can be functional inside photoreceptors. There are several possibilities for the modest decrease by Rz636. The rAAV titer was not very high (8×10^{10} particles/ml), and just 1 μl was injected into the retina. Therefore, the rAAV might not transduce a very large fraction of photoreceptors. However, when using the GFP reporter gene in a similar rAAV vector in rats, 20-30% of the photoreceptors were transduced (Flannery, et

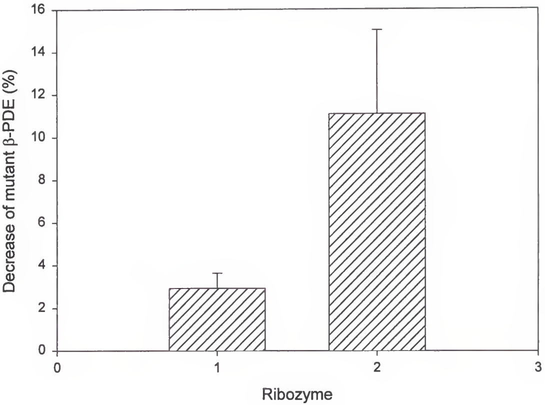

Figure 6-2: Reduction of mutant β-PDE mRNA in heterozygous *rd*/+ mice 8 weeks after subretinal injection with rAAV-pWRz (column 1) or rAAV-pRz636 (column 2). The amount of mutant β-PDE mRNA amount was determined by RT-PCR and RFLP from the total retinal RNA of the 8 week post injection *rd*/+ mice. The value given is the average±the standard deviation from three different digestions.

al 1997). If a similar fraction of mouse photoreceptors were transduced here by Rz636, a 15% reduction in β-PDE mutant transcript would be a significant reduction in most individual transformed photoreceptors. Alternatively, if the injection was not in the subretinal space, some viruses might diffuse to other tissues instead of penetrating photoreceptors, further reducing vector efficiency. The low level of endogenous mutant β-PDE transcripts (25% of the total β-PDE mRNA) might also result in the relatively modest reduction of nonsense target, since this low amount of target might decrease the binding probability between the ribozyme and target.

Even with a modest decrease of nonsense β-PDE mRNA, we may be able to see a phenotypic change in injected transgenic *rd* mouse. Several previous *in vivo* experiments have shown that the ribozymes could produce an altered phenotype without detectable target RNA cleavage (Saxena and Ackerman, 1990; Steinecke et al., 1992). In such cases, 100-1000 fold excess ribozyme might be needed to obtain a clear cleavage product. The mouse opsin promoter is a very strong promoter, and should produce relatively high ribozyme levels. Since transgenic *rd* mice (*rd/rd*/+) are likely to have more *rd* transcript relative to wild type transcript than the *rd*/+ heterozygote, any reduction of nonsense β-PDE mRNA could dramatically change this balance and extend rescue in transgenic *rd/rd*/+ mouse.

Currently ribozyme Rz838, specific to wild type β-PDE transcripts, is also being tested in heterozygous *rd*/+ mice. If successful, this ribozyme would induce retinal degeneration in *rd*/+ mouse by decreasing wild type vs *rd* transcript. To obtain a clean result, high titer recombinant virus and better injection techniques may be needed. All ribozymes have been cloned behind the mop500 promoter, and GFP can be used to monitor successful photoreceptor gene expression. On the negative side, the titer of rAAV containing ribozymes is currently not as high as other rAAV preps containing only reporter genes. It is possible that the secondary structure of ribozyme affects packaging efficiency, or that the size of the ribozyme clones is insufficient for efficient packaging.

It is currently unclear whether the transgene delivered by rAAV exists in the photoreceptors as an episome or is integrated into the genome. Preliminary results suggest rAAV might exist in an episomal form after initial infection, then eventually integrate into the genome (Yan et al., unpublished). Since the AAV Rep protein is necessary for efficient integration, without Rep, rAAV may stay as an episome until a less efficient integration mechanism pre-existing in photoreceptors can occur. It is not clear whether rAAV can integrate into specific sites in the mouse chromosome because the sequence of the human integration site for AAV 2 is not present in the mouse. However, if there is some wild type AAV contamination in the rAAV prep, the integration of the transgenes into mouse genome by rAAV may be enhanced even without the correct target sequence because some Rep protein would be made. Fisher et al. (1997) have shown that a *lacZ* reporter gene can exist as head to tail concatamers in mouse muscle cells, suggesting that this transgene is in the proper form for integration into the genome. Even though the exact nature and location of transgenes inside the cells *in vivo* is unclear presently, most rAAV-derived transgenes can be expressed for long periods. The expression of Factor IX can last for over half a year. If this is also the case for ribozyme expression in the transgenic *rd/rd/+* mouse, we should see an extended rescue phenotype appearing. Ribozymes can be a powerful tool for retinal degeneration therapy, and can be used for the study of gene regulation in photoreceptors. The best current example is for rAAV-derived ribozymes against the P23H transgenic rat with a P23H mutation in the rhodopsin gene (Lewin, unpublished).

CHAPTER 7
CONCLUSIONS AND PERSPECTIVES

This work has tested several elements required for a successful gene therapy approach for inherited retinal diseases:

1) To determine the *cis* elements in the upstream region of the bovine rhodopsin gene, an *in vitro* transcription system was set up using bovine retinal nuclear extract. Vectors containing a series of sequential deletions in the upstream region of rhodopsin based on the position of DNA footprints were constructed for *in vitro* transcription. The nuclear extract can direct correct transcription from the *in vivo* start site without supplementing with exogenous RNA polymerase II, indicating that Pol II and basal transcription factors for opsin expression are present. However, co-purifying nuclease activity in bovine nuclear extract was high, and caused an inconsistency in obtaining reproducible transcription. A G-rich region close to *in vivo* start site appears to lead to an artifactual transcription start site during *in vitro* transcription at position +10. It may be possible to test whether this G-rich track causes the artifactual start site by deleting them. 2.1 kb, 1.6 kb and 0.6 kb rod opsin promoters exhibited similar transcriptional activities. Therefore, *cis*-elements beyond 673 bp in rod opsin promoter are unnecessary for vector experiments but might be responsible for the developmental or more subtle tissue specific regulation.

2) To investigate the molecular mechanism relating phenotype and genotype in the *rd* mouse, I determined mRNA and pre-mRNA levels derived from the wild type and position 347 nonsense mutant β phosphodiesterase genes and compared these with the corresponding gene copy ratios. Quantitative RT-PCR and RFLP were used to determine the ratio between the wild type and mutant pre-mRNA and mature mRNA. The gene copy ratio between wild type and *rd* β PDE was determined by quantitative PCR. The pre-mRNA ratio of wild type verses nonsense mutant was close to 1:1, whereas the corresponding mRNA ratio was greater than 3:1 even though the gene copy ratio was confirmed to be 1:1. The equivalence of pre-mRNA levels for wild type and nonsense mutant in the *rd*/+ retina indicates that both genes are transcribed at similar levels. Thus, the intron 1 retroviral insertion also present in the *rd* gene does not affect gene transcription. In contrast, the strain-independent bias favoring wild type mRNA *in vivo* suggests a specific degradation of mutant transcript during or after pre-mRNA splicing. This allele-specific degradation serves to reduce mutant transcript levels dramatically in all *rd* strains, and suggests that a general mechanism may exist in photoreceptor cells for reducing the level of nonsense mutant mRNA. This observation may provide one possible explanation to the unexpected previous result that, although the *rd* mutation is recessive, rod cells in *rd*/*rd* animals provided with a wild type β-PDE transgene are not permanently rescued.

3) To eventually determine the role of the nonsense transcript of β-PDE in the retinal degeneration of *rd* mouse, I have designed a hammerhead ribozyme (Rz636) to selectively cleave the nonsense (codon 347) mutant mRNA and determined its activity *in*

vitro. Synthetic RNA targets and ribozymes were used in an *in vitro* cleavage reaction to determine catalytic efficiency. Total retinal RNA from heterozygous *rd* mice were also used as a substrates, and the cleavage of *rd* nonsense mRNA assayed by RT-PCR and RFLP. This hammerhead ribozyme cleaved the synthetic nonsense target specifically and did not digest the wild type sequence. Substrate cleavage can be seen in 10 mM Magnesium and was detectable within 30 minutes incubation. The kinetics of Rz636 were determined (k_{cat}/K_M ratio=$1.5x10^6$ $M^{-1}min^{-1}$). An inactive ribozyme control can cleave neither mutant nor wild-type target. Ribozyme Rz636 can also cleave the intact *rd* mRNA in the total retinal RNA from heterozygous *rd*/+ mouse. *In vivo* expression of this ribozyme should specifically decrease nonsense *rd* transcript, and might extend the rescue in the retinal degeneration of the transgenic *rd* mouse.

Another hammerhead ribozyme (Rz838) was designed to specifically cleave the wild type transcript of β-PDE at codon 347. If this ribozyme can specifically decrease the amount of wild type β-PDE, it might lead to the imbalance of the wild type and nonsense mutant β-PDE mRNA in the rd/+ heterozygous mouse, and induce retinal degeneration. This will prove our hypothesis in the complementary sense. Ribozyme Rz838 was found to specifically cleave mutant RNA oligonucleotide, and its kinetic constants are similar to that of Rz636. The cleavage rate of both ribozymes are within the range of natural ribozymes. Ribozyme Rz838 is also capable of specifically cleaving full length wild type β-PDE transcripts.

4) To test whether hnRNP A1 protein can enhance the rate of the ribozyme cleavage reaction, A1 binding sites were linked to ribozyme RZ636. Ribozyme cleavage was then

tested *in vitro*. The A1 protein could bind specifically to ribozymes with A1 binding sites, but did not enhance their cleavage rates. A trace of nuclease co-purifying with recombinant GST-A1 protein may have reduced the amount of active ribozyme in the *in vitro* assay, and could account for the reduction in ribozyme cleavage products. Ribozymes with A1 binding sites can also bind several other nuclear proteins in a Hela nuclear extract, indicating those proteins might interact with ribozymes *in vivo*.

5) Ribozyme Rz636 was delivered into the heterozygous *rd*/+ mouse by subretinal injection, and was shown to specifically decrease mutant β-PDE transcripts by 7 to 15 %. This demonstrates that ribozymes can function in the photoreceptor and alter its target mRNA level. This ribozyme is going to be delivered into retinas of transgenic *rd/rd*/+ mice to determine whether it can extend retinal rescue beyond 4 months by reducing the *rd* transcript level relative to the wild type transgene transcript.

Ribozyme Rz838 (cleaves wild type β-PDE mRNA) will be delivered into heterozygous *rd*/+ mice in order to determine whether its expression can create retinal degeneration in *rd*/+ mouse. Since injection efficiencies vary, a GFP reporter gene driven by its own mouse proximal promoter was linked with the ribozyme, thus giving us a direct way to determine the quality of each injection. It is important to know whether this ribozyme can result in a new phenotype. If so, other ribozymes targeting different genes could be created to produce "somatic knock out" retina, a very useful tool for understanding retinal diseases. It may also be possible to study some genes that are lethal in a whole animal knock out by targeting those genes in a particular tissue or organ.

Catalytic RNA is not only useful for autosomal dominant retinal diseases, but may also be effective in autosomal recessive diseases. RNA repair mediated by ribozyme cleavage/ligation activities can be used to correct a mutant transcript (Sullenger and Cech., 1994). This could have significant advantages over wild type gene addition because the wild type gene is usually regulated by a partially endogenous promoter or a viral promoter. It is therefore difficult to obtain levels of expression matching that of the original gene. Additionally, transgene expression might be repressed by methylation or insertional site effects. Correction of an endogenous defective gene at the RNA level could yield the precise genetic control required for effective rescue.

Many mutations in either photoreceptor-specific genes or non-photoreceptor-specific genes result in retinal degeneration. Ribozymes might be a general and effective way to relieve these symptoms *in vivo*. Ways to increase the efficiency of the ribozymes may be critical for obtaining an optimal therapeutic effect. Unfortunately, hnRNP A1, which binds to ribozymes *in vivo* and *in vitro*, had no measurable effect on cleavage activity. The length of helix arm may be an important factor in determining the specificity and cleavage rate of the ribozyme. Systematic analysis of this factor will be necessary to optimize each ribozyme for each different mutations. Asymmetric arm length might also increase the affinity of a ribozyme without losing specificity. Additionally, embedding the ribozyme in a stable tRNA or snRNA sequences might increase their stability and generate enhanced therapeutic effects (Michienzi et al., 1996). Multiple ribozymes for the same target can be expressed as a single RNA molecule to improve the ribozyme efficiency (Ohkawa et al., 1993). The design of novel ribozymes to target any mutation remains a challenge, but could be resolved through *in vitro* selection techniques.

The high specificity of ribozymes could also be a disadvantage when dealing with a board spectrum of mutations. There are more than 80 mutations in rhodopsin alone related to retinal degeneration. It will be very labor intensive to target each mutation with an efficient ribozyme. Since the clinical progression of most retinal diseases is slow, it may be possible to introduce genes more general effects to extend the survival of photoreceptors. The apoptosis pathway is ultimately responsible for most photoreceptor death from genetic defects. Therefore, ways to inhibit this process could be critical for therapeutic survival of photoreceptors. Cytokines, neurotrophic factors and neurophins appears to stimulate different pathways for extending cell survival. Introducing such therapeutic factors into the retina has been shown to protect photoreceptors from light damage in the rat (LaVail et al., 1992). Similar effects have also been found for the transgenic Bcl-2 mouse (Chen et al., 1996). Since Bcl-2 is an oncogene, it is critical to restrict gene expression to specifically affected tissues and the proximal rhodopsin promoter identified have satisfies that requirement. A further understanding of gene regulation in photoreceptors will be very important for reaching this goal. Another necessity is to identify the receptor and the signaling pathway in photoreceptors for each potential therapeutic factor. By dissecting these pathways, it should be possible to identify the optimal therapeutic factor or specific inhibitor of apoptosis.

Another consideration for the gene therapy for retinal degeneration is achieving efficient delivery of the desired gene to photoreceptors. Currently, the majority of delivery is through a subretinal or intravitreous injection, and damage to the eye by these injection routes can be substantial. Ways to target the genes into retinal cells without damaging the retina remains a problem. Since some viruses, such as herpesvirus, naturally and efficiently infect the eye, and it may be possible to use such viral vectors to target appropriate cell receptors for gene delivery. Adeno-associated virus is clearly promising gene delivery vector for the retina, and it is worth expanding routes of infection in photoreceptors using this system.

The eye is a relatively isolated compartment, and offers easy access to injections. These are very useful properties for any gene therapy approach to disease. Most genes in visual transduction have been cloned and sequenced, and many mutations related to retinal diseases have been identified in these genes. The eye is therefore a very attractive model for gene therapy, and should provide useful information for gene therapy in general.

LIST OF REFERENCES

Acsadi, G., Dickson, G., Love, D.R., Jani, A., Walsh, F.S., Gurusinghe, A., Wolff, J.A. and Davies, K.E. 1991. Human dystrophin expression in mdx mice after intramuscular injection of DNA constructs. Nature **352**: 815-8.

Aharon, T. and Schneider, R.J. 1993. Selective destabilization of short-lived mRNAs with the granulocyte-macrophage colony-stimulating factor AU-rich 3' noncoding region is mediated by a cotranslational mechanism. Mol Cell Biol **13**: 1971-80.

Alexander, I.E., Russell, D.W. and Miller, A.D. 1994. DNA-damaging agents greatly increase the transduction of nondividing cells by adeno-associated virus vectors. J Virol **68**: 8282-7.

Ali, R., Reichel, M., Thrasher, A., Levinsky, R., Kinnon, C., Kanuga, N., Hunt, D. and Bhattacharya, S. 1996. Gene transfer into the mouse retina mediated by an adeno-associated viral vector. Hum. Mol. Genet. **5**: 591-594.

Allikmets, R., Shroyer, N.F., Singh, N., Seddon, J.M., Lewis, R.A., Bernstein, P.S., Peiffer, A., Zabriskie, N.A., Li, Y., Hutchinson, A., Dean, M., Lupski, J.R. and Leppert, M. 1997a. Mutation of the Stargardt disease gene (ABCR) in age-related macular degeneration. Science **277**: 1805-7.

Allikmets, R., Singh, N., Sun, H., Shroyer, N.F., Hutchinson, A., Chidambaram, A., Gerrard, B., Baird, L., Stauffer, D., Peiffer, A., Rattner, A., Smallwood, P., Li, Y., Anderson, K.L., Lewis, R.A., Nathans, J., Leppert, M., Dean, M. and Lupski, J.R. 1997b. A photoreceptor cell-specific ATP-binding transporter gene (ABCR) is mutated in recessive Stargardt macular dystrophy. Nat Genet **15**: 236-46.

Altschuler, M., Tritz, R. and Hampel, A. 1992. A method for generating transcripts with defined 5' and 3' termini by autolytic processing. Gene 122:85-90

Anant, J.S., Ong, O.C., Xie, H.Y., Clarke, S., PJ, O.B. and Fung, B.K. 1992. In vivo differential prenylation of retinal cyclic GMP phosphodiesterase catalytic subunits. J Biol Chem **267**: 687-90.

Anderson, P., Monforte, J., Tritz, R., Nesbitt, S., Hearst, J. and Hampel, A. 1994. Mutagenesis of the hairpin ribozyme. Nucleic Acids Res **22**: 1096-100.

Apostolakos, M., Schuermann, W., Frampton, M., Utell, M. and Willey, J. 1993. Measurement of Gene Expression by Multiplex Competitive Polymerase Chain Reaction. Anal Biochem **213**: 277-284.

Baehr, W., Champagne, M.S., Lee, A.K. and Pittler, S.J. 1991. Complete cDNA sequences of mouse rod photoreceptor cGMP phosphodiesterase alpha- and beta-subunits, and identification of beta'-, a putative beta-subunit isozyme produced by alternative splicing of the beta-subunit gene. FEBS Lett **278**: 107-14.

Bajocchi, G., Feldman, S.H., Crystal, R.G. and Mastrangeli, A. 1993. Direct in vivo gene transfer to ependymal cells in the central nervous system using recombinant adenovirus vectors. Nat Genet **3**: 229-34.

Beelman, C. and Parker, R. 1995. Degradation of mRNA in Eukaryotes. Cell **81**: 179-183.

Been, M.D. 1994. Cis- and trans-acting ribozyme from a human pathogen, hepatitis delta virus. Trends Biol Sci **19**: 252-256.

Belgrader, P., Cheng, J. and Maquat, L.E. 1993. Evidence to implicate translation by ribosomes in the mechanism by which nonsense codons reduce the nuclear level of human triosephosphate isomerase mRNA. Proc Natl Acad Sci USA **90**: 482-486.

Belgrader, P., Cheng, J., Zhou, X., Stenphenson, L.S. and Maquat, L.E. 1994a. Mammalian nonsense codons can be cis effectors of nuclear mRNA half-Life. Mol Cell Biol **14**: 8219-8228.

Belgrader, P. and Maquat, L.E. 1994b. Nonsense but not missense mutations can decrease the abundance of nuclear mRNA for the mouse major urinary protein, while both types of mutations can facilitate exon skipping. Mol Cell Biol **14**: 6326-6336.

Bennett, J., Tanabe, T., Sun, D., Zeng, Y., Kjeldbye, H., Gouras, P. and Maguire, A.M. 1996. Photoreceptor cell rescue in retinal degeneration (rd) mice by in vivo gene therapy. Nat Med **2**: 649-54.

Bennett, J., Wilson, J., Sun, D., Forbes, B. and Maguire, A. 1994. Adenovirus vector-mediated in vivo gene transfer into adult murine retina. Invest Ophthalmol Vis Sci **35**: 2535-42.

Berget, S.M. 1995. Exon recognition in vertebrate splicing. J Biol Chem **270**: 2411-4.

Berson, E.L., Rosner, B., Sandberg, M.A., Hayes, K.C., Nicholson, B.W., Weigel DiFranco, C. and Willett, W. 1993. A randomized trial of vitamin A and vitamin E supplementation for retinitis pigmentosa. Arch Ophthalmol **111**: 761-72.

Bertrand, E., Pictet, R. and Grange, T. 1994. Can hammerhead ribozymes be efficient tools to inactivate gene function? Nucleic Acids Res **22**: 293-300.

Bertrand, E.L. and Rossi, J.J. 1994. Facilitation of hammerhead ribozyme catalysis by the nucleocapsid protein of HIV-1 and the heterogeneous nuclear ribonucleoprotein A1. EMBO J **13**: 2904-12.

Bird, A.C. 1995. Retinal photoreceptor dystrophies. Am. J. Ophthalmol **119**: 543-562.

Blomhoff, R., Green, M.H., Berg, T. and Norum, K.R. 1990. Transport and storage of vitamin A. Science **250**: 399-404.

Bok, D. 1985. Retinal photoreceptor-pigment epithelium interactions. Invest. Ophthalmol. Vis. Sci. **26**: 1659-1694.

Bonifacino, J.S., Suzuki, C.K., Lippincott Schwartz, J., Weissman, A.M. and Klausner, R.D. 1989. Pre-Golgi degradation of newly synthesized T-cell antigen receptor chains: intrinsic sensitivity and the role of subunit assembly. J Cell Biol 109: 73-89

Bowes, C., Danciger, M., Kozak, C.A. and Farber, D.B. 1989. Isolation of a candidate cDNA for the gene causing retinal degeneration in the rd mouse. Proc Natl Acad Sci U S A **86**: 9722-6.

Bowes, C., Li, T., Danciger, M., Baxter, L.C., Applebury, M.L. and Farber, D.B. 1990. Retinal degeneration in the rd mouse is caused by a defect in the beta subunit of rod cGMP-phosphodiesterase [see comments]. Nature **347**: 677-80.

Bowes, C., Li, T., Frankel, W.N., Danciger, M., Coffin, J.M., Applebury, M.L. and Farber, D.B. 1993. Localization of a retroviral element within the rd gene coding for the beta subunit of cGMP phosphodiesterase. Proc Natl Acad Sci U S A **90**: 2955-9.

Boyer, J.D., Ugen, K.E., Wang, B., Agadjanyan, M., Gilbert, L., Bagarazzi, M.L., Chattergoon, M., Frost, P., Javadian, A., Williams, W.V., Refaeli, Y., Ciccarelli, R.B., McCallus, D., Coney, L. and Weiner, D.B. 1997. Protection of chimpanzees from high-dose heterologous HIV-1 challenge by DNA vaccination. Nat Med **3**: 526-32.

Brawerman, G. 1990. Mechanisms of mRNA decay. Trends Biotechnol **8**: 171-4.

Breakefield, X.O. and DeLuca, N.A. 1991. Herpes simplex virus for gene delivery to neurons. New Biol **3**: 203-18.

Bridges, C.D. and Alvarez, R.A. 1987. The visual cycle operates via an isomerase acting on all-trans retinol in the pigment epithelium. Science **236**: 1678-1680.

Buchschacher, G.L., Jr. and Panganiban, A.T. 1992. Human immunodeficiency virus vectors for inducible expression of foreign genes. J Virol **66**: 2731-9.

Burd, C.G. and Dreyfuss, G. 1994. RNA binding specificity of hnRNP A1: significance of hnRNP A1 high-affinity binding sites in pre-mRNA splicing. EMBO J **13**: 1197-204.

Buvoli, M., Cobianchi, F., Biamonti, G. and Riva, S. 1990. Recombinant hnRNP protein A1 and its N-terminal domain show preferential affinity for oligodeoxynucleotides homologous to intron/exon acceptor sites. Nucleic Acids Res **18**: 6595-600.

Carey, M. 1998. The enhanceosome and transcription synergy. Cell **92**: 5-8.

Cartegni, L., Maconi, M., Morandi, E., Cobianchi, F., Riva, S. and Biamonti, G. 1996. hnRNP A1 selectively interacts through its Gly-rich domain with different RNA-binding proteins. J Mol Biol **259**: 337-48.

Carter Dawson, L.D. and LaVail, M.M. 1979a. Rods and cones in the mouse retina. I. Structural analysis using light and electron microscopy. J Comp Neurol **188**: 245-62.

Carter Dawson, L.D. and LaVail, M.M. 1979b. Rods and cones in the mouse retina. II. Autoradiographic analysis of cell generation using tritiated thymidine. J Comp Neurol **188**: 263-72.

Cech, T.R. 1990. Self-splicing of group I introns. Annu Rev Biochem. **59**: 543-68

Cepko, C.L., Austin, C.P., Yang, X., Alexiades, M. and Ezzeddine, D. 1996. Cell fate determination in the vertebrate retina. Proc Natl Acad Sci U S A **93**: 589-95.

Chang, G.Q., Hao, Y. and Wong, F. 1993. Apoptosis: final common pathway of photoreceptor death in rd, rds, and rhodopsin mutant mice. Neuron **11**: 595-605.

Chen, C.Y. and Shyu, A.B. 1995. AU-rich elements: characterization and importance in mRNA degradation. Trends Biochem Sci **20**: 465-70.

Chen, H.H., Mack, L.M., Kelly, R., Ontell, M., Kochanek, S. and Clemens, P.R. 1997. Persistence in muscle of an adenoviral vector that lacks all viral genes. Proc Natl Acad Sci U S A **94**: 1645-50.

Chen, J., Flannery, J.G., LaVail, M.M., Steinberg, R.H., Xu, J. and Simon, M.I. 1996. bcl-2 overexpression reduces apoptotic photoreceptor cell death in three different retinal degenerations. Proc Natl Acad Sci U S A **93**: 7042-7.

Chen, J., Makino, C.L., Peachey, N.S., Baylor, D.A. and Simon, M.I. 1995. Mechanisms of rhodopsin inactivation in vivo as revealed by a COOH-terminal truncation mutant. Science **267**: 374-7.

Chen, S. and Zack, D.J. 1996. Ret 4, a positive acting rhodopsin regulatory element identified using a bovine retina in vitro transcription system. J Biol Chem **271**: 28549-57.

Chowrira, B.M., Berzal, H.A. and Burke, J.M. 1993. Ionic requirements for RNA binding, cleavage, and ligation by the hairpin ribozyme. Biochemistry **32**: 1088-95.

Cideciyan, A.V., Zhao, X., Nielsen, L., Shani, S.C., Jacobson, S.G. and Palczewski, K. 1998. Null mutation in the rhodopsin kinase gene slows recovery kinetics of rod and cone phototransduction in man. Proc. Natl. Acad. Sci. U S A **96**: 328-333.

Cobianchi, F., Karpel, R.L., Williams, K.R., Notario, V. and Wilson, S.H. 1988. Mammalian heterogeneous nuclear ribonucleoprotein complex protein A1. Large-scale overproduction in Escherichia coli and cooperative binding to single-stranded nucleic acids. J Biol Chem **263**: 1063-71.

Coetzee, T., Herschlag, D. and Belfort, M. 1994. Escherichia coli proteins, including ribosomal protein S12, facilitate in vitro splicing of phage T4 introns by acting as RNA chaperones. Genes Dev **8**: 1575-88.

Colley, N.J., Cassill, J.A., Baker, E.K. and Zuker, C.S. 1995. Defective intracellular transport is the molecular basis of rhodopsin-dependent dominant retinal degeneration. Proc Natl Acad Sci U S A **92**: 3070-4.

Connell, G., Bascom, R., Molday, L., Reid, D., McInnes, R.R. and Molday, R.S. 1991. Photoreceptor peripherin is the normal product of the gene responsible for retinal degeneration in the rds mouse. Proc Natl Acad Sci U S A **88**: 723-6.

Cooper, D. 1993. Human Gene Mutations Affecting RNA Processing and Translation. Ann Med **25**: 11-17.

Cote, J., Quinn, J., Workman, J.L. and Peterson, C.L. 1994. Stimulation of GAL4 derivative binding to nucleosomal DNA by the yeast SWI/SNF complex. Science **265**: 53-60.

Couture, L.A. and Stinchcomb, D.T. 1996. Anti-gene therapy: the use of ribozymes to inhibit gene function. Trends Genet **12**: 510-5.

Crystal, R.G. 1995. Transfer of genes to humans: early lessons and obstacles to success. Science **270**: 404-10.

Curiel, D.T., Agarwal, S., Wagner, E. and Cotten, M. 1991. Adenovirus enhancement of transferrin-polylysine-mediated gene delivery. Proc Natl Acad Sci U S A **88**: 8850-4.

Dai, Y., Roman, M., Naviaux, R.K. and Verma, I.M. 1992. Gene therapy via primary myoblasts: long-term expression of factor IX protein following transplantation in vivo. Proc Natl Acad Sci U S A **89**: 10892-5.

Daiger, S.P., Sullivan, L.S. and Rodriguez, J.A. 1995. Correlation of phenotype with genotype in inherited retinal degeneration. Behavioral and Brain Science **18**: 452-467.

Davidson, B.L., Allen, E.D., Kozarsky, K.F., Wilson, J.M. and Roessler, B.J. 1993. A model system for in vivo gene transfer into the central nervous system using an adenoviral vector. Nat Genet **3**: 219-23.

Decker, C. and Parker, R. 1994. Mechanisms of mRNA degradation in eukaryotes. Trends Biochem Sci **19**: 336-340.

DesJardin, L.E. and Hauswirth, W.W. 1996. Developmentally important DNA elements within the bovine opsin upstream region. Invest Ophthalmol Vis Sci **37**: 154-65.

Doshi, M., Voaden, M.J. and Arden, G.B. 1985. Cyclic GMP in the Retinas of Normal Mice and those Heterozygous for Early-onset Photoreceptor Dystrophy. Exp eye Res **41**: 61-65.

Dreyfuss, G., Matunis, M.J., Pinol Roma, S. and Burd, C.G. 1993. hnRNP proteins and the biogenesis of mRNA. Annu Rev Biochem **62**: 289-321.

Dryja, T.P. 1997. Gene-based approach to human gene-phenotype correlations. Proc. Natl. Acad. Sci. USA **94**: 12117-12121.

Durrin, L.K., Mann, R.K., Kayne, P.S. and Grunstein, M. 1991. Yeast histone H4 N-terminal sequence is required for promoter activation in vivo. Cell **65**: 1023-31.

Emerich, D.F., Winn, S.R., Hantraye, P.M., Peschanski, M., Chen, E.Y., Chu, Y., McDermott, P., Baetge, E.E. and Kordower, J.H. 1997. Protective effect of encapsulated cells producing neurotrophic factor CNTF in a monkey model of Huntington's disease. Nature **386**: 395-9.

Faktorovich, E.G., Steinberg, R.H., Yasumura, D., Matthes, M.T. and LaVail, M.M. 1990. Photoreceptor degeneration in inherited retinal dystrophy delayed by basic fibroblast growth factor. Nature **347**: 83-6.

Farber, D.B., Park, S. and Yamashita, C. 1988. Cyclic GMP-phosphodiesterase of rd retina: biosynthesis and content. Exp Eye Res **46**: 363-74.

Farrar, G.J., Kenna, P., Jordan, S.A., Kumar Singh, R., Humphries, M.M., Sharp, E.M., Sheils, D.M. and Humphries, P. 1991. A three-base-pair deletion in the peripherin-RDS gene in one form of retinitis pigmentosa. Nature **354**: 478-80.

Fedor, M.J. and Uhlenbeck, O.C. 1990. Substrate sequence effects on "hammerhead" RNA catalytic efficiency. Proc Natl Acad Sci U S A **87**: 1668-72.

Fender, P., Ruigrok, R.W., Gout, E., Buffet, S. and Chroboczek, J. 1997. Adenovirus dodecahedron, a new vector for human gene transfer. Nat Biotechnol **15**: 52-6.

Ferrari, F.K., Samulski, T., Shenk, T. and Samulski, R.J. 1996. Second-strand synthesis is a rate-limiting step for efficient transduction by recombinant adeno-associated virus vectors. J Virol **70**: 3227-34.

Ferrendelli, J. and Cohen, A. 1976. The effects of light and dard adaptation on the levels of cyclic nucleotides in retinas of mice heterozygous for a gene for photoreceptor dystropy. Biochem Biophys Res Commun **73**: 421-427.

Fisher, K.J., Gao, G.P., Weitzman, M.D., DeMatteo, R., Burda, J.F. and Wilson, J.M. 1996. Transduction with recombinant adeno-associated virus for gene therapy is limited by leading-strand synthesis. J Virol **70**: 520-32.

Fisher, K.J., Jooss, K., Alston, J., Yang, Y., Haecker, S.E., High, K., Pathak, R., Raper, S.E. and Wilson, J.M. 1997. Recombinant adeno-associated virus for muscle directed gene therapy. Nat Med **3**: 306-12.

Flannery, J.G., Zolotukhin, S., Vaquero, M.I., LaVail, M.M., Muzyczka, N. and Hauswirth, W.W. 1997. Efficient photoreceptor-targeted gene expression in vivo by recombinant adeno-associated virus. Proc Natl Acad Sci U S A **94**: 6916-21.

Flotte, T.R., Afione, S.A., Conrad, C., McGrath, S.A., Solow, R., Oka, H., Zeitlin, P.L., Guggino, W.B. and Carter, B.J. 1993. Stable in vivo expression of the cystic fibrosis transmembrane conductance regulator with an adeno-associated virus vector. Proc Natl Acad Sci U S A **90**: 10613-7.

Forster, A.C. and Symons, R.H. 1987. Self-cleavage of virusoid RNA is performed by the proposed 55-nucleotide active site. Cell **50**: 9-16.

Freund, C., Gregory-Evans, C.Y., Furukawa, T., Papaioannou, M., Looser, J., Ploder, L., Bellingham, J., Ng, D., Herbrick, J.S., Duncan, A., Scherer, S.W., Tsui, L., Loutradis-Anagnostou, A., Jacobson, S.G., Cepko, C.L., Bhattacharya, S.S. and Mclnnes, R.R. 1997. Cone-rod dystrophy due to mutations in a novel photoreceptor-specific homeobox gene (CRX) essential for maintenance of the photoreceptor. Cell **91**: 543-553.

Freund, C., Horsford, D.J. and Mclnnes, R.R. 1996. Transcription factor genes and the developing eye: a genetic perspective. Hum Mol Genet **5 Spec No**: 1471-88.

Fujita, S., Koguma, T., Ohkawa, J., Mori, K., Kohda, T., Kise, H., Nishikawa, S., Iwakura, M. and Taira, K. 1997. Discrimination of a single base change in a ribozyme using the gene for dihydrofolate reductase as a selective marker in Escherichia coli. Proc Natl Acad Sci U S A **94**: 391-6.

Fung, B.K., K, Young, J., Yamane, H. and Griswold, P.I. 1990. Subunit Stoichiometry of Retinal Rod cGMP Phosphodiesterase. Biochemistry **29**: 2657-2664.

Furukawa, T., Kozak, C.A. and Cepko, C.L. 1997a. rax, a novel paired-type homeobox gene, shows expression in the anterior neural fold and developing retina. Proc Natl Acad Sci U S A **94**: 3088-93.

Furukawa, T., Morrow, E.M. and Cepko, C.L. 1997b. Crx, a novel otx-like homeobox gene, shows photoreceptor-specific expression and regulates photoreceptor differentiation. Cell **91**: 531-541.

Gal, A., Orth, U., Baehr, W., Schwinger, E. and Rosenberg, T. 1994. Heterozygous missense mutation in the rod cGMP phosphodiesterase beta-subunit gene in autosomal dominant stationary night blindness. Nat Genet **7**: 551.

Gilliland, G., Perrin, S., Blanchard, K. and Bunn, F. 1990. Analysis of cytokine mRNA and DNA: Detection and quantitation by competitive polymerase chain reaction. Proc Natl Acad Sci U S A **87**: 2725-2729.

Giraud, C., Winocour, E. and Berns, K.I. 1994. Site-specific integration by adeno-associated virus is directed by a cellular DNA sequence. Proc Natl Acad Sci U S A **91**: 10039-43.

Grunstein, M. 1997. Histone acetylation in chromatin structure and transcription. Nature **389**: 349-52.

Guo, H.C. and Collins, R.A. 1995. Efficient trans-cleavage of a stem-loop RNA substrate by a ribozyme derived from neurospora VS RNA. EMBO J. **14**: 368-76

Guo, Z. and Sherman, F. 1996. 3'-end-forming signals of yeast mRNA. Mol Cell Biol **15**: 5983-90.

Haase, G., Kennel, P., Pettmann, B., Vigne, E., Akli, S., Revah, F., Schmalbruch, H. and Kahn, A. 1997. Gene therapy of murine motor neuron disease using adenoviral vectors for neurotrophic factors. Nat Med **3**: 429-36.

Hafezi, F., Steinbach, J.P., Marti, A., Munz, K., Wang, Z.Q., Wagner, E.F., Aguzzi, A. and Reme, C.E. 1997. The absence of c-fos prevents light-induced apoptotic cell death of photoreceptors in retinal degeneration in vivo. Nat Med **3**: 346-9.

Hahn, L.B., Berson, E.L. and Dryja, T.P. 1994. Evaluation of the gene encoding the gamma subunit of rod phosphodiesterase in retinitis pigmentosa. Invest Ophthalmol Vis Sci **35**: 1077-82.

Hall, G. and Thein, S.L. 1994. Nonsense codon mutations in the terminal exon of the beta-globin gene are not associated with a reduction in beta-mRNA accumulation: A mechanism for the Phenotype of dominant beta-thalassemia. Blood **83**: 2031-2037.

Halle, J.P. and Meisterernst, M. 1996. Gene expression: increasing evidence for a transcriptosome. Trends Genet **12**: 161-3.

Hara, T., Tan, Y. and Huang, L. 1997. In vivo gene delivery to the liver using reconstituted chylomicron remnants as a novel vector. Proc Natl Acad Sci. U S A **94**:

Hargrave, P.A. and McDowell, H.J. 1992. Rhodopsin and phototransduction: a model system for G protein-linked receptors. FASEB J **6**: 2323-2331.

Haseloff, J. and Gerlach, W.L. 1988. Simple RNA enzymes with new and highly specific endoribonuclease activities. Nature **334**: 585-91.

Hassig, C.A., Fleischer, T.C., Billin, A.N., Schreiber, S.L. and Ayer, D.E. 1997. Histone deacetylase activity is required for full transcriptional repression by mSin3A. Cell **89**: 341-7.

Hegg, L.A. and Fedor, M.J. 1995. Kinetics and thermodynamics of intermolecular catalysis by hairpin ribozymes. Biochemistry **34**: 15813-28.

Heidenreich, O. and Eckstein, F. 1992. Hammerhead ribozyme-mediated cleavage of the long terminal repeat RNA of human immunodeficiency virus type 1. J Biol Chem **267**: 1904-1909.

Hermonat, P.L. and Muzyczka, N. 1984. Use of adeno-associated virus as a mammalian DNA cloning vector: transduction of neomycin resistance into mammalian tissue culture cells. Proc Natl Acad Sci U S A **81**: 6466-70.

Herschlag, D. 1995. RNA chaperones and the RNA folding problem. J Biol Chem **270**: 20871-4.

Herzog, R.W., Hagstrom, J.N., Kung, S.H., Tai, S.J., Wilson, J.M., Fisher, K.J. and High, K.A. 1997. Stable gene transfer and expression of human blood coagulation factor IX after intramuscular injection of recombinant adeno-associated virus. Proc Natl Acad Sci U S A **94**: 5804-9.

Holstege, F.C., van der Vliet, P.C. and Timmers, H.T. 1996. Opening of an RNA polymerase II promoter occurs in two distinct steps and requires the basal transcription factors IIE and IIH. EMBO J **15**: 1666-77.

Huang, S., Stupack, D., Mathias, P., Wang, Y. and Nemerow, G. 1997. Growth arrest of Epstein-Barr virus immortalized B lymphocytes by adenoviurs-delivery ribozymes. Proc Natl Acad Sci. U S A **94**: 8156-8161.

Huang, S.H., Pittler, S.J., Huang, X., Oliveira, L., Berson, E.L. and Dryja, T.P. 1995. Autosomal recessive retinitis pigmentosa caused by mutations in the alpha subunit of rod cGMP phosphodiesterase. Nat Genet **11**: 468-71.

Humphries, M.M., Rancourt, D., Farrar, J., Kenna, P., Hazel, M., Bush, R.A., Sieving, P.A., Sheils, D.M., McNally, N., Creighton, P., Erven, A., Boros, A., Gullya, K., Capecchi, M.R. and Humphries, P. 1997. Retinopathy induced in mice by targeted disruption of the rhodopsin gene. Nat. Gen. **15**: 216-219.

Hurley, J.B. and Stryer, L. 1982. Purification and characterization of the gamma regulatory subunit of the cyclic GMP phosphodiesterase from retinal rod outer segments. J Biol Chem **257**: 11094-9.

Jacobon, S., Kemp, c., Sung, C.H. and Nathans, J. 1991. Retinal Function and Rhodopsin Levels in Autosomal Dominant Retinitis Pigmentosa With Rhodopsin Mutations. Am J Ophthalmol **112**: 256-271.

Jaffe, H.A., Danel, C., Longenecker, G., Metzger, M., Setoguchi, Y., Rosenfeld, M.A., Gant, T.W., Thorgeirsson, S.S., Stratford Perricaudet, L.D., Perricaudet, M. and et al. 1992. Adenovirus-mediated in vivo gene transfer and expression in normal rat liver. Nat Genet **1**: 372-8.

Jayasena, V.K. and Gold, L. 1997. In vitro selection of self-cleaving RNAs with a low optimum. Proc Natl Acad Sci, U S A **94**: 10612-10617.

Kamakaka, R.T. and Kadonaga, J.T. 1994. The soluble nuclear fraction, a highly efficient transcription extract from Drosophila embryos. Methods Cell Biol **44**: 225-35.

Kaneko, A. 1979. Physiology of the retina. Ann. Rev. Neurosci. **2**: 169-91.

Kaplitt, M.G., Kwong, A.D., Kleopoulos, S.P., Mobbs, C.V., Rabkin, S.D. and Pfaff, D.W. 1994a. Preproenkephalin promoter yields region-specific and long-term expression in adult brain after direct in vivo gene transfer via a defective herpes simplex viral vector. Proc Natl Acad Sci U S A **91**: 8979-83.

Kaplitt, M.G., Leone, P., Samulski, R.J., Xiao, X., Pfaff, D.W., KL, O.M. and During, M.J. 1994b. Long-term gene expression and phenotypic correction using adeno-associated virus vectors in the mammalian brain. Nat Genet **8**: 148-54.

Kaufmann, J. and Smale, S.T. 1994. Direct recognition of initiator elements by a component of the transcription factor IID complex. Genes Dev **8**: 821-9.

Kay, M.A., Liu, D. and Hoogerbrugge, P.M. 1997. Gene therapy. Proc Natl Acad Sci. U S A **94**: 12744-12746.

Kazazian, H.H., Jr., Dowling, C.E., Hurwitz, R.L., Coleman, M., Stopeck, A. and Adams, J.G.d. 1992. Dominant thalassemia-like phenotypes associated with mutations in exon 3 of the beta-globin gene. Blood **79**: 3014-8.

Kenan, D.J., Query, C.C. and Keene, J.D. 1991. RNA recognition: towards identifying determinants of specificity. Trends Biochem Sci **16**: 214-20.

Khavari, P.A., Peterson, C.L., Tamkun, J.W., Mendel, D.B. and Crabtree, G.R. 1993. BRG1 contains a conserved domain of the SWI2/SNF2 family necessary for normal mitotic growth and transcription. Nature **366**: 170-4.

Kiledjian, M. and Dreyfuss, G. 1992. Primary structure and binding activity of the hnRNP U protein: binding RNA through RGG box. EMBO J **11**: 2655-64.

Koizumi, M., Iwai, S. and Ohtsuka, E. 1988. Construction of a series of several self-cleaving RNA duplexes using synthetic 21-mers. FEBS Lett **228**: 228-30.

Koleske, A.J. and Young, R.A. 1995. The RNA polymerase II holoenzyme and its implications for gene regulation. Trends Biochem Sci **20**: 113-6.

Kopito, R.R. 1997. ER quality control: the cytoplasmic connection. Cell **88**: 427-30.

Kotin, R.M., Siniscalco, M., Samulski, R.J., Zhu, X.D., Hunter, L., Laughlin, C.A., McLaughlin, S., Muzyczka, N., Rocchi, M. and Berns, K.I. 1990. Site-specific integration by adeno-associated virus. Proc Natl Acad Sci U S A **87**: 2211-5.

Kugler, W., Enssle, J., Hentze, M. and Kulozik, A. 1995. Nuclear degradation of nonsense mutated beta-globin mRNA: a post-translational mechanism to protect heterozygotes from severe clinical manifestations of beta-thalassemia. Nucleic Acids Res **23**: 413-418.

Kumar, R., Chen, S., Scheurer, D., Wang, Q.L., Duh, E., Sung, C.H., Rehemtulla, A., Swaroop, A., Adler, R. and Zack, D.J. 1996. The bZIP transcription factor Nrl stimulates rhodopsin promoter activity in primary retinal cell cultures. J Biol Chem **271**: 29612-8.

Kuo, M.Y., Goldberg, J., Coates, L., Mason, W., Gerin, J. and Taylor, J. 1988. Molecular cloning of hepatitis delta virus RNA from an infected woodchuck liver: sequence, structure, and applications. J Virol **62**: 1855-61.

Lai, Y.L., Wiggert, B., Liu, Y.P. and Chader, G.J. 1982. Interphotoreceptor retinol-binding proteins: possible transport vehicles between compartments of the retina. Nature **298**: 848-849.

LaVail, M., M., Rapaport, D.H. and Rakic, P. 1991. Cytogenesis in the monkey retina. J Comp Neurol **309**: 86-114.

LaVail, M.M., Unoki, K., Yasumura, D., Matthes, M.T., Yancopoulos, G.D. and Steinberg, R.H. 1992. Multiple growth factors, cytokines, and neurotrophins rescue photoreceptors from the damaging effects of constant light. Proc Natl Acad Sci U S A **89**: 11249-53.

Le, G.L.S.G., Robert, J.J., Berrard, S., Ridoux, V., Stratford, P.L., Perricaudet, M. and Mallet, J. 1993. An adenovirus vector for gene transfer into neurons and glia in the brain. Science **259**: 988-90.

Lee, D.Y., Hayes, J.J., Pruss, D. and Wolffe, A.P. 1993. A positive role for histone acetylation in transcription factor access to nucleosomal DNA. Cell **72**: 73-84.

Lee, R.H., Navon, S.E., Brown, B.M., Fung, B.K. and Lolley, R.N. 1988. Characterization of a phosphodiesterase-immunoreactive polypeptide from rod photoreceptors of developing rd mouse retinas. Invest Ophthalmol Vis Sci **29**: 1021-7.

Lem, J., Applebury, M.L., Falk, J.D., Flannery, J.G. and Simon, M.I. 1991. Tissue-specific and developmental regulation of rod opsin chimeric genes in transgenic mice. Neuron **6**: 201-10.

Lem, J., Flannery, J., Li, T., Applebury, M., Farber, D.B. and Simon, M.I. 1992. Retinal degeneration is rescued in transgenic rd mice by expression of the cGMP phosphodiesterase beta subunit. Proc Natl Acad Sci U S A **89**: 4422-4426.

Lewin A.L. 1998. Unpublished results.

Li, L. and Dowling, J.E. 1997. A dominant form of inherited retinal degeneration caused by a non-photoreceptor cell-specific mutation. Proc Natl Acad Sci USA **94**: 11645-11650.

Li, T., Adamian, M., Roof, D.J., Berson, E.L., Dryja, T.P., Roessler, B.J. and Davidson, B.L. 1994. In vivo transfer of a reporter gene to the retina mediated by an adenoviral vector. Invest Ophthalmol Vis Sci **35**: 2543-9.

Lieber, A., He, C.Y., Kirillova, I. and Kay, M.A. 1996. Recombinant adenoviruses with large deletions generated by Cre-mediated excision exhibit different biological properties compared with first-generation vectors in vitro and in vivo. J Virol **70**: 8944-60.

Lieber, A. and Kay, M.A. 1996. Adenovirus-mediated expression of ribozymes in mice. J Virol **70**: 3153-8.

Lieber, A. and Strauss, M. 1995. Selection of efficient cleavage sites in target RNAs by using a ribozyme expression library. Mol Cell Biol **15**: 540-51.

Lim, S.K., Sigmund, C.D., Gross, K.W. and Maquat, L.E. 1992. Nonsense codons in uman beta-globin mRNA result in the production of mRNA degradation products. Mol Cell Biol **12**: 1149-1161.

Lindsay, S., Inglehearn, C., Curtis, A. and Bhattacharya, S. 1992. Molecular genetics of inherited retinal degenerations. Curr Opin Gene Dev **2**: 459-466.

Liu, F., Qi, H., Huang, L. and Liu, D. 1997. Factors controlling the efficiency of cationic lipid-mediated transfection in vivo via intravenous administration. Gene Ther **4**: 517-523.

Liu, F., Yang, J., Huang, L. and Liu, D. 1996. New cationic lipid formulations for gene transfer. Pharm. Res. **13**: 1856-1860.

Liu, I.S., Chen, J.D., Ploder, L., Vidgen, D., van der Kooy, D., Kalnins, V.I. and McInnes, R.R. 1994. Developmental expression of a novel murine homeobox gene (Chx10): evidence for roles in determination of the neuroretina and inner nuclear layer. Neuron **13**: 377-93.

Long, D.M. and Uhlenbeck, O.C. 1993. Self-cleaving catalytic RNA. FASEB J **7**: 25-30.

Low, J.C. 1987. The corneal ERG of the heterozygous retinal degeneration mouse. Graefe's Arch Clin Exp Ophthalmol **225**: 413-417.

Luzi, E., Eckstein, F. and Barsacchi, G. 1997. The newt ribozyme is part of a riboprotein complex. Proc Natl Acad Sci U S A **94**: 9711-9716.

Maquat, L. 1995. When cells stop making sense: effects of nonsense codons on RNA metabolism in vertebrate cells. RNA **1**: 453-465.

Maquat, L. 1996. Defects in RNA Splicing and the Consequence of Shortened Translational Reading Frames. Am J Hum Genet **59**: 279-286.

Maquat, L., Kinniburgh, A., Rachmillewitz, E. and Ross, J. 1981. Unstable beta-globin mRNA in mRNA-deficient beta-0 thalassemia. Cell **27**: 543-553.

Mayeda, A., Helfman, D.M. and Krainer, A.R. 1993. Modulation of exon skipping and inclusion by heterogeneous nuclear ribonucleoprotein A1 and pre-mRNA splicing factor SF2/ASF. Mol Cell Biol **13**: 2993-3001.

Mayeda, A. and Krainer, A.R. 1992. Regulation of alternative pre-mRNA splicing by hnRNP A1 and splicing factor SF2. Cell **68**: 365-75.

Mayrand, S.H., Dwen, P. and Pederson, T. 1993. Serine/threonine phosphorylation regulates binding of C hnRNP proteins to pre-mRNA. Proc Natl Acad Sci U S A **90**: 7764-8.

McLaughlin, M.E., Ehrhart, T.L., Berson, E.L. and Dryja, T.P. 1995. Mutation spectrum of the gene encoding the beta subunit of rod phosphodiesterase among patients with autosomal recessive retinitis pigmentosa. Proc Natl Acad Sci U S A **92**: 3249-53.

McLaughlin, M.E., Sandberg, M.A., Berson, E.L. and Dryja, T.P. 1993. Recessive mutations in the gene encoding the beta-subunit of rod phosphodiesterase in patients with retinitis pigmentosa. Nat Genet **4**: 130-4.

McLaughlin, S.K., Collis, P., Hermonat, P.L. and Muzyczka, N. 1988. Adeno-associated virus general transduction vectors: analysis of proviral structures. J Virol **62**: 1963-73.

Meindl, A., Berger, W., Meitinger, T., van de Pol, D., Achatz, H., Dorner, C., Haasemann, M., Hellebrand, H., Gal, A., Cremers, F. and et al. 1992. Norrie disease is caused by mutations in an extracellular protein resembling C-terminal globular domain of mucins. Nat Genet **2**: 139-43.

Meindl, A., Dry, K., Herrmann, K., Manson, F., Ciccodicola, A., Edgar, A., Carvalho, M.R., Achatz, H., Hellebrand, H., Lennon, A., Migliaccio, C., Porter, K., Zrenner, E., Bird, A., Jay, M., Lorenz, B., Wittwer, B., M, D.U., Meitinger, T. and Wright, A. 1996. A gene (RPGR) with homology to the RCC1 guanine nucleotide exchange factor is mutated in X-linked retinitis pigmentosa (RP3). Nat Genet **13**: 35-42.

Meitinger, T., Meindl, A., Bork, P., Rost, B., Sander, C., Haasemann, M. and Murken, J. 1993. Molecular modelling of the Norrie disease protein predicts a cystine knot growth factor tertiary structure. Nat Genet **5**: 376-80.

Michienzi, A., Prislei, S. and Bozzoni, I. 1996. U1 small nuclear RNA chimeric ribozymes with substrate specificity for the rev pre-mRNA of human immunodeficiency virus. Proc Natl Acad Sci U S A **92**:

Miller, A.D. 1992. Human gene therapy comes of age. Nature **357**: 455-60.

Mitani, K., Graham, F.L., Caskey, C.T. and Kochanek, S. 1995. Rescue, propagation, and partial purification of a helper virus-dependent adenovirus vector. Proc Natl Acad Sci U S A **92**: 3854-8.

Mitchell, G.A., Brody, L.C., Sipila, I., Looney, J.E., Wong, C., Engelhardt, J.F., Patel, A.S., Steel, G., Obie, C., Kaiser Kupfer, M. and et al. 1989. At least two mutant alleles of ornithine delta-aminotransferase cause gyrate atrophy of the choroid and retina in Finns. Proc Natl Acad Sci U S A **86**: 197-201.

Miyoshi, H., Takahashi, M., Gage, F.H. and Verma, I.M. 1997. Stable and efficient gene transfer into the retina using an HIV-based lentiviral vector. Proc Natl Acad Sci U S A **94**: 10319-23.

Mizzen, C.A., Yang, X.J., Kokubo, T., Brownell, J.E., Bannister, A.J., Owen Hughes, T., Workman, J., Wang, L., Berger, S.L., Kouzarides, T., Nakatani, Y. and Allis, C.D. 1996. The TAF(II)250 subunit of TFIID has histone acetyltransferase activity. Cell **87**: 1261-70.

Mohr, G., Zhang, A., Gianelos, J.A., Belfort, M. and Lambowitz, A.M. 1992. The neurospora CYT-18 protein suppresses defects in the phage T4 td intron by stabilizing the catalytically active structure of the intron core. Cell **69**: 483-94.

Morabito, M.A., Yu, X. and Barnstable, C.J. 1991. Characterization of developmentally regulated and retina-specific nuclear protein binding to a site in the upstream region of the rat opsin gene. J Biol Chem **266**: 9667-72.

Muhlrad, D. and Parker, R. 1994. Premature translational temination triggers mRNA decapping. Nature **370**: 578-581.

Mulligan, R.C. 1993. The basic science of gene therapy. Science **260**: 926-32.

Muzyczka, N. 1992. Use of adeno-associated virus as a general transduction vector for mammalian cells. Curr Top Microbiol Immunol **158**: 97-129.

Nabel, E.G., Yang, Z.Y., Plautz, G., Forough, R., Zhan, X., Haudenschild, C.C., Maciag, T. and Nabel, G.J. 1993. Recombinant fibroblast growth factor-1 promotes intimal hyperplasia and angiogenesis in arteries in vivo. Nature **362**: 844-6.

Nadler, S.G., Merrill, B.M., Roberts, W.J., Keating, K.M., Lisbin, M.J., Barnett, S.F., Wilson, S.H. and Williams, K.R. 1991. Interactions of the A1 heterogeneous nuclear ribonucleoprotein and its proteolytic derivative, UP1, with RNA and DNA: evidence for multiple RNA binding domains and salt-dependent binding mode transitions. Biochemistry **30**: 2968-76.

Naldini, L., Blomer, U., Gallay, P., Ory, D., Mulligan, R., Gage, F.H., Verma, I.M. and Trono, D. 1996. In vivo gene delivery and stable transduction of nondividing cells by a lentiviral vector. Science **272**: 263-7

Nathans, J. and Hogness, D.S. 1983. Isolation, sequence analysis, and intron-exon arrangement of the gene encoding bovine rhodopsin. Cell **34**: 807-14.

Nie, Z., Chen, S., Kumar, R. and Zack, D.J. 1996. RER, an evolutionarily conserved sequence upstream of the rhodopsin gene, has enhancer activity. J Biol Chem **271**: 2667-75.

Ogryzko, V.V., Schiltz, R.L., Russanova, V., Howard, B.H. and Nakatani, Y. 1996. The transcriptional coactivators p300 and CBP are histone acetyltransferases. Cell **87**: 953-9.

Ohkawa, J., Yuyama, N., Takebe, Y., Nishikawa, S. and Taira, K. 1993. Importance of independence in ribozyme reactions: kinetic behavior of trimmed and of simply connected multiple ribozymes with potential activity against human immunodeficiency virus. Proc Natl Acad Sci U S A **90**: 11302-6.

Ohkuma, Y., Hashimoto, S., Wang, C.K., Horikoshi, M. and Roeder, R.G. 1995. Analysis of the role of TFIIE in basal transcription and TFIIH-mediated carboxy-terminal domain phosphorylation through structure-function studies of TFIIE-alpha. Mol Cell Biol **15**: 4856-66.

Olsson, J.E., Gordon, J.W., Pawlyk, B.S., Roof, D., Hayes, A., Molday, R.S., Mukai, S., Cowley, G.S., Berson, E.L. and Dryja, T.P. 1992. Transgenic mice with a rhodopsin mutation (Pro23His): a mouse model of autosomal dominant retinitis pigmentosa. Neuron **9**: 815-30.

Oudrhiri, N., Vigneron, J.P., Peuchmaur, M., Leclerc, T., Lehn, J.M. and Lehn, P. 1997. Gene transfer by guanidinium-cholesterol cationic lipids into airway epithelial cells in vitro and in vivo. Proc Natl Acad Sci U S A **94**: 1651-1656.

Palmer, T.D., Rosman, G.J., Osborne, W.R. and Miller, A.D. 1991. Genetically modified skin fibroblasts persist long after transplantation but gradually inactivate introduced genes. Proc Natl Acad Sci U S A **88**: 1330-4.

Pannetier, C., Delassus, S., Darche, S., Saucier, C. and Kourisky, P. 1993. Quantitative titration of nucleic acid by enzymatic amplification reactions run to saturation. Nucleic Acids Res **21**: 577-583.

Parks, R.J., Chen, L., Anton, M., Sankar, U., Rudnicki, M.A. and Graham, F.L. 1996. A helper-dependent adenovirus vector system: removal of helper virus by Cre-mediated excision of the viral packaging signal. Proc Natl Acad Sci U S A **93**: 13565-70.

Pazin, M.J. and Kadonaga, J.T. 1997. What's up and down with histone deacetylation and transcription? Cell **89**: 325-8.

Perriman, R., Delves, A. and Gerlach, W.L. 1992. Extended target-site specificity for a hammerhead ribozyme. Gene **113**: 157-63.

Peterson, C.L. and Tamkun, J.W. 1995. The SWI-SNF complex: a chromatin remodeling machine? Trends Biochem Sci **20**: 143-6.

Pinol Roma, S. and Dreyfuss, G. 1992. Shuttling of pre-mRNA binding proteins between nucleus and cytoplasm. Nature **355**: 730-2.

Pittler, S.J. and Baehr, W. 1991. Identification of a nonsense mutation in the rod photoreceptor cGMP phosphodiesterase beta-subunit gene of the rd mouse. Proc Natl Acad Sci U S A **88**: 8322-6.

Pittler, S.J., Keeler, C.E., Sidman, R.L. and Baehr, W. 1993. PCR analysis of DNA from 70-year-old sections of rodless retina demonstrates identity with the mouse rd defect. Proc Natl Acad Sci U S A **90**: 9616-9.

Poeschla, E. and Wong, S.F. 1994. Antiviral and anticancer ribozymes. Curr Opin Oncol **6**: 601-6.

Pontius, B.W. 1993. Close encounters: why unstructured, polymeric domains can increase rates of specific macromolecular association. Trends Biochem Sci **18**: 181-6.

Portera, C.C., Sung, C.H., Nathans, J. and Adler, R. 1994. Apoptotic photoreceptor cell death in mouse models of retinitis pigmentosa. Proc Natl Acad Sci U S A **91**: 974-8.

Portman, D.S. and Dreyfuss, G. 1994. RNA annealing activities in HeLa nuclei. EMBO J **13**: 213-21.

Poznansky, M., Lever, A., Bergeron, L., Haseltine, W. and Sodroski, J. 1991. Gene transfer into human lymphocytes by a defective human immunodeficiency virus type 1 vector. J Virol **65**: 532-6.

Ptashne, M. and Gann, A. 1997. Transcriptional activation by recruitment. Nature **386**: 569-77.

Pulak, R. and Anderson, P. 1993. mRNA surveillance by the Caenorhabditis elegans smg genes. Genes & Dev **7**: 1885-1897.

Qin, N., Pittler, S.J. and Baehr, W. 1992. In vitro isoprenylation and membrane association of mouse rod photoreceptor cGMP phosphodiesterase alpha and beta subunits expressed in bacteria. J Biol Chem **267**: 8458-63.

Quantin, B., Perricaudet, L.D., Tajbakhsh, S. and Mandel, J.L. 1992. Adenovirus as an expression vector in muscle cells in vivo. Proc Natl Acad Sci U S A **89**: 2581-4.

Rehemtulla, A., Warwar, R., Kumar, R., Ji, X., Zack, D.J. and Swaroop, A. 1996. The basic motif-leucine zipper transcription factor Nrl can positively regulate rhodopsin gene expression. Proc Natl Acad Sci U S A **93**: 191-5.

Roeder, R.G. 1996. The role of general initiation factors in transcription by RNA polymerase II. Trends Biochem Sci **21**: 327-35.

Roof, D.J., Adamian, M. and Hayes, A. 1994. Rhodopsin accumulation at abnormal sites in retinas of mice with a human P23H rhodopsin transgene. Invest Ophthalmol Vis Sci **35**: 4049-62.

Rosenfeld, M.A., Yoshimura, K., Trapnell, B.C., Yoneyama, K., Rosenthal, E.R., Dalemans, W., Fukayama, M., Bargon, J., Stier, L.E., Stratford-Perricaudet, L., Perricaudet, M., Guggino, W.B., Pavirani, A., Lecocq, J. and Crystal, R.G. 1992a. In vivo transfer of the human cystic fibrosis transmembrane conductance regulator gene to the airway epithelium. Cell **68**: 143-155.

Rosenfeld, P.J., Cowley, G.S., McGee, T.L., Sandberg, M.A., Berson, E.L. and Dryja, T.P. 1992b. A null mutation in the rhodopsin gene causes rod photoreceptor dysfunction and autosomal recessive retinitis pigmentosa. Nat Genet **1**: 209-13.

Roush, W. 1997. Antisense aims for a renaissance. Science **276**: 1192-1193.

Ruffner, D.E., Stormo, G.D. and Uhlenbeck, O.C. 1990. Sequence requirements of the hammerhead RNA self-cleavage reaction. Biochemistry **29**: 10695-702.

Samulski, R.J., Zhu, X., Xiao, X., Brook, J.D., Housman, D.E., Epstein, N. and Hunter, L.A. 1991. Targeted integration of adeno-associated virus (AAV) into human chromosome 19. EMBO J **10**: 3941-50.

Sarver, N. and Rossi, J.J. 1993. Gene therapy for HIV-1 infection: progress and prospects. J NIH Res. **5**: 63-67.

Sauer, F., Wassarman, D.A., Rubin, G.M. and Tjian, R. 1996. TAF(II)s mediate activation of transcription in the Drosophila embryo. Cell **87**: 1271-84.

Savant Bhonsale, S. and Cleveland, D.W. 1992. Evidence for instability of mRNAs containing AUUUA motifs mediated through translation-dependent assembly of a > 20S degradation complex. Genes Dev **6**: 1927-39.

Saxena, S.K. and Ackerman, E.J. 1990. Microinjected oligonucleotides complementary to the alpha-sarcin loop of 28 S RNA abolish protein synthesis in Xenopus oocytes. J Biol Chem **265**: 3263-9.

Scanlon, K.J., Jiao, L., Funato, T., Wang, W., Tone, T., Rossi, J.J. and Kashani Sabet, M. 1991. Ribozyme-mediated cleavage of c-fos mRNA reduces gene expression of DNA synthesis enzymes and metallothionein. Proc Natl Acad Sci U S A **88**: 10591-5.

Seabra, M.C., Brown, M.S. and Goldstein, J.L. 1993. Retinal degeneration in choroideremia: deficiency of rab geranylgeranyl transferase. Science **259**: 377-81.

Semple Rowland, S.L., Lee, N.R., Van Hooser, J.P., Palczewski, K. and Baehr, W. 1998. A null mutation in the photoreceptor guanylate cyclase gene causes the retinal degeneration chicken phenotype. Proc Natl Acad Sci U S A **95**: 1271-6.

Sharmeen, L., Kuo, M.Y., Dinter Gottlieb, G. and Taylor, J. 1988. Antigenomic RNA of human hepatitis delta virus can undergo self-cleavage. J Virol **62**: 2674-9.

Sherman, P.M., Sun, H., Macke, J.P., Williams, J., Smallwood, P.M. and Nathans, J. 1997. Identification and characterization of a conserved family of protein serine/threonine phosphatases homologous to Drosophila retinal degeneration C. Proc Natl Acad Sci U S A **94**: 11639-44.

Siebert, P. and Larrick, J. 1992. Competitive PCR. Nature **359**: 557-558.

Snyder, R.O., Miao, C.H., Patijn, G.A., Spratt, S.K., Danos, O., Nagy, D., Gown, A.M., Winther, B., Meuse, L., Cohen, L.K., Thompson, A.R. and Kay, M.A. 1997. Persistent and therapeutic concentrations of human factor IX in mice after hepatic gene transfer of recombinant AAV vectors. Nat Genet **16**: 270-6.

Souaze, F., Ntodou, T.A. and Tran, C.Y. 1996. Quantitative RT-PCR: Limits and accuracy. BioTechniques **21**: 280-285.

Spaete, R.R. and Frenkel, N. 1982. The herpes simplex virus amplicon: a new eucaryotic defective-virus cloning-amplifying vector. Cell **30**: 295-304.

Steinecke, P., Herget, T. and Schreier, P.H. 1992. Expression of a chimeric ribozyme gene results in endonucleolytic cleavage of target mRNA and a concomitant reduction of gene expression in vivo. EMBO J **11**: 1525-30.

Steinmetz, E.J. 1997. Pre-mRNA processing and the CTD of RNA polymerase II: the tail that wags the dog? Cell **89**: 491-4.

Stone, E.M., Fingert, J.H., Alward, W.L.M., Nguyen, T.D., Polansky, J.R., Sunden, S.L.F., Nishimura, D., Clark, A.F., Nystuen, A., Nichols, B.E., Mackey, D.A., Ritch, R., Kalenak, J.W., Craven, E.R. and Sheffield, V.C. 1997. Identification of a gene that causes primary open angle glaucoma. Science **275**: 668-670.

Stryer, L. 1986. Cyclic GMP cascade of vision. Ann. Rev. Neurosci. **9**: 87-119.

Stryer, L. and Bourne, H.R. 1986. G proteins: a family of signal transducers. Annu Rev Cell Biol **2**: 391-419.

Suber, M.L., Pittler, S.J., Qin, N., Wright, G.C., Holcombe, V., Lee, R.H., Craft, C.M., Lolley, R.N., Baehr, W. and Hurwitz, R.L. 1993. Irish setter dogs affected with rod/cone dysplasia contain a nonsense mutation in the rod cGMP phosphodiesterase beta-subunit gene. Proc Natl Acad Sci U S A **90**: 3968-72.

Sullenger, B.A. and Cech, T.R. 1993. Tethering ribozymes to a retroviral packaging signal for destruction of viral RNA. Science **262**: 1566-9.

Sullenger, B.A. and Cech, T.R. 1994. Ribozyme-mediated repair of defective mRNA by targeted, trans-splicing. Nature **371**: 619-22.

Sung, C.H., Davenport, C.M., and Nathans, J. 1993. Rhodopsin mutations responsible for autosomal dominant retinitis pigmentosa. Clustering of functional classes along the polypeptide chain. J Biol Chem 268: 26645-49

Sung, C.H., Makino, C., Baylor, D. and Nathans, J. 1994. A rhodopsin gene mutation responsible for autosomal dominant retinitis pigmentosa results in a protein that is defective in localization to the photoreceptor outer segment. J Neurosci **14**: 5818-33.

Sung, C.H., Schneider, B.G., Agarwal, N., Papermaster, D.S. and Nathans, J. 1991. Functional heterogeneity of mutant rhodopsins responsible for autosomal dominant retinitis pigmentosa. Proc Natl Acad Sci U S A 88:8840-4

Swanson, M.S. and Dreyfuss, G. 1988. RNA binding specificity of hnRNP proteins: a subset bind to the 3' end of introns. EMBO J **7**: 3519-29.

Symons, R.H. 1989. Self-cleavage of RNA in the replication of small pathogens of plants and animals. Trends Biochem Sci **14**: 445-50.

Tamkun, J.W., Deuring, R., Scott, M.P., Kissinger, M., Pattatucci, A.M., Kaufman, T.C. and J.A., K. 1992. brahma: a regulator of Drosophila homeotic genes structurally related to the yeast transcriptional activator SNF2/SWI2. Cell **68**: 561-72.

Taubes, G. 1997. Salvation in a snippet of DNA. Science **278**: 1711-1714.

Taylor, R.M. and Wolfe, J.H. 1997. Decreased lysosomal storage in the adult MPS VII mouse brain in the vicinity of grafts of retroviral vector-corrected fibroblasts secreting high levels of beta-glucuronidase [see comments]. Nat Med **3**: 771-4.

Thein, S.L., Hesketh, C., Taylor, P., Temperley, I.J., Hutchinson, R.M., Old, J.M., Wood, W.G., Clegg, J.B. and Weatherall, D.J. 1990. Molecular basis for dominantly inherited inclusion body beta-thalassemia. Proc Natl Acad Sci U S A **87**: 3924-3928.

Timmers, A.M., Newton, B.R. and Hauswirth, W.W. 1993. Synthesis and stability of retinal photoreceptor mRNAs are coordinately regulated during bovine fetal development. Exp Eye Res **56**: 257-65.

Travis, G.H., Groshan, K.R., Lloyd, M. and Bok, D. 1992. Complete rescue of photoreceptor dysplasia and degeneration in transgenic retinal degeneration slow (rds) mice. Neuron **9**: 113-9.

Treisman, J.E., Morabito, M.A. and Barnstable, C.J. 1988. Opsin expression in the rat retina is developmentally regulated by transcriptional activation. Mol Cell Biol **8**: 1570-9.

Tsang, S.H., Gouras, P., Yamashita, C.K., Kjeldbye, H., Fisher, J., Farber, D.B. and Goff, S.P. 1996. Retinal degeneration in mice lacking the gamma subunit of the rod cGMP phosphodiesterase. Science **272**: 1026-9.

Tsuchihashi, Z., Khosla, M. and Herschlag, D. 1993. Protein enhancement of hammerhead ribozyme catalysis. Science **262**: 99-102.

Tuite, M. 1996. Death by decapitation for mRNA. Nature **382**: 577-579.

Turner, D.L. and Cepko, C.L. 1987. A common progenitor for neurons and glia persists in rat retina late in development. Nature **328**: 131-6.

Turner, D.L., Snyder, E.Y. and Cepko, C.L. 1990. Lineage-independent determination of cell type in the embryonic mouse retina. Neuron **4**: 833-45.

Uhlenbeck, O.C. 1987. A small catalytic oligoribonucleotide. Nature **328**: 596-600.

Verrijzer, C.P. and Tjian, R. 1996. TAFs mediate transcriptional activation and promoter selectivity. Trends Biochem Sci **21**: 338-42.

Wang, Y., Macke, J.P., Merbs, S.L., Zack, D.J., Klaunberg, B., Bennett, J., Gearhart, J. and Nathans, J. 1992. A locus control region adjacent to the human red and green visual pigment genes. Neuron **9**: 429-40.

Watanabe, T. and Raff, M.C. 1990. Rod photoreceptor development in vitro: intrinsic properties of porliferating neuroepithelial cells change as development proceeds in the rat retina. Neuron **2**: 461-467.

Weber, B.H., Vogt, G., Pruett, R.C., Stohr, H. and Felbor, U. 1994. Mutations in the tissue inhibitor of metalloproteinases-3 (TIMP3) in patients with Sorsby's fundus dystrophy. Nat Genet **8**: 352-6.

Wetts, R. and Fraser, S.E. 1988. Multipotent precursors can give rise to all major cell types of the frog retina. Science **239**: 1142-5.

Wieland, T., Chen, C.K. and Simon, M.I. 1997. The retinal specific protein RGS-r competes with the gamma subunit of cGMP phosphodiesterase for the alpha subunit of transducin and facilitates signal termination. J Biol Chem **272**: 8853-6.

Wiertz, E.J., Tortorella, D., Bogyo, M., Yu, J., Mothes, W., Jones, T.R., Rapoport, T.A. and Ploegh, H.L. 1996. Sec61-mediated transfer of a membrane protein from the endoplasmic reticulum to the proteasome for destruction. Nature **384**: 432-8.

Wileman, T., Carson, G.R., Concino, M., Ahmed, A. and Terhorst, C. 1990. The gamma and epsilon subunits of the CD3 complex inhibit pre-Golgi degradation of newly synthesized T cell antigen receptors. J Cell Biol **110**: 973-86.

Wolff, J.A., Malone, R.W., Williams, P., Chong, W., Acsadi, G., Jani, A. and Felgner, P.L. 1990. Direct gene transfer into mouse muscle in vivo. Science **247**: 1468-9.

Wong, P. 1994. Apoptosis, retinitis pigmentosa, and degeneration. Biochem Cell Biol **72**: 489-498.

Woodford, B.J., Chen, J. and Simon, M.I. 1994. Expression of rhodopsin promoter transgene product in both rods and cones. Exp Eye Res **58**: 631-5.

Wu, G.Y., Wilson, J.M., Shalaby, F., Grossman, M., Shafritz, D.A. and Wu, C.H. 1991. Receptor-mediated gene delivery in vivo. Partial correction of genetic analbuminemia in Nagase rats. J Biol Chem **266**: 14338-42.

Xiao, X., Xiao, W., Li, J. and Samulski, R.J. 1997. A novel 165-base-pair terminal repeat sequence is the sole cis requirement for the adeno-associated virus life cycle. J Virol **71**: 941-8.

Xie, Y., Chen, X. and Wagner, T.E. 1997. A ribozyme-mediated, gene "kncokdown" strategy for the identification of gene function in zebrafish. Proc Natl Acad Sci U S A **94**: 13777-13781.

Xu, J., Dodd, R.L., Makino, C.L., Simon, M.I., Baylor, D.A. and Chen, J. 1997. Prolonged photoresponses in transgenic mouse rods lacking arrestin. Science **389**: 505-511.

Yan, W.M., Flannery, J.G. and Hauswirth, W.W. 1998. Unpublished results.

Yu, M., Ojwang, J., Yamada, O., Hampel, A., Rapapport, J., Looney, D. and Wong Staal, F. 1993a. A hairpin ribozyme inhibits expression of diverse strains of human immunodeficiency virus type 1. Proc Natl Acad Sci U S A **90**: 6340-4.

Yu, X., Chung, M., Morabito, M.A. and Barnstable, C.J. 1993b. Shared nuclear protein binding sites in the upstream region of the rat opsin gene. Biochem Biophys Res Commun **191**: 76-82.

Zack, D.J. 1993. Use of transgenic mice to study retinal gene expression. Methods in Neuroscience **15**: 331-342.

Zack, D.J., Bennett, J., Wang, Y., Davenport, C., Klaunberg, B., Gearhart, J. and Nathans, J. 1991. Unusual topography of bovine rhodopsin promoter-lacZ fusion gene expression in transgenic mouse retinas. Neuron **6**: 187-99.

Zawel, L. and Reinberg, D. 1995. Common themes in assembly and function of eukaryotic transcription complexes. Annu Rev Biochem **64**: 533-61.

Zhang, J. and Maquat, L. 1996. Evidence that the decay of nucleus-associated nonsense mRNA for human triosephosphate isomerase involves nonsense codon recognition after splicing. RNA **2**: 235-243.

Zhang, J. and Maquat, L. 1997. Evidence that translation reinitiation abrogates nonsense-mediated mRNA decay in mammalian cells. EMBO J **16**: 826-833.

Zhao, J.J. and Pick, L. 1993. Generating loss-of-function phenotypes of the fushi tarazu gene with a targeted ribozyme in Drosophila. Nature **365**: 448-51.

Zolotukhin, S., Potter, M., Hauswirth, W.W., Guy, J. and Muzyczka, N. 1996. A "humanized" green fluorescent protein cDNA adapted for high-level expression in mammalian cells. J Virol **70**: 4646-54.

BIOGRAPHICAL SKETCH

Weiming Yan graduated in 1991 with a Bachelor of Science in Biochemistry from Zhongshan University. In 1994, he entered the graduate program at University of Florida.

I certify that I have read this study and that in my opinion it conforms to acceptable standards of scholarly presentation and is fully adequate, in scope and quality, as a dissertation for the degree of Doctor of Philosophy.

William W. Hauswirth, Chair
Eminent Scholar of Molecular Genetics
and Microbiology

I certify that I have read this study and that in my opinion it conforms to acceptable standards of scholarly presentation and is fully adequate, in scope and quality, as a dissertation for the degree of Doctor of Philosophy.

Paul A Hargrave

Paul A. Hargrave
Eminent Scholar of Ophthalmology

I certify that I have read this study and that in my opinion it conforms to acceptable standards of scholarly presentation and is fully adequate, in scope and quality, as a dissertation for the degree of Doctor of Philosophy.

Alfred Lewin

Alfred S. Lewin
Professor of Molecular Genetics
and Microbiology

I certify that I have read this study and that in my opinion it conforms to acceptable standards of scholarly presentation and is fully adequate, in scope and quality, as a dissertation for the degree of Doctor of Philosophy.

Nicholas Muzyczka

Nicholas Muzyczka
Eminent Scholar of Molecular Genetics
and Microbiology

This dissertation was submitted to the Graduate Faculty of the College of Medicine and to the Graduate School and was accepted as partially fulfillment of the requirements for the degree of Doctor of Philosophy.

December, 1998

Dean, College of Medicine

Dean, Graduate School